UNIVERSITY of TASMANIA

University of Tasmania Open Access Repository

Cover sheet

Title
The character, origin and significance of the Howards Basalt, within the Cambrian Tyndall Group, Western Tasmania

Author
Scott, H

Bibliographic citation
Scott, H (2000). The character, origin and significance of the Howards Basalt, within the Cambrian Tyndall Group, Western Tasmania. University Of Tasmania. Thesis. https://doi.org/10.25959/23211530.v1

Is published in:

Copyright information
This version of work is made accessible in the repository with the permission of the copyright holder/s under the following,

Licence.

Rights statement: Copyright the Author - The University is continuing to endeavour to trace the copyright owner(s) and in the meantime this item has been reproduced here in good faith. We would be pleased to hear from the copyright owner(s).

If you believe that this work infringes copyright, please email details to: oa.repository@utas.edu.au

Downloaded from University of Tasmania Open Access Repository

Please do not remove this coversheet as it contains citation and copyright information.

University of Tasmania Open Access Repository

Library and Cultural Collections
University of Tasmania
Private Bag 3
Hobart, TAS 7005 Australia
E oa.repository@utas.edu.au CRICOS Provider Code 00586B | ABN 30 764 374 782 utas.edu.au

The Character, Origin and Significance of the Howards Basalt, within the Cambrian Tyndall Group, Western Tasmania

Helen J. Scott
BAppSc

University of Tasmania

CODES SRC
Centre for Ore Deposit Research

A research thesis submitted in partial fulfilment of the requirements of the Degree of Bachelor of Science with Honours

School of Earth Sciences
November 2000

Abstract

The Howards Basalt forms a minor mafic unit in the basal Lynchford Member of the Cambrian Tyndall Group. The unit is andesitic in character, and occurs most frequently as a monomictic breccia, strongly altered by chlorite, sericite and haematite.

The unit was formed by the eruption of lava both explosively and effusively, in an extensional and subaqueous environment, to produce five main facies.

The Howards Basalt can be geochemically correlated with the Suite III rocks of the Mount Read Volcanics, which include the high K Que-Hellyer footwall volcanic rocks, and the shoshonitic Lynch Creek Basalt.

The Howards Basalt occurs on the Comstock - Mt Lyell prospective horizon, on the same stratigraphic horizon as the Henty deposit. It is also thought to have formed in a similar fashion to the Spillway Basalt, which occupies another favourable horizon. The mode of emplacement of the Howards Basalt unit may have been conducive to mineralisation.

Acknowledgments

☺ First of all I have to thank my supervisors: Dr Jocelyn McPhie & Wally Herrmann

☺ The government for the money (scholarship)

☺ All the other students for putting up with me

☺ The guys at Goldfields – Mike (thanks for the maps, logs and other little bits and pieces), Bruce (thanks for helping me with the saw and the truck) and Scott & Dale (thanks for laying out all that core and cutting those samples for me)

☺ My computer, and other associated bits of technology (for working most of the time)

☺ The soccer ball and kicking partners (for relieving stress in the last coupla months)

☺ My Mum (for putting up with me even though I never told her enough about what was going on)

☺ And last, but not least, my Dad (for the technical expertise when the puter decided not to work)

"Reality is nothing but a collective hunch."
- Lily Tomlin

Contents

Abstract i

Acknowledgments ii

List of Illustrations vi

Maps ..... **vi**

Figures ..... **vi**

Plates ..... **vii**

Chapter 1: Introduction 1

1.1 Aims and Significance 1

1.2 Location 1

1.3 Methods 4

1.4 Previous work 5

1.5 Outline 6

Chapter 2: Regional Geology 7

2.1 Lithostratigraphy and Tectonic History of Western Tasmania 7

2.2 Mount Read Volcanics 8

2.2.1 Tyndall Group (TG) **9**

Chapter 3: Local Geology 11

3.1 Introduction 11

3.2 Stratigraphy, Facies, and Structure Between the South Henty Fault and the Great Lyell Fault 11

3.2.1 Central Volcanic Complex **12**

3.2.2 Tyndall Group **13**

Comstock Formation *15*

Zig Zag Hill Formation *16*
3.3 Mineral Deposits and Exploration Targets 16

Chapter 4: Textural and Lithofacies Characteristics of the Howards Basalt 18

4.1 Introduction 18
4.2 Alteration and Deformation 22
4.3 Facies Descriptions 25
4.3.1 Type 1 Monomictic Breccia Facies 25
4.3.2 Type 2 Monomictic Breccia Facies 25
4.3.3 Polymictic Breccia Facies 25
4.3.4 Coherent Basalt Facies 27
4.3.5 Volcaniclastic Sandstone Facies 27
4.4 Internal Stratigraphy and Relation to Associated Units 27
4.5 Interpretation 28

Chapter 5: Petrography and Geochemistry of the Howards Basalt 31

5.1 Introduction 31
5.2 Petrographic Analyses 31
5.3 XRF Analyses 32
5.4 Carlo-Erba Analyses 33
5.5 Short-wave Infra-red Spectral Analyses 33
5.6 Geochemical Plots - Discrimination and Comparison to other Mount Read Volcanic Successions 34
5.7 Interpretation 40

Chapter 6: Discussion **41**

6.1 Tectonic 41

6.2 Regional Correlations 41

6.3 Eruption Style and Setting 41

6.4 Implications for Mineralisation 44

Chapter 7: Conclusions **45**

References **46**

List of Abbreviations **49**

Appendices **50**

A- Drill core logs 50

B- 120

1- XRF analyses 121

2- Carlo-Erba analyses and recalculations 122

3a- Short-wave infra-red spectrum stack 123

3b- PIMA Results 124

C- Literature Review - Fire Fountain Basalts 125

D- Rock Catalogue 151

List of Illustrations - Maps

Map 1 Geological units of the central part of the Mount Read Volcanics, western Tasmania [modified after White & McPhie, 1997]. The area of study is shown. 2

Map 2 Geology map of the study area between the South Henty and Great Lyell Faults [modified Goldfields Exploration, in-house map]. 3

- Figures

Figure 3.1 Stratigraphic column displaying main units within the slice of Mount Read Volcanics between the South Henty Fault and Great Lyell Fault (Map 2) [modified after Herrmann & MacDonald, 1996]. 14

Figure 4.1 Summary of cores logged. 19

Figure 4.2 Interpretative cross-section along line A-B (Map 2), showing geometry of the basalt bodies. 20

Figure 4.3 Interpretative longitudinal projection along the line C-D (Map 2), showing the geometry of the basalt. 21

Figure 5.1 Plot of TiO_2 Vs Zr, to determine immobility of components (author's dataset only). 35

Figure 5.2 Plot of TiO_2 Vs Zr, to determine immobility of components (multiple data sources, see text). 35

Figure 5.3 Plot of P_2O_5/TiO_2 Vs SiO_2, showing the medium K calc-alkaline to shoshonitic fields described by Crawford *et al.* [1992], and MRV Suites I - V. 37

Figure 5.4 Plot of Ti/Zr Vs SiO_2, showing fields of MRV Suites of Crawford *et al.* [1992]. 37

Figure 5.5 Plot of light rare earth elements, showing samples from Crawford *et al.* [1992]. 38

Figure 5.6 Plot of Zr/TiO_2 Vs Nb/Y, showing fields of Floyd & Winchester [1977]. 38

Figure 5.7 Plot of Ti/100 - Zr - Y×3, showing fields of Pearce & Cann [1973]. 39
Figure 5.8 Plot of chlorite-carbonate-pyrite index Vs Ishikawa alteration index, showing fields of Large *et al.* [2000]. 39
Figure 6.1 Schematic section, outlining the environment and mode of eruption of the Howards Basalt and related units 43

- Plates

4.1 Monomictic breccia with strong haematite (maroon), chlorite (green) and sericite (cream) alteration to clasts and matrix [NC4_3]. 23
4.2 Recrystallised carbonate (C- calcite, cross polarized light, field of view is 8.4 mm × 6.4 mm) [NC1_7]. 23
4.3 Monomictic breccia with altered rims (B- basalt, Ch- chlorite, P- plagioclase, plane polarized light, field of view is 4.2 mm × 3.2 mm) [SHD13_5]. 23
4.4 Basalt with sericite (cream) alteration along fractures [NC4_17]. 23
4.5 Basalt clast with multiple alteration rims, and uncompressed amygdales (B- basalt inner, A- amygdales, H- haematite, M- muscovite, plane polarized light, field of view is 8.4 mm × 6.4 mm) [SHD25_4]. 23
4.6 Carbonate altered basalt clast, with uncompressed concentrically zoned amygdales (C- calcite, A- amygdales, plane polarized light, field of view is 1.05 mm × 0.8 mm) [NC1_7]. 23
4.7 Monomictic breccia altered by sericite (pink) and pyrite (grey), darker pink spots are relict plagioclase glomerocrysts [NC1_13]. 24
4.8 Carbonate vein with quartz central fill (C- carbonate, Q- quartz, cross polarized light, field of view is 8.4 mm × 6.4 mm) [NC1_9]. 24

4.9 Shistose texture in volcaniclastic sandstone (?) (M- muscovite, P?- plagioclase (?), cross polarized light, field of view is 8.4 mm × 6.4 mm) [NC4_18]. 24
4.10 Chlorite (dark green) and sericite (light cream) altered lensoidal monomictic breccia [NC4_1]. 24
4.11 Chlorite (green) and sericite (cream) altered monomictic breccia (large basalt clast in upper right) [SHD14_2]. 24
4.12 Haematite (red-brown) and chlorite (dark green) altered basalt clasts (B- basalt, plane polarized light, field of view 8.4 mm × 6.4 mm) [NC4_3]. 24
4.13 Polymictic breccia with basalt (dark green) and rhyolite/dacite (pink) clasts [NC4_14]. 26
4.14 Coherent basalt with plagioclase glomerocrysts (P- plagioclase, cross polarized light, field of view is 8.4 mm × 6.4 mm) [SHD1_1]. 26
4.15 Coherent basalt with altered plagioclase glomerocrysts (P- plagioclase, plane polarized light, field of view is 8.4 mm × 6.4 mm) [NC1_16]. 26
4.16 Volcaniclastic sandstone with abundant quartz, plagioclase and basalt fragments (Q- quartz, P- plagioclase, B- basalt, plane polarized light, filed of view is 8.6 mm × 6.4 mm) [SHD1_3]. 26

Chapter 1: Introduction

1.1 Aims and Significance

The aims of the project were to determine the character of the Howards Basalt (HB), including its internal stratigraphy, contact relationships, geometry and spatial extent. By using geochemistry it was aimed to ascertain a tectonic origin for the basalt, and its relation to other mafic successions within the Mount Read Volcanics (MRV). Interpretation of the mode of eruption of the basalt, and the depositional and tectonic setting into which the eruption took place was the main volcanological objective. The final aim was to consider the significance of the HB as an indicator of proximity to the eruptive vent(s), and any implications for volcanic-hosted massive sulfide mineralisation.

The MRV have been intensively explored for massive sulfide and gold deposits. Developments in stratigraphic correlation [White & McPhie, 1996] and metallogenic interpretation of the Henty deposit during the last decade have led to the recognition that the Henty, Mt Lyell and Comstock deposits exist at approximately the same stratigraphic horizon near the base of the Tyndall Group (TG). This is the same stratigraphic level as the HB. The Spillway Basalt, a fire fountain breccia unit similar to the HB but at much lower stratigraphic level within the Central Volcanic Complex (CVC), underlies polymictic breccia which contains clasts of massive sulfide, of unknown source. Given that association, and the occurrence of some VHMS deposits at felsic-mafic stratigraphic boundaries [Stolz *et al.*, 1997] the HB may have favourable exploration potential.

1.2 Location

The HB is a thin mafic unit occurring at the base of the Lynchford Member (LM) within the Cambrian TG of the MRV (Map 1). Formerly referred to as the "Howards Tuff", it is exposed in the vicinity of the "Howards Anomaly" prospect. It is south of the Henty gold mine, within the South Henty EL 8/96, and about halfway between Rosebery and Queenstown, in western Tasmania. It is exposed on the eastern shore of Lake

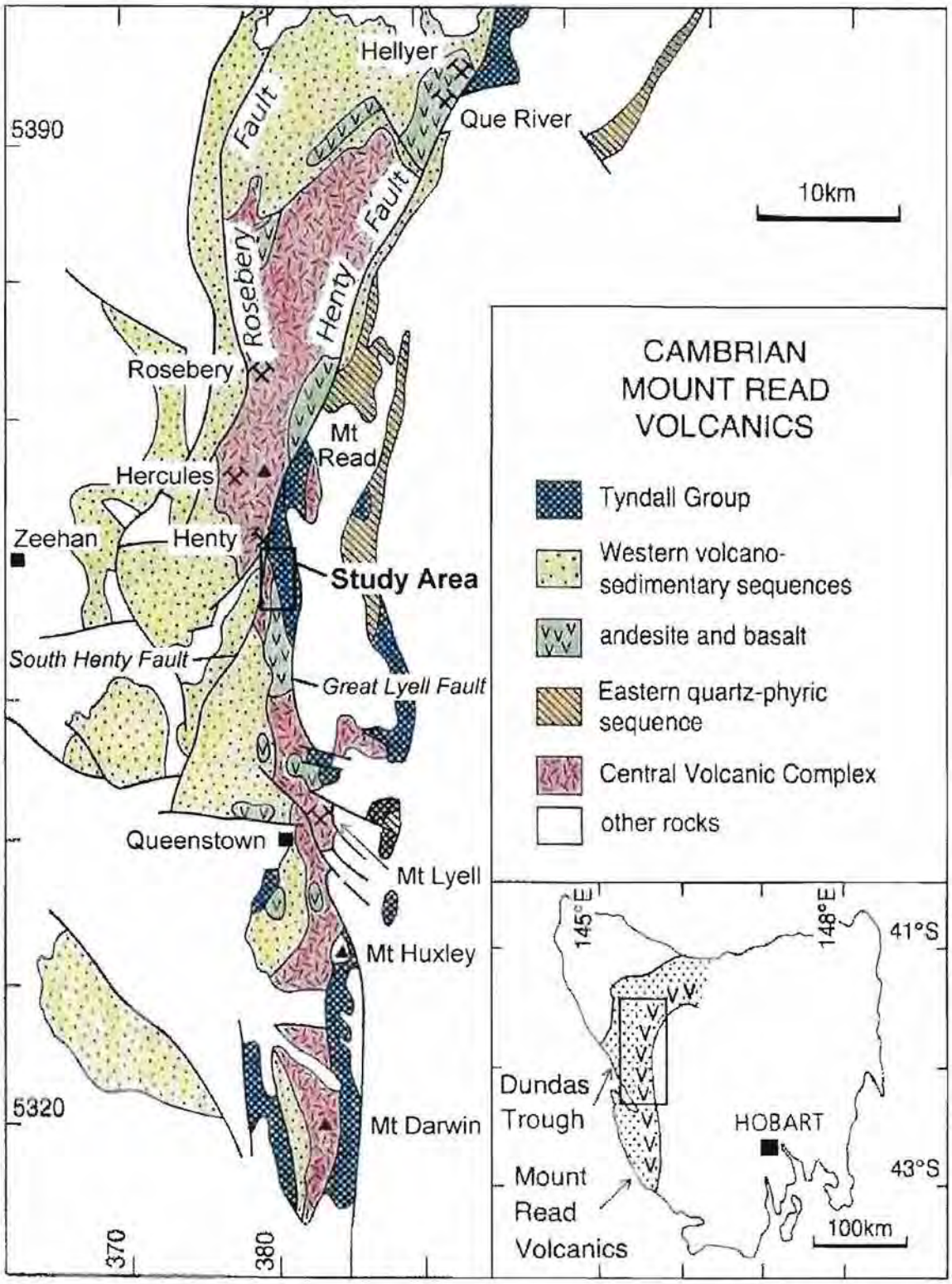

Map 1 Geological units of the central part of the Mount Read Volcanics, western Tasmania [modified after White & McPhie, 1997]. The area of study is shown.

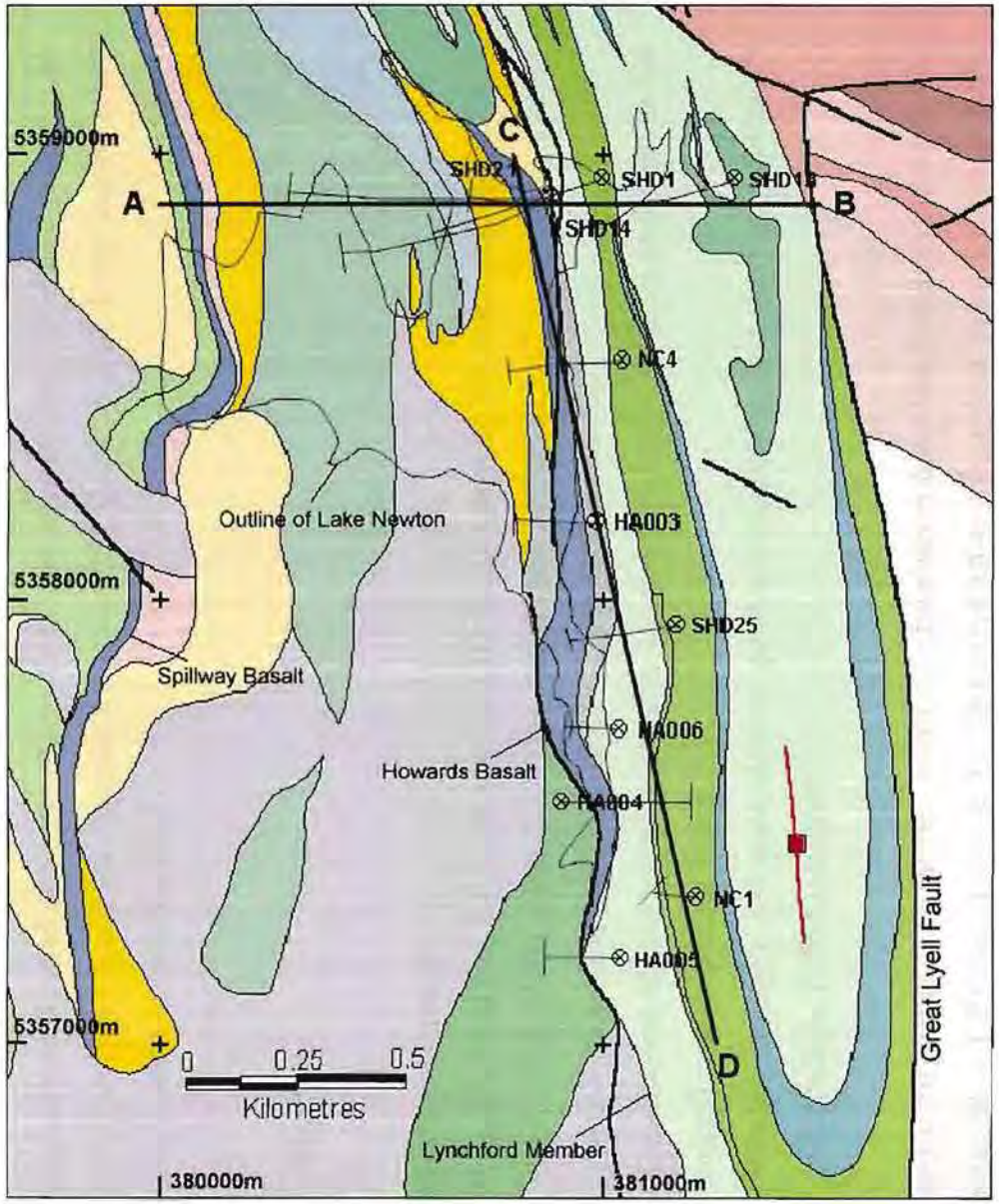

Geology Legend

- Ccvl - Newton Creek Dacite
- Ccarb - massive carbonate (Tyndall Group)
- Cb - Bas (Central Volcanic Complex & Tyndall Group)
- Cymt/Cymtq - Footwall volcaniclastic rocks (Central Volcanic Complex)
- Ccv - Central Volcanic Complex
- Ccvag - Spillway Polymictic Breccia (Central Volcanic Complex)
- Ca - And intrusions (Anthony Road Andesite)
- Cp - Q-F porphyry (Anthony Road Andesite)
- Cal - And lavas (Anthony Road Andesite)
- Cts - (Tyndall Group)
- Ctl - (Tyndall Group)
- Cto/Cttl - (Tyndall Group)
- COon - Newton Creek Sandstone (Denison Group)
- COonsh - Newton Creek Sandstone (Denison Group)
- COomcs - Newton Creek Sandstone (Denison Group)
- Ctt/Cttpl - Comstock Formation (Tyndall Group)
- COou - Upper Owen Formation (Denison Group)
- COom - Middle Owen Formation (Denison Group)
- Cttls - (Tyndall Group)

Symbols Legend

- Diamond drill hole
- Fold - syncline
- Fault - inferred
- Fault - accurate
- Fold axial trace
- Geological boundary

N

Map 2. Geology map of the study area between the South Henty and Great Lyell Faults [modified Goldfields Exploration, in-house map].

Newton (Map 2), and is known (from drill hole intersections) to extend laterally for approximately 3.4 km from its southern termination against a fault, to the northernmost outcrops, north of Lake Newton.

1.3 Methods

Methods used include:

- Logging of seven drill cores spanning the strike extent of the main outcropping body (NC1, NC4, SHD1, SHD13, SHD14, SHD21 and SHD25 Map 2).
- Volcanic facies analysis on the basis of core and thin sections.
- Construction of cross-sections (Figures 4.2 & 4.3; A-B, C-D Map 2) to determine the overall geometry of the basalt.
- Whole-rock major and trace element geochemical analysis, and short-wave infra-red spectroscopic (PIMA) analysis.

Detailed logging of 2750 metres of drill core from seven holes that intersected the HB was conducted at 1:200 and 1:100 scale. This provided coverage over about 1.6 km of strike and 800 m of down dip extent (refer to Figure 4.1 & Appendix A). Goldfields drill core logs of holes drilled between those logged by the author (HA003, HA004, HA005 and HA006 Map 2), were used to aid in correlation of units in cross section. The clast distribution, abundance and size were recorded to aid in the later analysis of the breccias, and samples representing different facies of the basalt (coherent, breccias, sandstones and intrusions) were taken for thin section and geochemical analysis.

Geochemical analysis of samples was done by XRF for whole-rock major (SiO_2, TiO_2, Fe_2O_3, MnO, MgO, CaO, Na_2O, K_2O, P_2O_5), and selected trace elements (Y, Zr, Nb, La, Ce, Nd; Appendix B-1). These various analyses were used to aid in comparison of the basalt to other MRV mafic units, and to determine the tectonic origin and setting of the basalt.

The Carlo-Erba elemental analyser was used to measure the concentration of volatile elements (C, H, S) in selected samples. This data was then used for recalculation purposes (Appendix B-2), to aid in the analysis of alteration intensities and mineralogies. Short-

wave infra-red spectral analyses (Appendix B-3) were conducted by the author, with the CODES' PIMA instrument, on selected diamond drill core samples. Veins, as well as sericitic alteration zones were analysed to aid in the determination of some of the alteration mineralogies within the HB.

The computer program IgPet was implemented to graph the geochemical data resulting from the above methods, together with data gathered from several external sources. Plots (Figures 5.1 – 5.7) were constructed to determine the immobility of the selected trace elements, as well as to compare the results with those of previous researchers (e.g. MRV suites of Crawford *et al.* [1992]), and against established discrimination diagrams (e.g. Floyd & Winchester [1977] diagram; Pearce & Cann [1973]). An alteration box plot [Large *et al.*, in prep.] was also constructed (Figure 5.8) to determine the degree and type of alteration occurring in the HB.

A literature review (Appendix C) on fire fountain basalts, addressing processes and products was conducted. This was done to compare and contrast the deposits of known fire fountain events, with those in the logged core. An understanding of the processes would aid in the determination of likely environments of eruption and deposition, as well as to assess the feasibility of basaltic fire fountaining having occurred in the area of study.

1.4 Previous work

In previous work on the volcanic facies in the MRV and the TG by McPhie & Allen [1992] it has been found that the TG and other closely associated units are dominantly subaqueous and volcano-sedimentary in nature. Further work by Allen [1994] on the Spillway Basalt raised the possibility that fire fountain activity could be a cause for the unit. This indicates an environment/tectonic setting conducive to sulfide mineralisation, in which extension allows for the high velocity release of basaltic magma. Herrmann & MacDonald [1996] commented on the similarity of the HB to the Spillway facies, and drew on the possibility of a similar fire fountain origin.

Within the area of study there are several non-economic deposits including the Howards Anomaly prospect, the gossan of which was discovered by Pickands Mather during 1950's

and 60's exploration [Street, 1999]. Later drilling intercepted the barite and haematite veins and silver mineralisation responsible for early geochemical and geophysical anomalies. Silver grades of 49 m at 8 g/t, 35 m at 34 g/t, 8.6 m at 11 g/t and 4.1 m at 6.3 g/t were recorded in diamond drill holes (DDH) HA3, HA4, HA5 and HA6 respectively [Herrmann & MacDonald, 1996].

Recent exploration in the South Henty area has been conducted by Pasminco, Aberfoyle, Resolute Samantha and Goldfields Exploration. It has concentrated on the Spillway Polymictic Breccia, which contains clasts of massive sulfide, the Tyndall Creek sulfide-barite mineralisation, and the intersection of the Great Lyell Fault and the basal TG [Herrmann & MacDonald, 1996]. Exploration has involved geochemical soil and rockchip sampling and, geophysical electromagnetic surveys, and the drilling of several thousand metres of diamond core.

Work by White [1996] on the TG has helped in defining the volcanological setting and processes that occurred in late stage MRV volcanism.

1.5 Outline

This thesis will address three main areas, the large scale characteristics, basically the geometry of the HB; small scale characteristics, namely the facies attributes and significance of the HB; and the geochemical nature of the HB, comparing and contrasting the HB to identified suites/groups.

Chapter 2: Regional Geology

2.1 Lithostratigraphy and Tectonic History of Western Tasmania

The three main geological provinces of western Tasmania are the Precambrian Rocky Cape and Tyennan Regions, the Cambrian MRV, and Dundas and Smithton Troughs. The Precambrian basement is composed of meta-sedimentary rocks, and comprises shallow marine quartzarenite, and deeper water turbiditic quartzose sandstone [Turner **in** Burrett & Martin, 1989].

The tectonic history of western Tasmania is complex and is still not fully understood. During the Late Proterozoic, eastward intraoceanic subduction produced an island arc with low Ti basalts and boninites in the forearc setting. Further eastward-subducting movement resulted in the collision of arc and thinned passive continental margin [Crawford & Berry, 1992], represented by the Precambrian basement and overlying shelf sedimentary units of the Success Creek Group and Crimson Creek Formation. This led to obduction of forearc basalts and boninites, represented by the ultramafic-mafic complexes of western Tasmania, and reversing of subduction for a short time. Post-collisional extension resulted in development of the Dundas Trough (DT), eruption of the MRV and uplift and exhumation of underthrust Precambrian basement [Crawford & Berry, 1992]. Volcaniclastic sediments originating from large-volume, explosive eruptions were deposited in the DT, over the earlier shelf sediments of the Success Creek Group and Crimson Creek Formation, which in turn unconformably overlie the Precambrian Rocky Cape Region [Brown **in** Burrett & Martin, 1989]. Uplift of the basement continued into the Ordovician, allowing for the flooding of primarily siliciclastic sediments into the DT and burial of the MRV. Movement on the Great Lyell Fault during deposition resulted in the greater thickness of the Owen Conglomerate (OC) to the east of the fault. Later in the Ordovician deposition of the Gordon Limestone and other sedimentary units occurred, further burying the volcanic succession. Major fault movement and folding occurred in the late Early to Middle Devonian, causing large scale folding and regional cleavage development [Corbett & Lees, 1987]. This deformation coincided with the Tabberabberan Orogeny on the east Australian mainland [Burrett & Martin, 1989]. The Late Devonian saw the intrusion of post-tectonic granitoid bodies, and the development of contact metamorphic aureoles, some of which

host tin-tungsten mineralisation in western Tasmania [Corbett & Lees, 1987; Renison, Zeehan, Mt Bischoff & Cleveland, Collins *et al.* **in** Burrett & Martin, 1989].

Both the Henty Fault and the Great Lyell Fault were active in the Cambrian, during deposition of the TG [Corbett & Lees, 1987; Halley & Roberts, 1997], and were therefore likely to have been, in part, responsible for any structurally controlled deposition and intrusion [White & McPhie, 1996]. Other Cambrian structures include pre-TG deformation in the Darwin-Murchison area, likely early movement on the Rosebery Fault [Corbett & Lees, 1987], and folding and disruption of Dundas Group rocks during Late Cambrian to Early Ordovician.

The regional cleavage developed in the Devonian is only weakly expressed in the TG [White & McPhie, 1996]. The HB is an exception to this, as it shows well-developed cleavage especially in areas of strong phyllosilicate alteration. The basalt may have been the focus of shearing during the Devonian deformation, as it displays strong shearing, straining and alteration at both hand specimen and thin-section scales.

2.2 Mount Read Volcanics

The Mid to Late Cambrian MRV, dated at 502.6 ± 3.5 Ma [majority of the belt, Perkins & Walshe, 1993], comprise a range of felsic to mafic lavas and intrusions, numerous volcaniclastic rocks, and minor non-volcanic sedimentary assemblages [Crawford *et al.*, 1992; McPhie & Allen, 1992; Corbett, 1992; White & McPhie, 1996]. They form an arcuate belt separating the Cambrian sedimentary, volcano-sedimentary sequences and ultramafic to mafic complexes of the DT to the west, from the Precambrian Tyennan Block to the east [Corbett & Lees, 1987].

The MRV (Map 1) comprises an eastern volcanic dominated zone, and a broad western volcano-sedimentary dominated zone. The MRV abut the Precambrian Tyennan Block in the east represented by the thin clastic Sticht Range Beds. The Eastern quartz-porphyritic sequence is the other component of the eastern zone, and is composed of quartz-porphyritic volcanic rocks. The Central Volcanic Complex (CVC) feldspar-porphyritic lava-rich volcanic and volcaniclastic rocks, TG volcanic intrusions and mass-flow volcaniclastic

deposits, and the andesitic lavas and breccias and minor felsic lavas and intrusive rocks of the Western Volcano-sedimentary Sequences (WVSS), make up the western zone. The WVSS has been divided into three main groups by different researchers, mostly based on geographic location. These are the Yolande River Sequence (YRS), located south of the South Henty Fault; Dundas Group, north of the North Henty Fault; Mt Charter Group, in the Hellyer area [Corbett, 1992]. The units contained in the Henty Fault Wedge (wedge of mismatch rocks between the North and South Henty Faults) are seen as independent of the documented successions of the MRV, and are believed to represent the remnants of an inter-arc basin [Corbett & Lees, 1987].

The MRV have undergone regional metamorphism of prehnite-pumpellyite to lower greenschist facies intensity [Corbett & Lees, 1987], with locally intense alteration from hydrothermal systems occurring in the Cambrian. The fine grained matrix of TG volcaniclastic rocks has been replaced by secondary metamorphic and alteration minerals [White & McPhie, 1996].

Alteration is very widespread in the geological units of the MRV. Many different alteration assemblages exist, the distribution of which is strongly structurally controlled by fault systems (e.g. Henty fault system), syn- and post-depositional, and hydrothermal systems that were active at the time of deposition of units.

2.2.1 Tyndall Group (TG)

The TG has been studied in detail by White [1996] and White & McPhie [1996], with emphasis applied to the volcanic source of components of the group. Classification of major lithologies was based on compositional differences, and facies architecture. The TG is divided into two formations representing different mechanisms of deposition, the Comstock Formation (CF) and the Zig Zag Hill Formation (ZZHF). The CF is further divided based on changes in provenance characteristics into the Lynchford Member (LM) and the Mt Julia Member (MJM). Of special interest are the many and varied units within the CF, which include the major quartz-rich and quartz-poor, crystal-rich volcaniclastic rocks of the MJM and the LM respectively. Less voluminously important units include fossiliferous limestones, welded ignimbrites [White & McPhie, 1997] and a minor mafic

unit, here referred to as the Howards Basalt. The ZZHF is dominated by redeposited volcaniclastic units, with mixed Cambrian-Precambrian basement source, and increasing basement input to the top of the sequence [White & McPhie, 1996].

The TG unconformably overlies a Cambrian granite near Mt Darwin that intrudes earlier MRV units [White & McPhie, 1997]. This relationship shows that the TG is of younger Cambrian age than much of the MRV. $^{206}Pb/^{238}U$ dates obtained from magmatic zircons in the Comstock tuff of the upper TG, by Perkins & Walshe [1993], yield ages of 494.4 ± 3.8 Ma. Fossils recovered from limestone units at Mt Lyell (within TG) by Jago *et al.* [1972], and from the base of the Owen Conglomerate by Corbett [cited in Corbett & Lees, 1987, p50], are of late Mid and mid Late Cambrian age. Therefore, the age of the TG is approximately Mid-Late Cambrian (~500 Ma).

The TG and correlates are spread throughout the central MRV (Map 1), but are restricted to the eastern side of the Henty Fault (Map 1). Numerous similar units have been correlated with the TG, but most associations have been invalidated by further work. The Cambrian CVC is, in general, conformably overlain by the TG. The TG in turn is unconformably overlain by the Ordovician Newton Creek Sandstone (NCS) and OC of the Denison Group.

Chapter 3: Local Geology

3.1 Introduction

The CVC conformably and unconformably underlies the TG, and consists of predominantly intermediate to felsic lavas and intrusions, and associated volcaniclastic rocks, with minor amounts of mafic material. The depositional environment of the CVC is thought to have been subaqueous, and below storm wave base [Corbett, 1992]. Sources for volcaniclastic sediments are thought to have been from submarine lavas and domes.

The TG is the youngest unit within the MRV, and almost exclusively comprises volcaniclastic sedimentary rocks, with minor lavas and non-volcanic sedimentary rocks. From fossil assemblages and facies associations it is interpreted to have been predominantly deposited in a subaqueous, below storm wave base, shelf setting [White & McPhie, 1996], with locally important shallow marine carbonate deposition [Jago *et al.*, 1972]. Volcanic debris is thought to have been sourced from both subaerial and subaqueous centres, and is represented in the TG as primary and reworked deposits [White & McPhie, 1996].

Within the area of the South Henty EL 8/96, between the South Henty and Great Lyell Faults, the basal TG includes a minor mafic unit known as the HB. This unit marks the transition from the commonly felsic coherent lavas, intrusive units and volcaniclastic rocks of the CVC, to the intermediate and felsic crystal-rich volcaniclastic units that dominate the TG.

3.2 Stratigraphy, Facies, and Structure Between the South Henty Fault and the Great Lyell Fault

The HB occurs in the slice of MRV occurring between the steep, west-dipping reverse South Henty and Great Lyell Faults. The local sequence consists of three major units: the Cambrian CVC, the Cambrian TG and the Ordovician Owen Conglomerate (OC). The Cambrian units have been interpreted as shallow to deep marine deposits [Corbett, 1992], whereas the Ordovician units are considered to have been deposited in shallow marine to

fluvial settings [Corbett & Lees, 1987]. The sequence displays consistent younging to the east, and has been recognised as the western limb of a syncline, which has been faulted over the eastern limb by movement on the Great Lyell Fault [Halley & Roberts, 1997].

The stratigraphy of the study area was summarised by Herrmann & MacDonald [1996] (Figure 3.1) and, to a lesser extent, Halley & Roberts [1997].

3.2.1 Central Volcanic Complex (CVC)

The Footwall Pumice Breccia (FPB) is the lowest stratigraphic unit in the South Henty area. It is dominated by massive, pink or green, feldspar-phyric, sericitic pumice breccias [Herrmann & MacDonald, 1996]; they are rhyolitic and have affinities to Suite I of Crawford *et al.* [1992]. The FPB was interpreted by Herrmann & MacDonald [1996] as subaqueous mass-flow deposits, from large, felsic explosive eruptions. Allen [cited by Herrmann & MacDonald, 1996, p7] suggested that the FPB could represent a southern correlate of the lithologically similar footwall pumice breccia of the Rosebery-Hercules sequence.

The unit overlying the FPB is the Spillway Basalt Breccia (SBB), which ranges from monomictic breccia to sandstone, and within the upper part of the unit intersected in northern drill holes, there are mafic polymictic breccias. The breccias consist of framework supported lensoidal, amygdaloidal, chloritic basalt clasts in a fine-grained matrix [Herrmann & MacDonald, 1996]. Allen [1994] interpreted the unit to be the result of subaqueous fire fountaining, due to the nature of the deposit, and the Spillway section to be a proximal to medial facies.

The SBB is conformably overlain by the Spillway Polymictic Breccia (SPB), known for its polymetallic, massive sulfide clasts. It predominantly comprises clasts of dacite, with lesser basalt and felsic lava clasts [Herrmann & MacDonald, 1996]. The SPB was interpreted by Allen [cited in Herrmann & MacDonald, 1996, p9] to be deposited by mass flows resultant from a partly emergent dacitic cryptodome, and seafloor volcaniclastic debris.

The Newton Creek Dacites (NCD) are near aphyric to feldspar phyric, coherent intrusions, hyaloclastite breccias and minor volcaniclastic rocks [Herrmann & MacDonald, 1996]. They are partially intercalated with the SPB, and chemically belong to MRV Suite I of Crawford *et al.* [1992].

The Anthony Road Andesites (ARA) comprise volcanic and volcaniclastic rocks of basaltic to dacitic composition [Herrmann & MacDonald, 1996], and immediately underlie (in places) the HB of the TG (Map 2). The units that make up the ARA range from intrusions to volcaniclastic rocks, and are intercalated with carbonates in the upper sequence. Herrmann & MacDonald [1996] interpreted the ARA to represent a submarine strato-volcano in which the coherent facies represent feeder stocks and sills, volcaniclastic rocks represent mass-flow reworking of the volcano, and the associated carbonates have formed around the shallow-water shoulders of the volcano. The NCD are thought to have continued erupting contemporaneously with the ARA, due to the occurrence of NCD (in southern holes) in the same stratigraphic position as the ARA (in northern holes) [Herrmann & MacDonald, 1996].

3.2.2 Tyndall Group (TG)

The TG comprises two formations, the Zig Zag Hill (ZZHF) and the Comstock [White & McPhie, 1996]. The CF is further divided into the Mt Julia (MJM) and Lynchford Members (LM). Volcaniclastic facies are well represented in both formations, but vary in that the CF was deposited by syn-eruptive processes, involving water-supported mass-flow resedimentation of pyroclastic deposits. The ZZHF, on the other hand, represents post-eruptive deposition, and includes variably reworked volcanic and Precambrian debris. The HB occurs at the base of the CF, interlayered with volcaniclastic units, dacitic and rhyolitic intrusions and breccias, as well as carbonates. The close relation between the basalt and carbonates within the dominantly volcanic succession may indicate a relatively shallow subaqueous environment for eruption of the basalt.

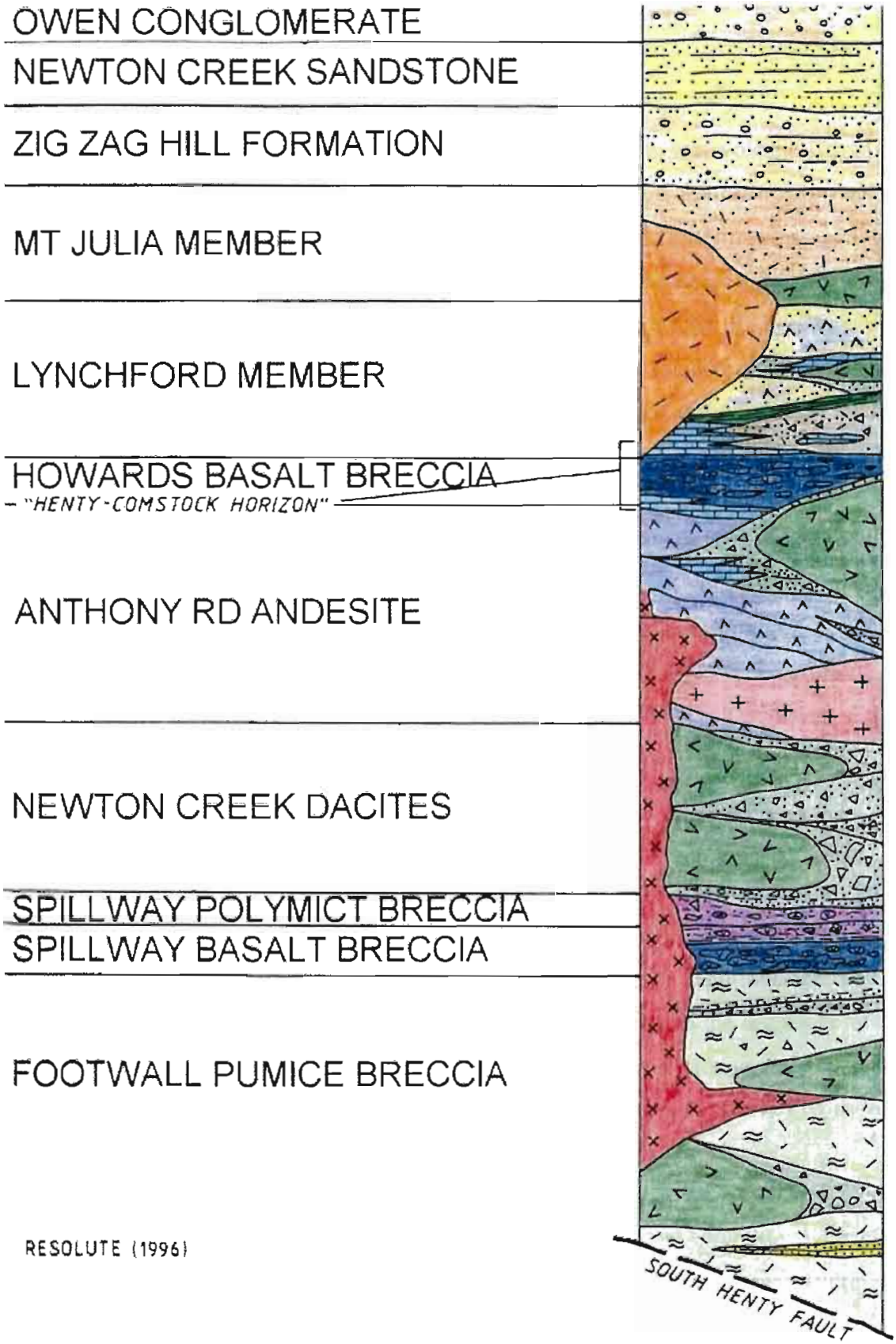

Figure 3.1 Stratigraphic column displaying main units within the slice of Mount Read Volcanics between the South Henty Fault and Great Lyell Fault (Map 2) [modified after Herrmann & MacDonald, 1996].

Comstock Formation (CF)

The CF comprises primary volcaniclastic units, with minor coherent volcanic (rhyolite, dacite, basalt) and sedimentary units. The volcaniclastic rocks of this formation are the result of pyroclastic flows from subaerial volcanic centres entering the sea and transforming into water-supported mass-flows. Sorting during transport generated vitric-ash-poor, crystal-enriched mass-flows to be deposited below wave base. Rapid deposition, plus tectonically induced uplift, resulted in local shallowing and welded ignimbrites were locally deposited in a subaqueous environment, as is evident in the CF [Zig Zag Hill ignimbrite, White & McPhie, 1997].

The LM comprises quartz-poor, feldspar crystal-rich volcaniclastic sandstones and breccias of andesitic to dacitic composition, with minor carbonate and non-volcanic sedimentary units [White & McPhie, 1996]. It is the lowest stratigraphic unit in the CF, and overlies the YRS at Lynchford [Corbett, 1979 cited in Poltock, 1992; Dower, 1991]. The nature of the contact between the two units, however, is complex [Dower, 1991]. The Ewart Creek Track volcaniclastic rocks of Poltock [1992] are assigned as TG correlates, and overlie the YRS in that area.

The HB is part of the LM of the CF (Map 2), occurring at the base, and shows some interfingering with other lower LM units. It is noted that the TG is both conformable and unconformable with the underlying CVC in the area of the Henty Fault Wedge, and in places interfingers with it. This shows that the HB is co-eruptive with the last stage of the ARA, and the early stages of extra-basinal intermediate to felsic, explosive eruptions that generated the LM. Herrmann & MacDonald [1996] described textures in the HB as very similar to the SBB, and suggested it may have had a similar eruptive origin.

The MJM is compositionally different from the LM. Dacitic to rhyolitic volcanism followed the earlier intermediate to felsic volcanism of the Lynchford source, resulting in higher quartz content of quartz and feldspar crystal-rich volcaniclastic sandstones and breccias of the MJM [White & McPhie, 1996]. The MJM consists primarily of volcaniclastic facies with lesser degrees of coherent rhyolite and associated autoclastic intervals.

Zig Zag Hill Formation (ZZHF)

The ZZHF comprises post-eruptive volcaniclastic units resulting from mass-flow redeposition of earlier volcaniclastic rocks. The ZZHF marks the end of large-volume, explosive volcanic eruptions [Herrmann & MacDonald, 1996]. It is conformably overlain by the NCS and OC, units that are predominantly derived of eroded and redeposited Precambrian basement. The sequence from ZZHF through NCS and OC shows the change in sediment source from volcanic to Precambrian basement with the uplift of basement from Late Cambrian to Ordovician. The ZZHF comprises mostly volcanic and minor siliciclastic rocks to the top [White & McPhie, 1996], and the NCS and OC solely comprise siliciclastic sedimentary rocks originating from the Tyennan Block.

The TG shows rapid changes in facies near to the Henty Fault, and the fault is therefore thought to have been active during the deposition of the succession [Halley & Roberts, 1997]. The Great Lyell Fault is also thought to have been active during deposition due to the stratigraphic change in the TG across the fault [Halley & Roberts, 1997].

3.3 Mineral Deposits and Exploration Targets in the Tyndall Group

The Henty deposit is located at the base of the TG in the footwall block of the Henty Fault [Halley & Roberts, 1997]. The Comstock and Mt Lyell deposits also occur in basal TG near the contact with the CVC [Herrmann & MacDonald, 1996]. The prospects of South Henty and Basin Lake occur in the upper CVC. The South Henty alteration style has some elements of high sulfidation epithermal systems [Street, 1999]. Street [1999] suggested that the South Henty prospect occurred within a spectrum from the copper-rich Mt Lyell end member, to the gold-rich Henty-Mt Julia end member.

The Howards Anomaly barite-silver mineralisation occurs as late stage veins in strongly haematite altered rocks, possibly of the HB. The silver is present in the rocks as freibergite, pyrargyrite and native silver [Herrmann & MacDonald, 1996].

The HB itself has, in the past, been generally thought of as an extremely chlorite - haematite ± calcite altered, sheared felsic sequence. Variously named over the years, based

upon these interpretations, it has only recently been recognised as basaltic in character, through work in lithogeochemistry [W. Herrmann pers. comm.].

Chapter 4: Textural and Lithofacies Characteristics of the Howards Basalt

4.1 Introduction

The HB is a minor mafic unit occurring within the lower part of the LM of the CF. Its most common form is as a monomictic breccia comprising commonly lensoidal clasts of amygdaloidal basalt in a fine-grained chloritic matrix. Clast size and abundance in the breccia units is variable, but clasts are on average about 15 - 25 mm; units are generally clast-supported. Intervals of the basalt are also coherent, frequently with breccia margins, and less frequently interstices. Mafic intrusions are also in evidence, though show no obvious differences from the coherent and breccia facies in hand specimen or thin section. A large majority of the HB is amygdaloidal.

On the basis of drill core information (Figure 4.1, Appendix A), the HB isn't a discrete unit and the unit's thickness varies laterally from north to south. The distribution of brecciated basalt to coherent basalt is seen, in cross section (Figure 4.2), to be dominantly due to the presence of two basalt bodies. The abundance of the breccia facies is influenced by the position within the sequence (stratigraphically, Figure 4.2; north to south, Figure 4.3). Brecciation is also partly associated with faulting within the sequence, and is probably post-depositional (Late Cambrian &/or Devonian).

The HB (refer Map 2 for DDH and C-D longitudinal projection line, Figure 4.3), in the north, has a true thickness of approximately 70 m for the upper basalt and from 100 - 140 m for the lower. Further to the south the upper unit thins to about 30 m, the lower unit is absent until DDH SHD25 (about halfway along the logged extent) where it is about 110 m thick. Further south the lower unit thins to DDH HA006, then thickens greatly to DDH NC1 (probably due to faulting). In the southern section there are two units, but both have the morphology of the lower unit in the north. Two intervals of approximately 80 m each are encountered in DDH NC1 separated by a large carbonate unit. DDH HA5 does not intersect the HB, and there is no further outcrop or intersection of the target body in any other southern DDHs.

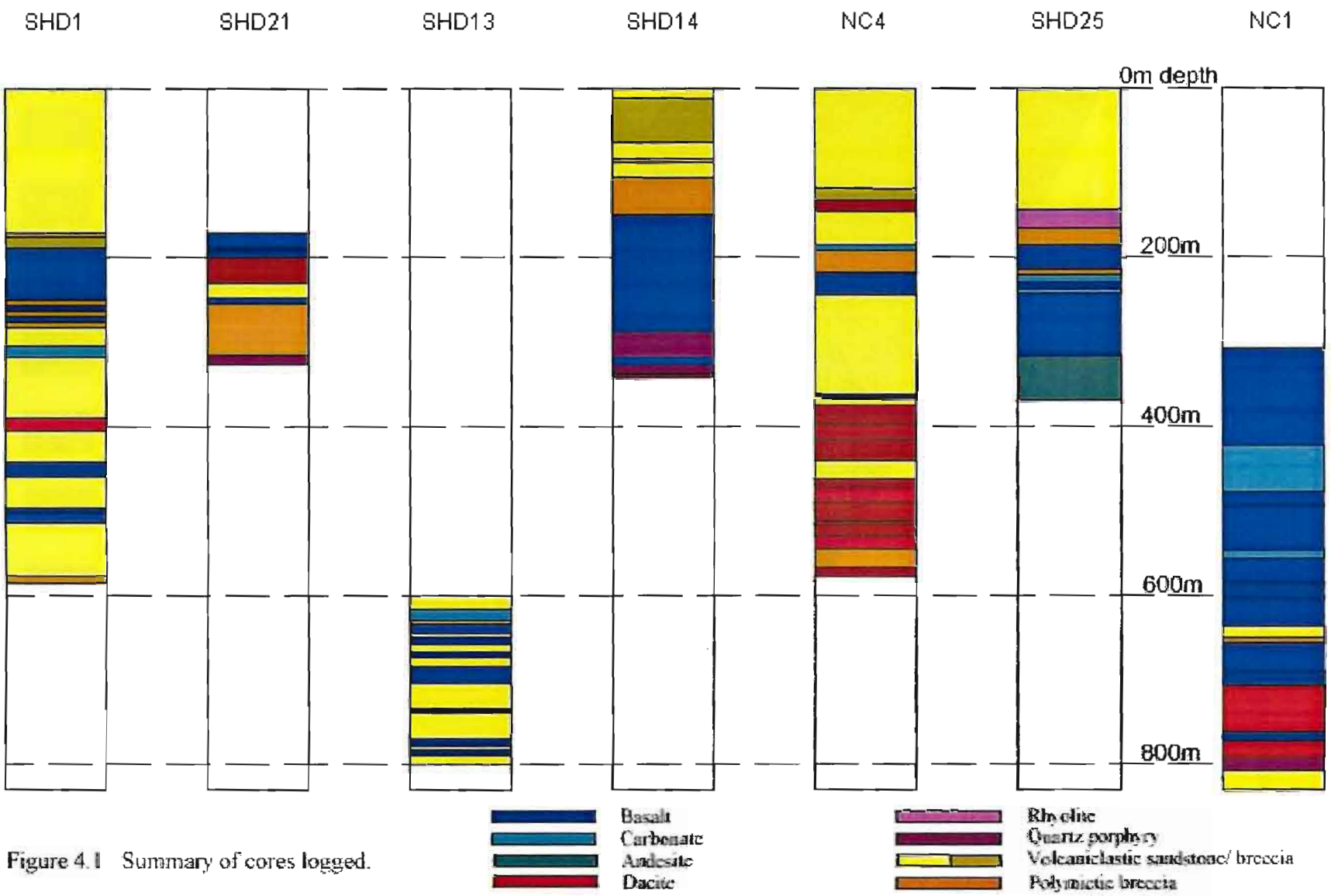

Figure 4.1 Summary of cores logged.

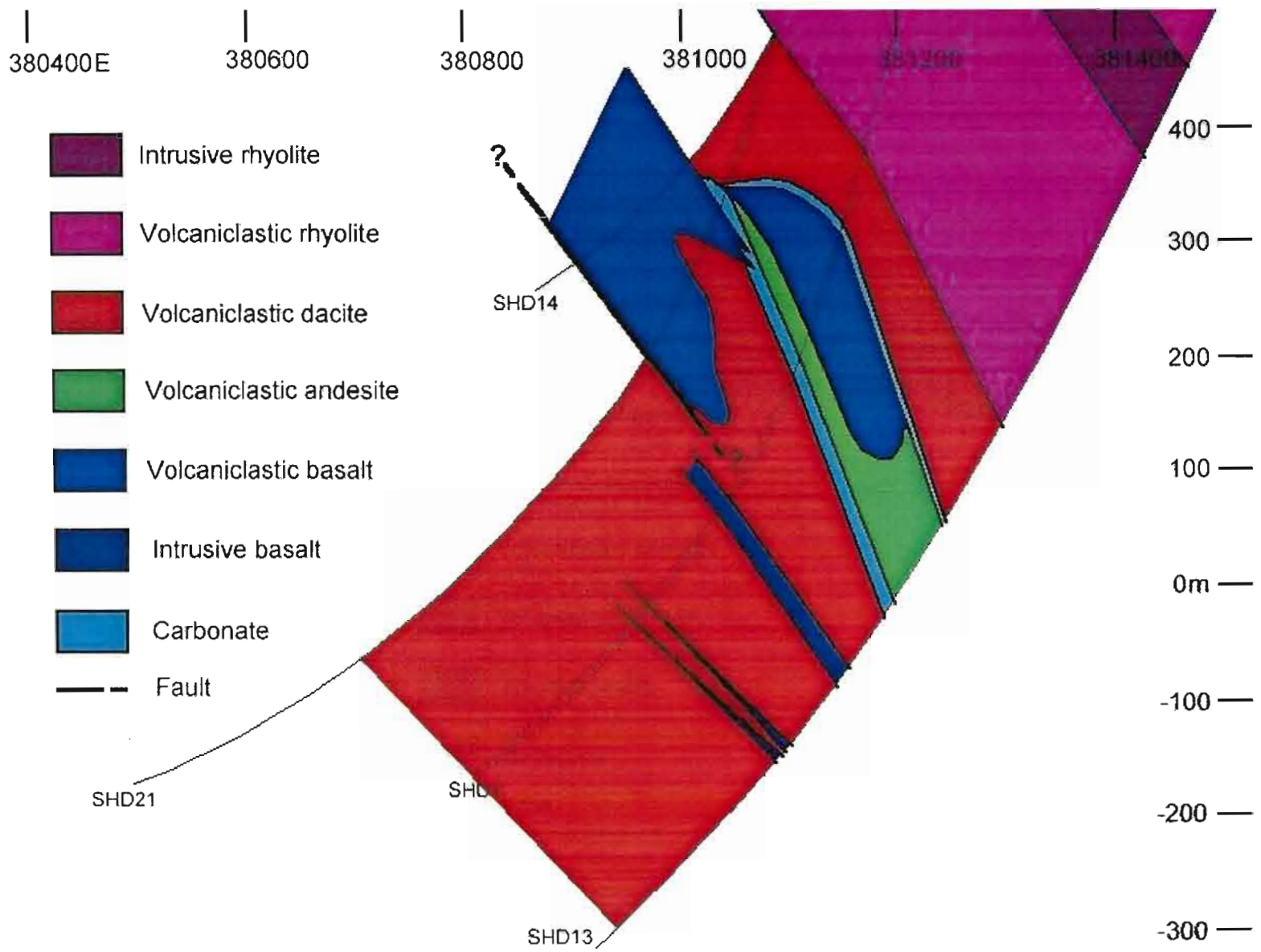

Figure 4.2 Interpretive cross-section along line A-B (Map 2), showing geometry of the basalt bodies.

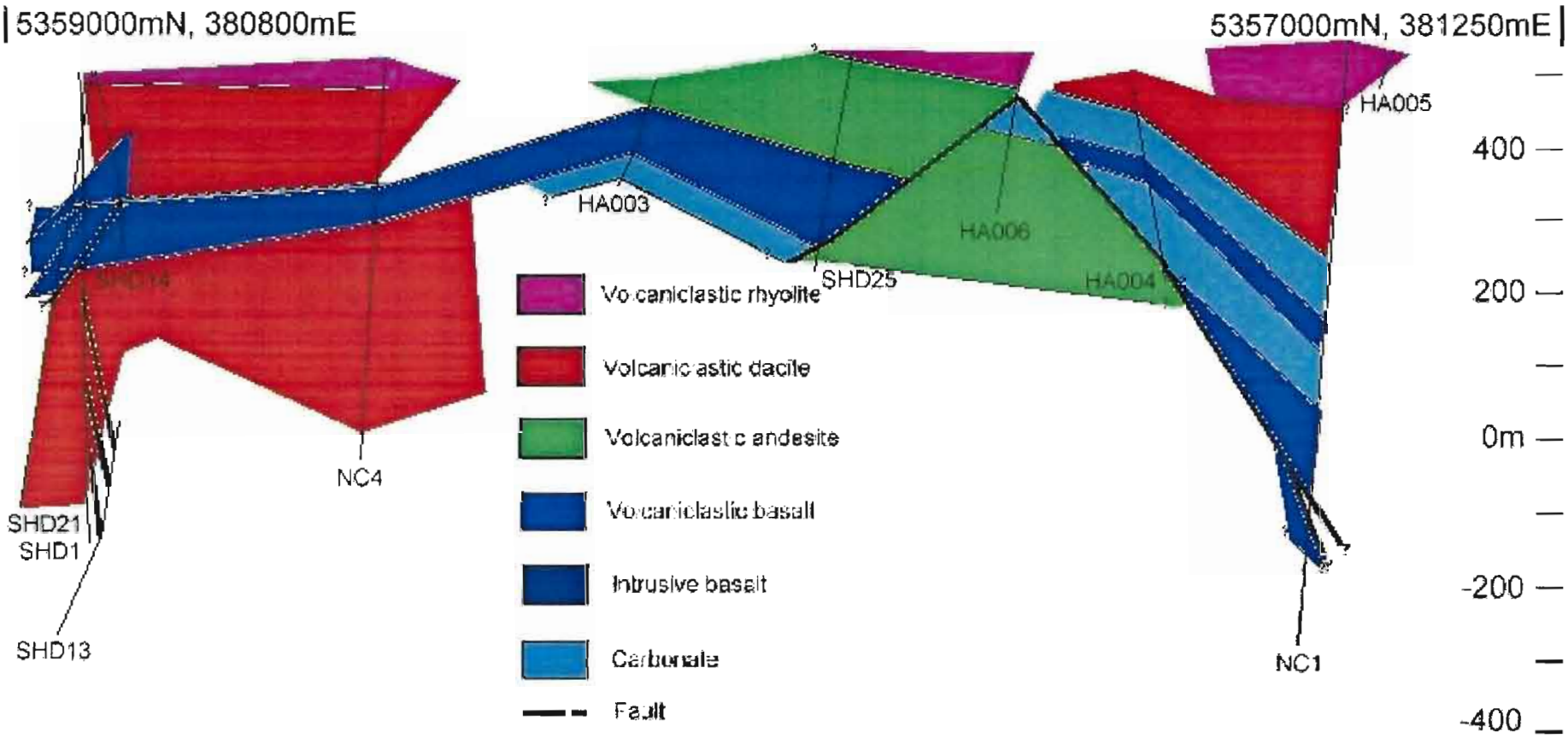

Figure 4.3 Interpretive longitudinal projection along the line C-D (Map 2), showing the geometry of the basalt.

4.2 Alteration and Deformation

There is pervasive chlorite alteration throughout most of the HB, with sections of the sequence strongly altered by sericite, haematite (Plate 4.1) and carbonate. Usually the alteration in any area of the basalt is a combination of at least two of the above, most commonly chlorite and sericite. Carbonate is frequently represented within deformational veins, and in southern cores is frequently pervasive and in higher abundance than sericite. The carbonate units that occur in close proximity to the HB are usually either a green &/or pink colour due to chlorite and haematite alteration respectively. In thin section (Plate 4.2) the carbonate appears to have been recrystallised.

Frequently the breccia texture is exaggerated by alteration in the basalt, with sericite lightening the quenched rims of clasts (Plate 4.3), or picking out fractures (Plate 4.4). Chlorite, and sometimes carbonate, replaces, to differing degrees, the fine grained matrix of the breccias.

The majority of the HB is vesicular, with the brecciated facies generally more vesicular than the coherent facies. All vesicles have been filled, and are frequently zoned concentrically, primarily by carbonate and chlorite, with lesser sericite. Some amygdales appear almost unaffected by the deformation that has compressed and sheared the HB. Closer examination of unaffected amygdales has revealed different zones of alteration in the parent clasts (Plate 4.5). A few relict basalt clasts are completely altered by carbonate, and amygdales throughout appear as if they may be unaffected by deformation (Plate 4.6).

Veins are very common in the succession, and are most frequently of carbonate, as mentioned above. Chemically the carbonate is calcite, sometimes with ankerite influence. There are also occasional ankerite veins, usually within zones of higher iron content, that are identifiable in weathered core as having red-brown coatings. Lesser veins of epidote (usually fault-related), barite (southern cores only, probably related to Tyndall Creek barite mineralised zone), pyrite (iron-rich areas - fluid focus e.g. Plate 4.7) and quartz (very rare, associated with faults and sometimes the central fill of large carbonate veins as shown in Plate 4.8).

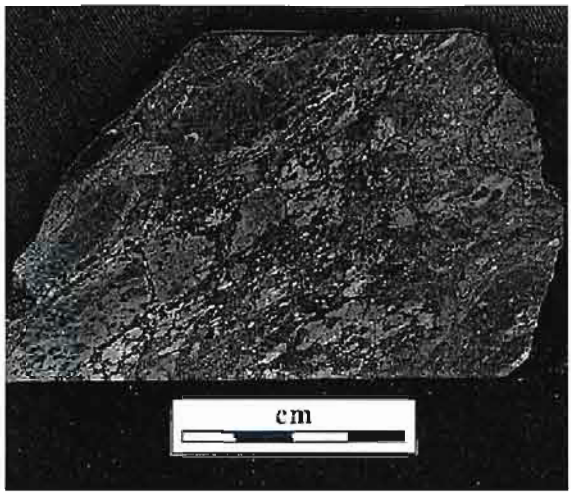

1

2

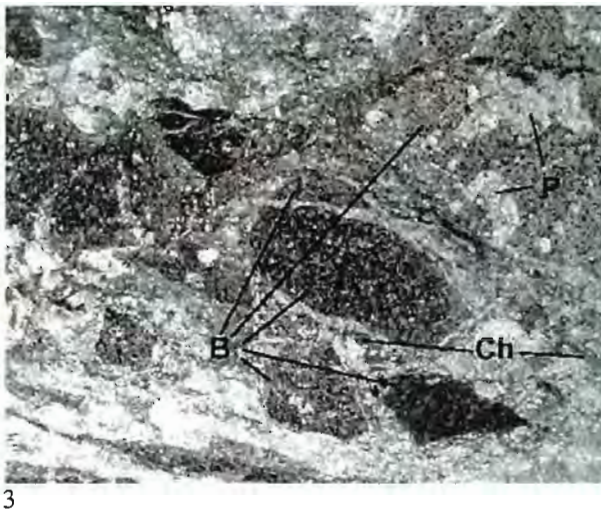

3

4

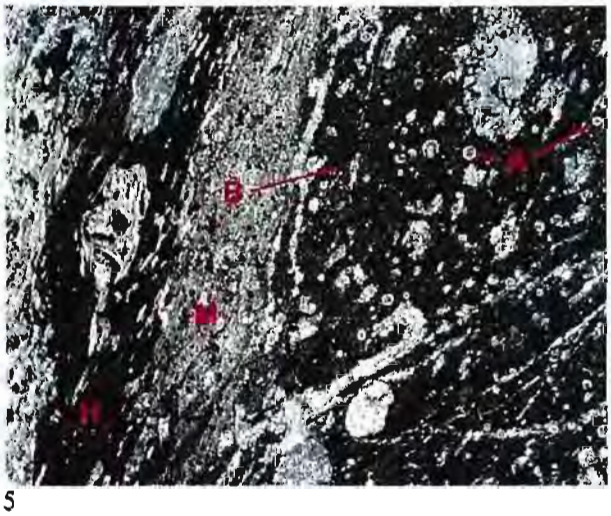

5

6

Plate 4.1 - 4.6

4.1 Monomictic breccia with strong haematite (maroon), chlorite (green) and sericite (cream) alteration to clasts and matrix [NC4_3].

4.2 Recrystallised carbonate (C- calcite, cross polarized light, field of view is 8.4 mm × 6.4 mm) [NC1_7].

4.3 Monomictic breccia with altered rims (B- basalt, Ch- chlorite, P- plagioclase, plane polarized light, field of view is 4.2 mm × 3.2 mm) [SHD13_5].

4.4 Basalt with sericite (cream) alteration along fractures [NC4_17].

4.5 Basalt clast with multiple alteration rims, and uncompressed amygdales (B- basalt inner, A- amygdales, H- haematite, M- muscovite, plane polarized light, field of view is 8.4 mm × 6.4 mm) [SHD25_4].

4.6 Carbonate altered basalt clast, with uncompressed concentrically zoned amygdales (C- calcite, A- amygdales, plane polarized light, field of view is 1.05 mm × 0.8 mm) [NC1_7].

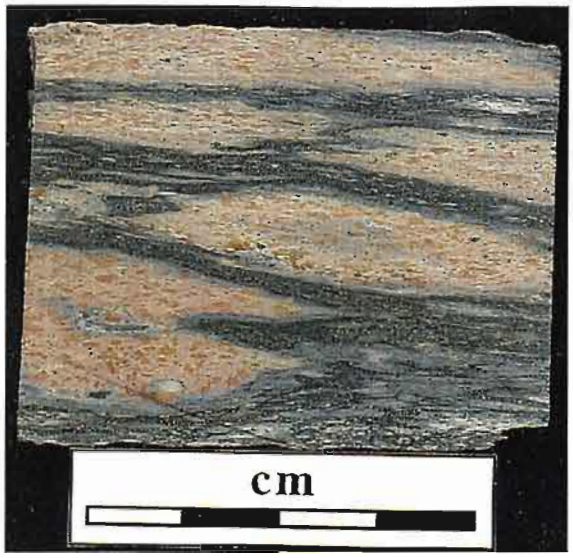

7

8

9

10

11

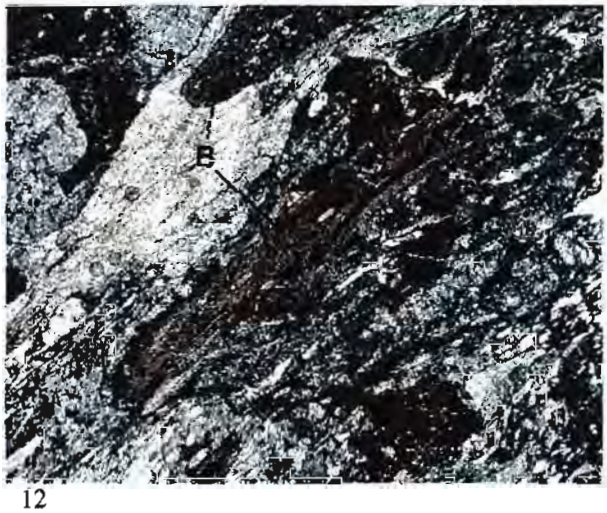

12

Plate 4.7 - 4.12

4.7 Monomictic breccia altered by sericite (pink) and pyrite (grey), darker pink spots are relict plagioclase glomerocrysts [NC1_13].

4.8 Carbonate vein with quartz central fill (C- carbonate, Q- quartz, cross polarized light, field of view is 8.4 mm × 6.4 mm) [NC1_9].

4.9 Shistose texture in volcaniclastic sandstone (?) (M- muscovite, P?- plagioclase (?), cross polarized light, field of view is 8.4 mm × 6.4 mm) [NC4_18].

4.10 Chlorite (dark green) and sericite (light cream) altered lensoidal monomictic breccia [NC4_1].

4.11 Chlorite (green) and sericite (cream) altered monomictic breccia (large basalt clast in upper right) [SHD14_2].

4.12 Haematite (red-brown) and chlorite (dark green) altered basalt clasts (B- basalt, plane polarized light, field of view 8.4 mm × 6.4 mm) [NC4_3].

Due to the strong phyllosilicate (chlorite and sericite) alteration through the majority of the HB, deformation has resulted in the development of strong cleavage in places (Plate 4.9). The strain has also imparted the HB with its characteristic appearance (Plates 4.10, 4.11 & 4.12).

4.3 Facies Descriptions

There are five main volcanic and volcaniclastic facies that make up the HB. The facies are: type 1 and 2 monomictic breccias, polymictic breccias, coherent units and volcaniclastic sandstones. In this study rocks that contain greater than 50% sand-size (2 mm) particles are classified as sandstones, and those containing greater than 50% >2 mm clasts as breccias.

4.3.1 Type 1 Monomictic Breccia Facies

Type one monomictic breccias are clast-supported, in a fine-grained, dark, chloritic or haematitic matrix. Clasts are generally lensoidal, moderately vesicular and compacted (Plates 4.10 & 4.11). Clast sizes are on average 15-20 mm, but may vary from 5 mm up to about 50 mm.

4.3.2 Type 2 Monomictic Breccia Facies

Type two monomictic breccias are plagioclase glomeroporphyritic, clast-supported, in a fine- to medium-grained chloritic matrix. Clasts are angular to subangular, non vesicular to poorly vesicular and frequently display jig-saw fit textures. The average clast size is about 45 mm, but can range from 3 mm to 65 mm.

4.3.3 Polymictic Breccia Facies

Polymictic breccias are clast- to matrix-supported, in a medium-grained chloritic matrix (Plate 4.13). Clasts within these breccias range from basalt, dacite and rhyolite to carbonate. The clasts within the breccias can be mafic dominated, or they may be more

13

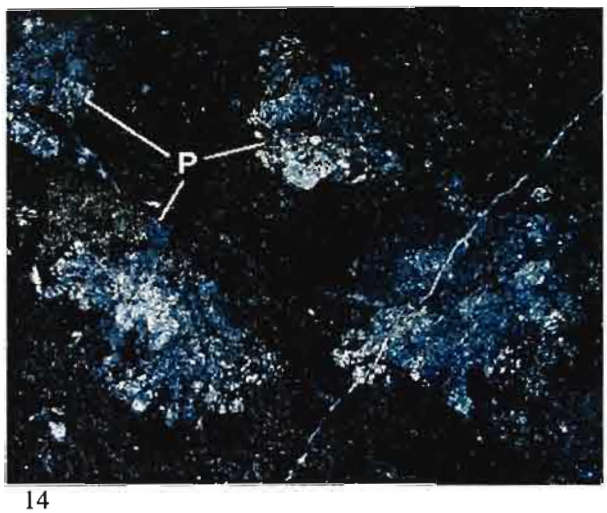

14

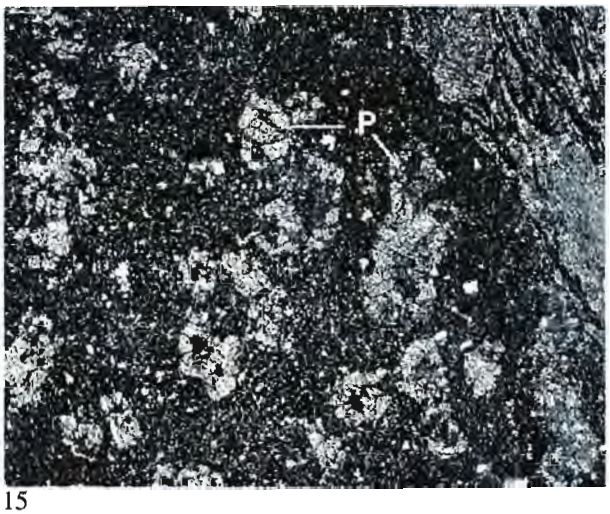

15

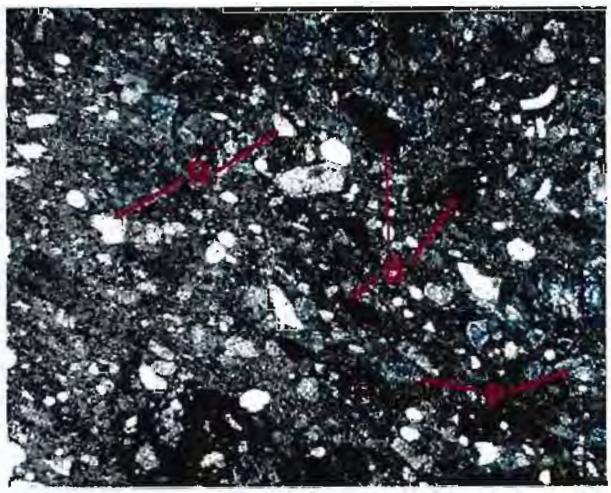

16

Plate 4.13 - 4.16

4.13 Polymictic breccia with basalt (dark green) and rhyolite/dacite (pink) clasts [NC4_14].

4.14 Coherent basalt with plagioclase glomerocrysts (P- plagioclase, cross polarized light, field of view is 8.4 mm × 6.4 mm) [SHD1_1].

4.15 Coherent basalt with altered plagioclase glomerocrysts (P- plagioclase, plane polarized light, field of view is 8.4 mm × 6.4 mm) [NC1_16].

4.16 Volcaniclastic sandstone with abundant quartz, plagioclase and basalt fragments (Q- quartz, P- plagioclase, B- basalt, plane polarized light, filed of view is 8.6 mm × 6.4 mm) [SHD1_3].

felsic. Within the HB sequence the polymictic breccias are generally more mafic in character than those over- and under-lying it. Clasts are usually angular to sub-angular, with lesser clasts being sub-rounded to rounded. Size of clasts varies from sand up to about 60 mm, but are on average about 25 mm.

4.3.4 Coherent Basalt Facies

The coherent basalts are generally green to blue-green, non-vesicular to poorly vesicular, and plagioclase glomeroporphyritic (Plates 4.14 & 4.15) within a fine-grained chloritic to sericitic groundmass. This facies also represents the intrusive basalts occurring within the HB.

4.3.5 Volcaniclastic Sandstone Facies

The volcaniclastic sandstones display a range of compositions from basaltic to dacitic (Plate 4.16). This facies is very similar to the polymictic breccias, with clast size being the only difference.

4.4 Internal Stratigraphy and Relation to Associated Units

The HB consists of an upper and a lower unit. These two units are separated by a carbonate unit (Figure 4.2). The upper unit throughout the logged extent, and both units in the south, are represented by the coherent and type two monomictic breccias (Figure 4.3). The plagioclase glomeroporphyritic nature of both the coherent and type two monomictic breccia facies, distinguishes them from the type one monomictic breccia facies. The lower unit in the north is represented by type one monomictic breccias. The polymictic breccias and volcaniclastic sandstones occur above the upper basalt along the complete extent, but is in greater abundance in the northern section. They are also present in lesser amounts between the monomictic breccia units.

The carbonate units, which locally bear shallow marine trilobite fossils, are closely associated to the HB, and interfinger with the breccia units in places. In the DDHs SHD25

and NC1 the relationship between the carbonate and the HB is very close with the occurrence of many carbonate units, both major and minor, and common occurrences where the two units are interfingering.

Summary logs (Figure 4.1) give an overall impression of change in facies along strike and down dip. For greater detail see graphic logs (Appendix A).

4.5 Interpretation

From work on core logs (Figure 4.1), cross-sections (Figure 4.2 & 4.3), rock characteristics in hand and thin section and geochemistry, the following theory has been developed on the nature of the basalt, its eruption and emplacement styles.

An early basalt was erupted in a fountaining manner due to high discharge rate and low hydrostatic pressure to form a scoria cone/ breccia pile [Cas & Wright, 1987]. This basalt formed a discrete basalt breccia lens (type one monomictic breccia – proximal to vent), which displays interfingering relationships with some of the surrounding units. Later effusive eruption of basalt occurred at a lower discharge rate producing two lavas (coherent facies, north – proximal to medial from vent, south – medial to distal from vent). Only one of these lava units is present in the northern section. Both are present in the southern cores, however, separated by a large carbonate unit. The basalt units in the south are much thicker than in the north, and are thought to have accumulated in a basinal structure, possibly the result of growth faulting.

Although the majority of the HB has been interpreted, by the author, to represent a lava (coherent facies), a great deal of it has been brecciated (type two monomictic breccia facies), either primarily during flowage, or through secondary events such as faulting. The brecciation of the interpreted lavas (type two monomictic breccia – medial to distal from vent) was generally restricted to the more southern parts of the HB. This coincides with a fault that passes through the basalt for almost two kilometres lateral extent, from the southern termination of the basalt against the same fault. This fault, though showing little or no displacement in the northern section, superimposes the HB over the ARA in the south. This fault may have been instrumental in the degree of shearing that has occurred in

the HB, but by the way that it affects the basalt is interpreted to have been absent, or inactive, at the time of deposition. Another possible reason for the degree of brecciation of the lavas in the southern section is by quenching and brecciation through slumping. As the HB is thought to be subaqueously erupted, contact between the seawater and hot lavas would cause some degree of quench fragmentation. Schmincke & von Rad [cited in Cas, 1992, p523] noted that non-explosive fragmentation of lava would produce hyaloclastites that may be resedimented great distances from the eruptive vent. As the lavas moved out down the flanks of the basaltic pile they may have become more brecciated as further cooling occurred, and they became more susceptible to brittle fragmentation.

The strong association between the HB and carbonate units, especially in DDHs SHD25 and NC1, may mean that there was continued growth of a carbonate shelf with fluxes of basaltic volcanic debris entering the system and disrupting growth. The presence of carbonate clasts in some of the breccias probably indicates that transport and deposition of the basalt was due to mass flows or slumping, or at least emplacement methods violent enough to scrape carbonate material off the shelf.

The polymictic breccias may be formed by primary mixing of several different source volcanics and sediments that were deposited simultaneously, or they may be the result of reworking. The latter is favoured as the facies is most abundant in the northern section and lies upon the interpreted breccia pile and closely associated lavas (proximal to vent). The presence of polymictic breccias in this location may be due to reworking of basalt from the pile, as well as carbonates and local felsic volcaniclastic units in the area. Reworking is most likely due to currents in an above storm wave base environment. The near absence of a similar facies in the southern section supports this theory, as it is thought to be a basinal environment resulting in the pooling of lavas and associated volcaniclastic units, as well as the deposition of large carbonate units.

The volcaniclastic sandstones are present throughout the studied area, and are thought to be a further progression, through reworking, of the polymictic breccias. This is due to the similarity of the two facies, both compositionally and stratigraphically. Some of the volcaniclastic sandstones are thought to be representative of the underlying dacitic volcaniclastic rocks (Figure 4.2).

A possible explanation for the difference in shape of amygdales in altered basalt clasts is that there was more than one phase of alteration, perhaps one before and then one after the deformation event. Another idea is that one alteration assemblage may be more susceptible to compression and deformational events than another.

Chapter 5: Petrography and Geochemistry of the Howards Basalt

5.1 Introduction

Petrographic analysis was carried out on thin-sections representing the five facies of the HB: monomictic breccias, coherent basalt, polymictic breccias and volcaniclastic sandstones. Some samples were also taken from surrounding units including carbonates. Seven samples from the logged cores were analysed by XRF for major elements and some trace elements (Appendix B-1), and by Carlo-Erba (Appendix B-2) for the volatiles C, H and S. In addition PIMA (Appendix B-3) and petrographic analyses were used to aid in determination of the alteration mineralogy in the HB.

In addition the major and trace element analytical data of Gibson [1991], Herrmann & MacDonald [1996], Aberfoyle and Goldfields Exploration, were used for support and comparison on some geochemical plots.

5.2 Petrographic Analyses

Petrographic analyses of samples, thin-sectioned by the author, were carried out to determine textural differences between facies in and around the HB, and the different alteration mineralogies. The textural differences have been described in Chapter 4. Mineralogically the sections analysed are quite simple, comprising of generally only a few minerals. Most of these minerals are due to alteration, namely chlorite, sericite (muscovite), carbonate and haematite, with lesser opaque phases and quartz. Plagioclase survives in samples to varying degrees, with some almost pristine, and others completely altered (Plate 4.7).

The most common mineral assemblage in the altered rocks of the HB is chlorite + sericite + carbonate ± plagioclase ± opaque phase. Some sections are more enriched in haematite, with occasional precipitation of metallic haematite.

Plagioclase is the most common, and usually sole, phenocryst phase. The phenocrysts occur primarily as large glomerocrysts (up to about 5 mm diameter, Plates 4.14 & 4.15), and occasionally as subhedral to euhedral crystals. In a few samples there are relict pyroxene phenocrysts, which are typically embayed and altered to carbonate.

Plagioclase is also present as fine grained, euhedral to subhedral, laths (sometimes altered) within the groundmass of some of the fine-grained monomictic breccias. In most samples, however, the mineralogy of the groundmass is either dominated by chlorite and sericite (muscovite), or is very difficult to ascertain. This difficulty is due to "dirtiness", which may be devitrified glass, or due to iron staining.

Relict glass was recognised in only three thin-sections, two of which are from the polymictic breccia facies. The other sample occurs at depth in the core, and is dissimilar, geochemically, from most other samples. This sample will be discussed further in subsequent subchapters. The relict glass samples display perlitic fracturing within clasts of about 2 - 3 mm diameter. The samples are now composed of: haematite + carbonate, carbonate, chlorite + sericite (muscovite).

A quartz porphyry similar to those mentioned by Poltock [1992] exists in several of the drill cores logged, directly underlying the HB, and may represent the YRS in the South Henty region, or alternatively may belong to a similar unit within the compositionally diverse ARA of Herrmann & MacDonald [1996]. Crawford *et al.* [1992] also describes some of the ARA (MRV Suite II) with partly resorbed quartz phenocrysts or xenocrysts. Whether the quartz porphyry mentioned belongs to the YRS or the ARA, the contact between it and the TG is difficult to ascertain, with the locally intense shearing further obscuring the relationship. Suspected basalt clasts, however, are seen in the porphyry in proximity to the contact between the units and may therefore represent either a sheared contact relationship, or may indicate that the 'porphyry' is in fact a volcano-sedimentary unit.

5.3 XRF Analyses

Geochemical analysis was conducted on seven core samples each of about 10cm length of halved diamond drill core or equivalent. Preparation (by the author) involved crushing of the samples in a hydraulic crusher, followed by milling with the tungsten carbide ring mill. Further preparation of the powdered samples was conducted by Katie McGoldrick for XRF analysis for the major elements (SiO_2, TiO_2, Al_2O_3, Fe_2O_3, MnO, MgO, CaO, Na_2O, K_2O, P_2O_5) using fused glass discs. Powder pellets were prepared for analysing the selected immobile trace elements (Y, Zr, Nb, La, Ce, Nd). The XRF analyses were conducted at the School of Earth Sciences, University of Tasmania, by Phil Robinson. The analyses are tabulated in Appendix B-1.

Analyses of the samples revealed that silica is an extremely mobile component in the system, together with iron, magnesium and the alkali elements. The most reliable elements analysed were titanium, phosphorous, zirconium, yttrium and niobium. These elements were the components upon which classification of the HB was predominately based.

5.4 Carlo-Erba Analyses

Carbon, hydrogen and sulfur (XRF is more accurate) were analysed, using the Carlo-Erba elemental analyser, by Dr Graham Rowbottom at the Central Science Laboratory, University of Tasmania, using the sample powders prepared by the author as mentioned above. This data was then used to recalculate the contribution of volatile components to the geochemistry of the samples. Recalculation was based on the assumption that carbon occurred as carbonate, and hydrogen as water in hydrous minerals (e.g. chlorite), (refer Appendix B-2).

Results from these analyses showed that there is considerable carbon and lesser hydrogen. When the figures were recalculated to read as weight percent CO_2 and H_2O, expressing carbonate and hydrous minerals, values ranged from 0.33 - 8.57% CO_2 and 3.O4 - 7.95% H_2O.

5.5 Short Wave Infra Red Spectral Analyses

Short wave infra red spectral analysis (PIMA) was conducted on numerous hand samples to aid in determination of alteration mineralogy. Only carbonate and sericite rich samples were reflective enough for reliable spectral identification. Carbonates analysed were predominantly in vein form. Sericitic samples with only minor chlorite, were used for white mica determinations. A wavelength spectrum stack of samples analysed, and a list of samples and results, is included as Appendix B-3.

Analyses determined the main carbonate mineral was calcite, with occasional ankerite-influenced calcite and ankerite veins. The white mica was found to be muscovite, with some samples gaining influence from Mg-chlorite.

5.6 Geochemical Plots – Discrimination and Comparison to other Mount Read Volcanic Successions

Geochemical discrimination diagrams were used to determine the affinities and tectonic origin of the HB, and its relation to other mafic successions within the MRV. The trace elements analysed for are considered to be relatively immobile in hydrothermally altered [Herrmann, 1998], and metamorphosed systems [MacLean & Barrett, 1993]. The first of the plots implemented is TiO_2 Vs Zr to test the immobility of these components [MacLean & Barrett, 1993], and their usefulness as geochemical discriminants (Figures 5.1 & 5.2). Figure 5.1 shows only the seven samples of the author's dataset, Figure 5.2 includes data from Gibson [1991], Herrmann & MacDonald [1996], Aberfoyle and Goldfields Exploration (gives more concise regression line). Plots shows a clear linear regression trend, for the HB samples, with correlation factor of $r \sim 0.9$, that passes close to the origin. The spread of samples to the origin end indicate dilution of TiO_2 and Zr, probably due to alteration mass gains.

A second regression line, with correlation factor of $r > 0.9$ passing close to the origin, contains two samples (SHD1_14 & SHD21_6) taken from the logged core. These two samples fall on the line with samples from Gibson [1991] of the ARA (Suite II).

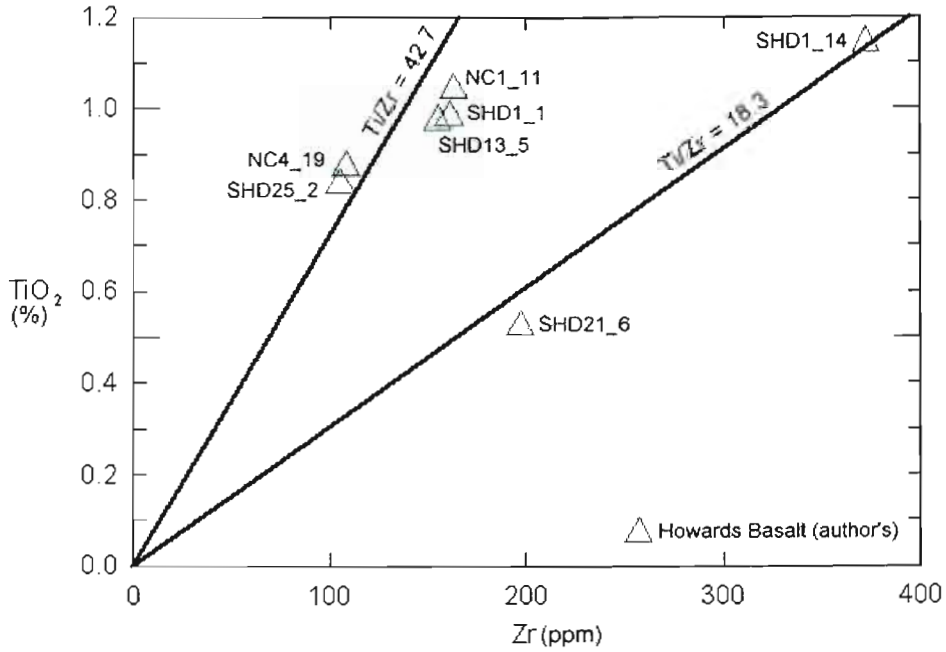

Figure 5.1 Plot of TiO_2 Vs Zr, to determine immobility of components (author's dataset only).

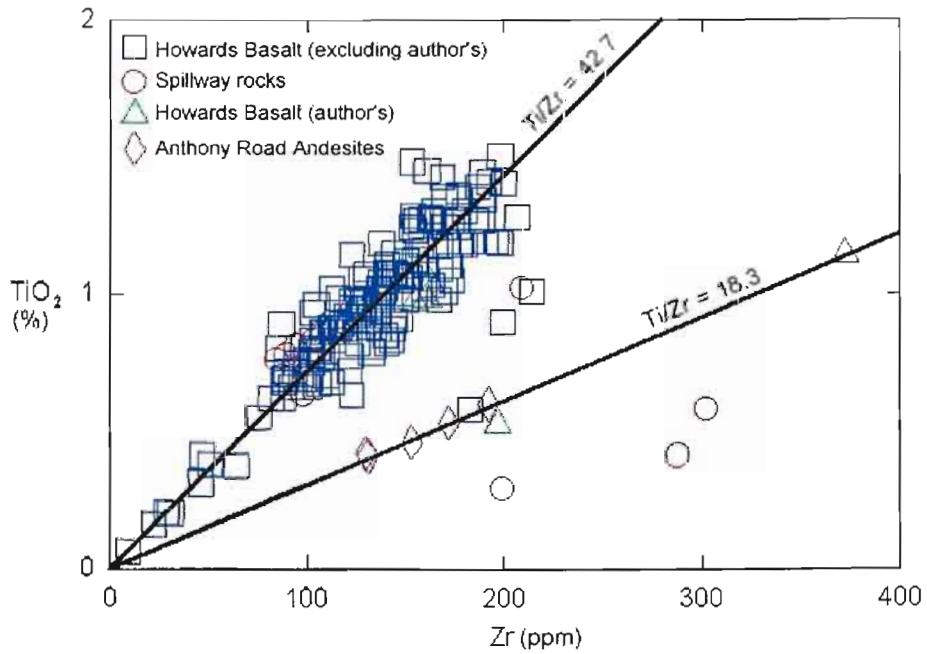

Figure 5.2 Plot of TiO_2 Vs Zr, to determine immobility of components (multiple data sources, see text).

Another important plot used in differentiation and correlation was P_2O_5/TiO_2 Vs SiO_2. Comparison of this plot (Figure 5.3) and the MRV Suites of Crawford *et al.* [1992], shows that the HB data falls in the Suite III field. Suite III includes the Que-Hellyer Volcanics, Lynch Creek Basalt and Howards Plains Basalt [Crawford *et al.*, 1992], and displays a spectrum of volcanics from medium K calc-alkaline to shoshonitic. Of the dacitic (Ti/Zr = 18.3) samples, SHD21_6 displays a major loss of SiO_2, while SHD1_14 falls within Suite III. Due to the loss of SiO_2, both SHD21_6 and SHD1_14 may have originated in the Suite II field.

Other plots, including Ti/Zr Vs SiO_2 (Figure 5.4) and rare earth elements (REE) (Figure 5.5), also point to a Suite III association. Ti/Zr Vs SiO_2 distinguishes the calc-alkaline suites (I, II & III) from the tholeiitic (V & IV). As the immobility of Ti and Zr has been confirmed (Figures 5.1 & 5.2), it can be safely assumed that the Ti/Zr ratio is the same as in the precursor volcanics [Herrmann, 1998], therefore the HB falls into the Suite III field, as well as being confirmed as having calc-alkaline affinities. The possible Suite II samples again may fall in the same field, given SiO_2 loss. The REE plot is only based on three of the light elements, but display a strong similarity to the Suite III samples of Crawford *et al.* [1992]. Suite II REE patterns for the light end are very similar to Suite III, therefore no differentiation can be made between the normal HB samples and the anomalous ones.

The tectono-magmatic Winchester & Floyd [1977] diagram, and Pearce & Cann [1973] are included (Figures 5.6 & 5.7) to determine magmatic character and tectonic regime or eruption of the HB. These show that the HB, based on immobile element geochemistry, is actually an andesite, and that it formed within a volcanic arc regime. The anomalous samples plot within the rhyodacite/dacite field, the same as Suite II rocks.

An alteration box plot [Large *et al.*, in prep.] was constructed to aid in constraint of alteration trends. It shows that there are two main trends, one to the chlorite-pyrite-sericite end, and one to the calcite-albite end (Figure 5.8).

The two basalt units, mentioned in Chapter 4, that are petrographically different, are found, from the limited geochemistry available, to be inseparable. The only geochemical

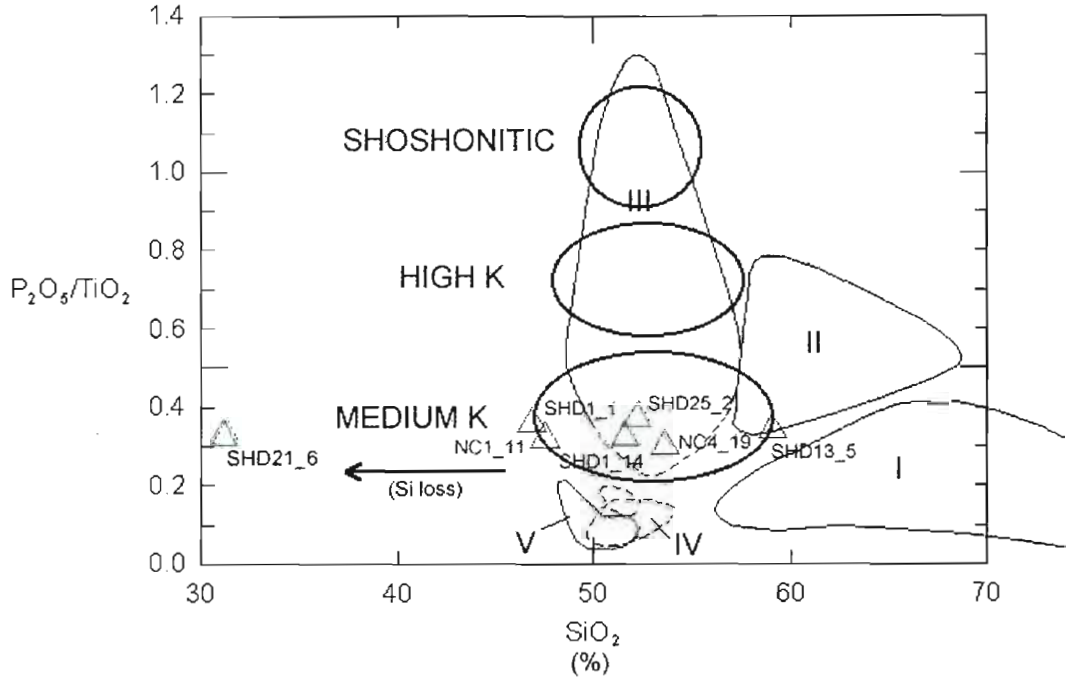

Figure 5.3 Plot of P_2O_5/TiO_2 Vs SiO_2, showing the medium K calc-alkaline to shoshonitic fields described by Crawford *et al.* [1992], and MRV Suites I - V.

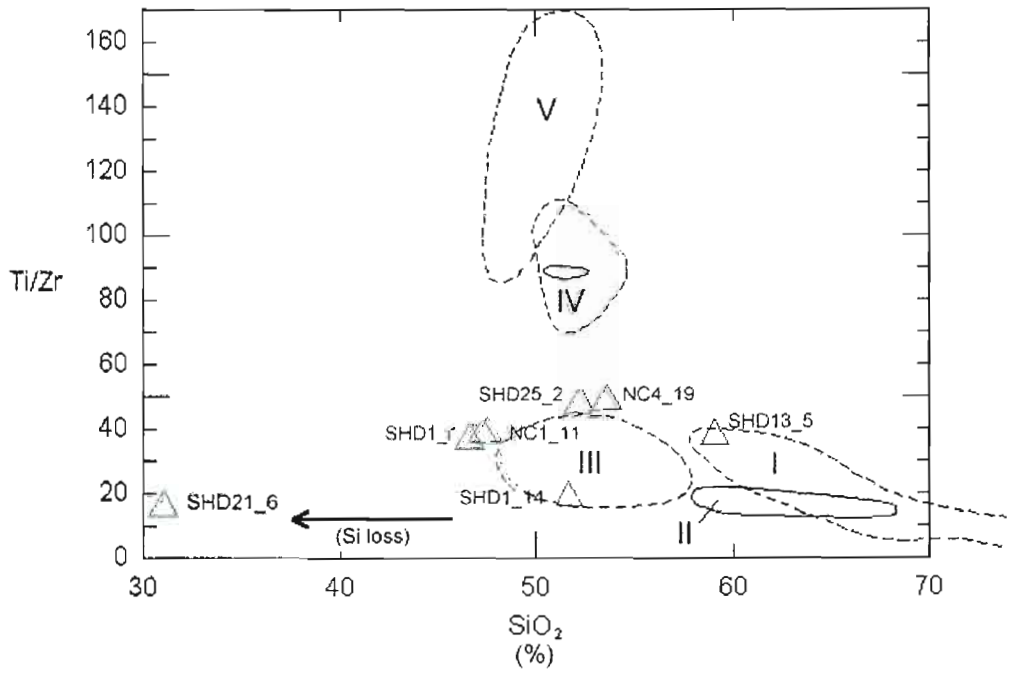

Figure 5.4 Plot of Ti/Zr Vs SiO_2, showing fields of MRV Suites of Crawford *et al.* [1992].

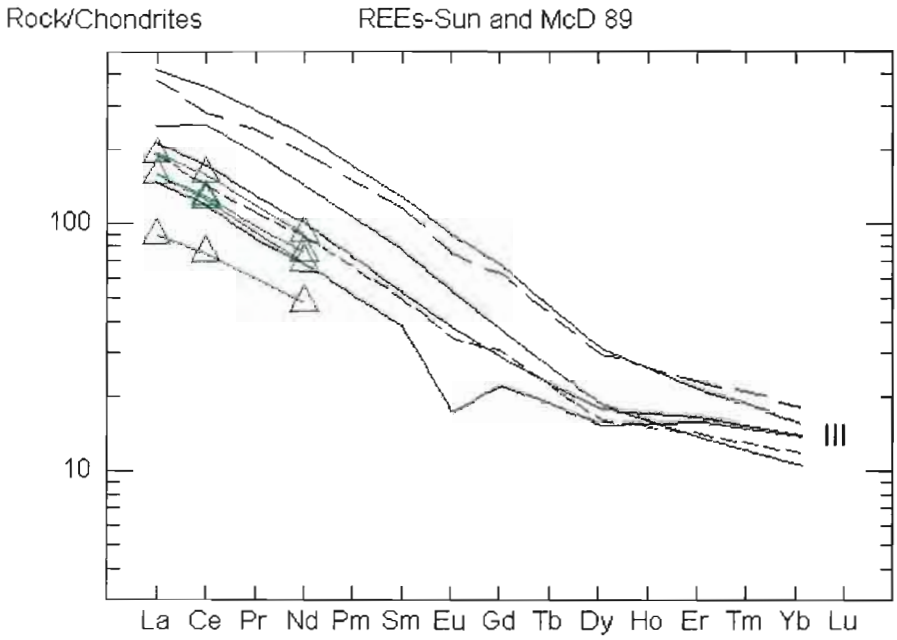

Figure 5.5 Plot of light rare earth elements, showing samples from Crawford *et al.* [1992].

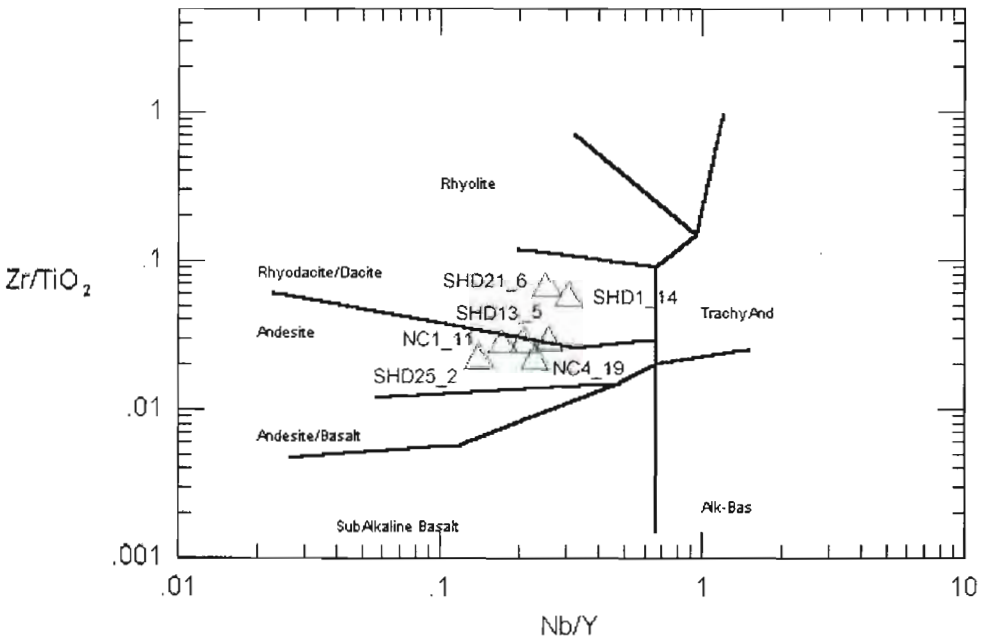

Figure 5.6 Plot of Zr/TiO_2 Vs Nb/Y, showing fields of Winchester & Floyd [1977] diagram.

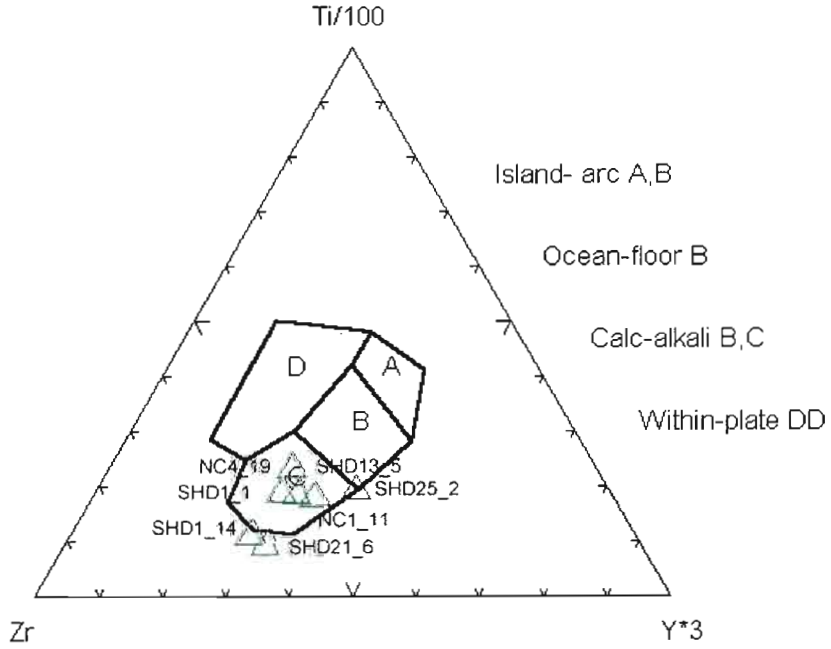

Figure 5.7 Plot of Ti/100 - Zr - Y×3, showing fields of Pearce & Cann [1973].

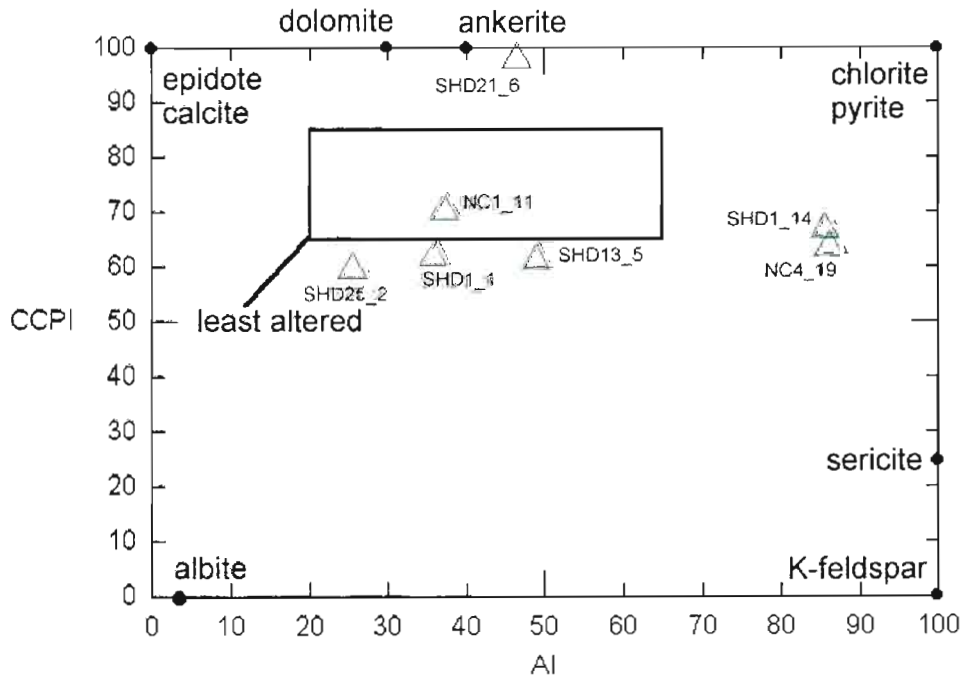

Figure 5.8 Plot of chlorite-carbonate-pyrite index Vs Ishikawa alteration index, showing fields of Large *et al.* [2000].

difference is in the abundances of alkali elements, which on the basis of local alteration, are quite mobile and therefore cannot be relied upon for discrimination purposes.

5.7 Interpretation

Based on geochemistry, the HB is interpreted to belong to the MRV Suite III of Crawford *et al.* [1992]. It falls within the medium K calc-alkaline end of the Suite III spectrum. The two anomalous samples are interpreted to have Suite II affinities. Due to their stratigraphic locations, one near the base of the breccia pile, and the other closely related to the possible feeder system of the basaltic eruption, they are roughly interpreted as xenoliths from underlying Suite II (ARA) units (Figure 4.3). Definitive classification can not be reached with the limited geochemical data available on only a few specimens.

Chapter 6: Discussion

6.1 Tectonic

From geochemical modeling, and facies identification, the HB is interpreted to have been formed in an extensional setting. When geochemical data is applied to tectonic discrimination plots, they come out in the calc-alkaline arc setting. This is supported by work on the tectonic history of the MRV by Crawford & Berry [1992], and geochemical work by Crawford *et al.* [1992].

6.2 Regional Correlations

Through geochemical discrimination the HB has been assigned to the medium K calc-alkaline end of Suite III. The increase from medium K through shoshonitic rocks in Suite III is the result of post-collisional volcanism induced by an arc-continent or continent-continent collision [Crawford *et al.*, 1992]. From this the HB may be said to be one of the earlier erupted units with medium K calc-alkaline affinities. Progressive magma evolution produced more K-rich and shoshonitic volcanic units (e.g. Que-Hellyer Volcanics, Lynch Creek Basalt).

6.3 Eruption Style and Setting

As the MRV were evolving in an post-collisional setting, there would have been active extension [Crawford & Berry, 1992]. This extension would have facilitated basaltic eruption, and would have allowed for a high rate of discharge for the eruption if hydrostatic, and overburden pressure were low enough. This leads to the possible eruption of magma in a fountaining manner, and the accumulation of a localised fire fountain deposit around the vent [Cas & Wright, 1987].

Two distinct stages of basalt eruption are envisaged to have formed the unit known as the HB. An initial explosive eruption produced a basalt breccia which formed a pile in the northern section of the sequence. The HB type one monomictic breccia may be part of the original breccia pile formed by subaqueous fountaining of lava, and would therefore be

representative of a proximal setting. After a hiatus during which volcaniclastic units and carbonates were deposited around the flanks of the pile, a stage of effusive basaltic eruption occurred. The first lava spread out, especially in a southward direction, where it appears there was perhaps a growth fault facilitated depression into which the could accumulate. A second lava followed, after the intermediary deposition of more carbonate, pooling in the southern depression, representing the distal setting. Sections of this second lava located on the slopes of the basaltic pile were subject to reworking and erosion, given their position above storm wave base. Breccias formed on the slopes of the pile, from both lavas, were redeposited downslope during slumping events, resulting in the interfingering of carbonate (which continued to grow) and basalt breccia units. Reworking, and subsequent resedimentation of the second lava, parts of the breccia pile, carbonate units and other local volcaniclastic units above storm wave base, resulted in the polymict breccias that occur in the northern area almost exclusively. Units deposited in the basin were below wave base, and therefore protected from severe reworking, hence the near absence of large polymictic breccia units. This interpretation is summarised in a schematic section (Figure 6.1).

Eruption and subsequent deposition of the HB is thought to be shallow subaqueous because of the fossiliferous carbonate that displays interbedding relationships with the basalt in place. Reworking of isolated parts of the basalt (northern pile and closely related flows) implies currents, and therefore above storm wave base conditions.

This theory isn't easily confirmed, or disproved, with the data available. The reason why this is so, is because of the sparse number of diamond drill holes in the southern area as compared to the northern, as well as limited depth reached in some holes.

After the basaltic volcanism there was subsidence, and the beginnings of large-volume intermediate to felsic explosive subaerial eruptions (source for TG). Deposition of resulting mass flows is known to have been in a subaqueous below storm wave base setting [White & McPhie, 1996], hence the subsidence during and/or after basaltic volcanism..

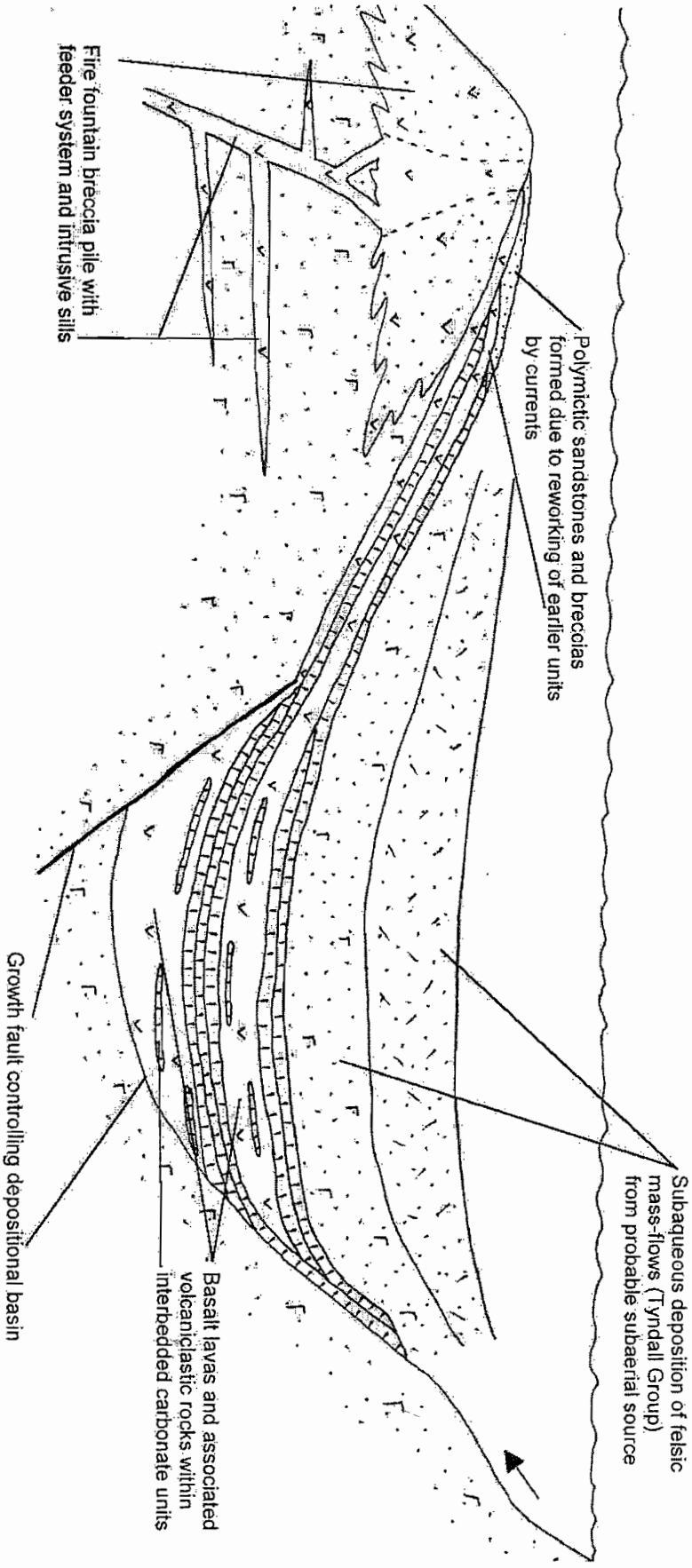

Figure 6.1 Schematic section, outlining the environment and mode of eruption of the Howards Basalt and related units.

6.4 Implications for Mineralisation

Crawford *et al* [1992] noted the occurrence of several mineral deposits in close proximity to Suite II and Suite III units (Hellyer, Mt Lyell). Suite I units are also known to be prospective (e.g. Henty). As the HB is thought to be subaqueously erupted the chances of there being mineralisation is greater than for subaerially erupted lavas. The associated magma source could have provided heat to drive hydrothermal convection cells [Stolz, 1995], and later faulting may have focussed fluids. Halley & Roberts [1997] noted that the main factors important in the formation of gold-rich volcanogenic massive sulfide deposits, are evident in the Henty deposit.

The horizon upon which the HB occurs is already a prospective horizon because of the Mt Lyell and Comstock deposits. The possibility of a heat source, and therefore a higher capacity to form VHMS style mineralisation, increases the viability of the HB horizon. This same horizon may have been fault displaced (Figure 4.3) during a later event, and if mineralisation has occurred, it may still be preserved at depth.

Chapter 7: Conclusions

The HB is a non-vesicular to moderately vesicular, commonly brecciated and highly altered sequence of andesitic volcanic and volcaniclastic rocks, comprising of two monomictic breccias, a polymictic breccia, a volcaniclastic sandstone and a coherent facies. The units of the HB were formed through an explosive (possibly fire fountaining), and effusive phase of subaqueous eruption (petrographically dissimilar), and subsequent reworking and redeposition of some units.

The HB was formed in the early stage of the progression from medium K calc-alkaline rocks to shoshonitic rocks, during a time of post-collisional extension, after the collision of an island arc and a continent. The sequence is part of the MRV Suite III of Crawford *et al.* [1992] which include the more evolved of the calc-alkaline to shoshonitic spectrum.

The heat of the magma source for the HB may have fueled convective cells in a volcanogenic massive sulfide generating system. Cambrian and Devonian deformations reactivated the major South Henty and Great Lyell Faults, which may have directed hydrothermal fluids generated by continued volcanic activity, to sites of precipitation in the brecciated facies of the HB.

References

Allen, R.L., 1994 *Interpretation of the volcanic sequence and mineralization, Yolande-Newton Creek area* **in** Pasminco report TCR-94-3590

Burrett, C.F., & Martin, E.L. (Eds.), *1989 Geology and mineral resources of Tasmania* Geol. Soc. Aust., Special Publication 15: 574p

Cas, R.A.F., 1992 *Submarine volcanism: Eruption styles, products, and relevance to understanding the host-rock successions to volcanic-hosted massive sulfide deposits* Econ. Geol. 87: 511-541

Cas, R.A.F. & Wright, J.V., 1987 *Volcanic successions, modern and ancient* Chapman & Hall: London 528p

Corbett, K.D., 1992 *Stratigraphic-volcanic setting of massive sulfide deposits in the Cambrian Mount Read Volcanics, Tasmania* Econ. Geol. 87: 564-586

Corbett, K.D. & Lees, T.C., 1987 *Stratigraphic and structural relationships and evidence for Cambrian deformation at the western margin of the Mt Read Volcanics, Tasmania* Aust. J. Earth Sci. 34: 45-67

Crawford, A.J. & Berry, R.F., 1992 *Tectonic implications of late Proterozoic - early Palaeozoic igneous rock associations in western Tasmania* Tectonophysics 214: 37-56

Crawford, A.J., Corbett, K.D. & Everard, J.L., 1992 *Geochemistry of the Cambrian volcanic-hosted massive sulfide-rich Mount Read Volcanics, Tasmania, and some tectonic implications* Econ. Geol. 87: 597-619

Dower, B., 1991 *The geology, geochemistry and tectonic setting of the Miners Ridge Basalt and Lynch Creek Basalt in the Mount Read Volcanic belt, Western Tasmania* BSc (Hons) thesis (unpubl.) University of Tasmania

Gibson, R.P., 1991 *The geology of the Mt Read Volcanics in the Anthony Road-Newton Creek area, western Tasmania* BSc (Hons) thesis (unpubl.) University of Tasmania

Halley, S.W. & Roberts, R.H., 1997 *Henty: A shallow-water gold-rich volcanogenic massive sulfide deposit in western Tasmania* Econ. Geol. 92: 438-447

Herrmann, W., 1998 *Use of immobile elements and chemostratigraphy to determine precursor volcanics* AMIRA/ARC Project P439, Report 6: 1-12

Herrmann, W. & MacDonald, G., 1996 *Volcanic facies, alteration and exploration targets in EL 8/96 South Henty, Tasmania* Resolute Samantha Ltd. (unpubl.)

Jago, J.B., Reid, K.O., Quilty, P.G., Green, G.R. & Daily B., 1972 *Fossiliferous Cambrian limestone from within the Mt Read Volcanics, Mt Lyell mine area, Tasmania* J. Geol. Soc. Aust. 19: 379-382

Large, R.R., Gemmell, J.B., Paulick, H. & Huston, D.L., *The alteration box plot: A simple approach to understanding the relationship between alteration mineralogy and lithogeochemistry associated with VHMS deposits* Econ. Geol. (in prep.)

MacLean, W.H., & Barrett, T.J., 1993 *Lithogeochemical techniques using immobile elements* J. Geochem. Expl. 48: 109-133

McPhie, J. & Allen, R.L., 1992 *Facies architecture of mineralized submarine volcanic sequences: Cambrian Mount Read Volcanics, western Tasmania* Econ. Geol. 87: 587-596

Pearce, J.A. & Cann, J.R., 1973 *Tectonic setting of basic volcanic rocks determined using trace element analyses* Earth Planet. Sci. Let. 19: 290-300

Perkins, C. & Walshe, J.L., 1993 *Geochronology of the Mount Read Volcanics, Tasmania, Australia* Econ. Geol. 88: 1176-1197

Poltock, R.A., 1992 *Henty fault wedge* BSc (Masters) thesis (unpubl.) University of Tasmania

Stolz, A.J., 1995 *Geochemistry of the Mount Windsor Volcanics; implications for the tectonic setting of Cambro-Ordovician volcanic-hosted massive sulfide mineralization in northeastern Australia* Econ. Geol. 90: 1080-1097

Stolz, A.J., Davies, G.R. & Allen, R.L., 1997 *The importance of different types of magmatism in VHMS mineralisation; evidence from the geochemistry of the host volcanic rocks to the Benambra massive sulphide deposits, Victoria, Australia* Mineral. Petr. 59: 251-286

Street, M., 1999 *Alteration of the South Henty Prospect* BSc (Hons) thesis (unpubl.) University of Tasmania

White, M.J., 1996 *Stratigraphy, volcanology and sedimentology of the Cambrian Tyndall Group, Mount Read Volcanics, western Tasmania* PhD thesis (unpubl.) University of Tasmania

White, M.J. & McPhie, J., 1996 *Stratigraphy and palaeovolcanology of the Cambrian Tyndall Group, Mt Read Volcanics, western Tasmania* Aust. J. Earth Sci. 43: 147-159

White, M.J. & McPhie, J., 1997 *A submarine welded ignimbrite-crystal-rich sandstone facies association in the Cambrian Tyndall Group, western Tasmania, Australia* J. Volc. Geotherm. Res. 76: 277-295

List of Abbreviations

ARA	Anthony Road Andesites
CF	Comstock Formation
CVC	Central Volcanic Complex
DDH	Diamond drill hole
DT	Dundas Trough
FPB	Footwall Pumice Breccia
HB	Howards Basalt
K	Potassium
LM	Lynchford Member
MJM	Mt Julia Member
MRV	Mount Read Volcanics
NCD	Newton Creek Dacites
NCS	Newton Creek Sandstone
OC	Owen Conglomerate
PIMA	Short-wave infra-red spectroscopy
REE	Rare earth elements
SBB	Spillway Basalt Breccia
SPB	Spillway Polymictic Breccia
TG	Tyndall Group
VHMS	Volcanic-hosted massive sulfide
WVSS	Western Volcano-sedimentary Sequences
XRF	X-ray fluorescence
YRS	Yolande River Sequence
ZZHF	Zig Zag Hill Formation

Appendix A

SHD1

SHD13

SHD14

SHD21

SHD25

NC1

NC4

LOG

SHD 1

date: 14/03/00

scale 1:200

structure	m	grainsize (.063, 1, 2, 8, 32, 64, 256 mm)		s	description
alt^n	0				0-1.50 no core recovery glacials?
					strongly weathered
					vc ss (Q+F)
	10				
	20				
Art L Sp bedding					
					fairly massive Q+F vc ss
	30				
	40				
	50				

LOG

SHD1

date: 14/03/00

scale 1:200

alt^n	structure	m	grainsize (.063, 1, 2, 8, 32, 64, 256 mm)		s	description
		50				
		60				
		70				
A+C						
		80				
		90				gradually larger clasts to base
		100				

LOG

SHD1

date: 14/03/00

scale 1:200

structure	alt^n	m	grainsize (.063, 1, 2, 8, 32, 64, 256 mm)		s	description
		100				
		110				
		120				
A+C		130				
		140				
		150				

F vc ss little gtn

LOG

SHD1

date: 14/03/00 | grainsize | scale 1:200 / 1:100

structure / alt^n		m	grainsize (.063, 1, 2, 8, 32, 64, 256 mm)		s	description
		150				← rhy clasts.
A+C		160				
	fairly sharp	170				← more fluidal at base plus a little polymictic
C+ CARB (minor veining) - A						silty top polymictic lithic bx clasts - limestone, cherty?
	sharp fault?					ls breccia. (clasts w/ tr/tos) pm BX (broken/fractured core) - fault?
A+C						VC SS
C+CARB H+C+ CARB	sharp fault?					ls 178.45 - 179.0 broken core - fault? pm BX
C-A	sharp?	180				pm BX (CARB ONLY AS VEINS/ALT).
C+CARB + H	sharp					massive (bedded) ls w/ few bx bits some tr/tos.
	sharp					pm lithic, vc? BX
C≈A						Dacite clasts (larger), rounded ls clasts, cherty + poss. mafic (c alt).
	sharp					
		190				
C≈ CARB (mostly as veins throughout)				SHD1_1		basaltic breccia
		195				

1:200

1:100

LOG

SHD 1

date: 15/03/00 | scale 1:100

alt^n	structure	m	grainsize (.063 1 2 8 32 64 256 mm)		s	description
		195				
	sharp	200		SHD1-2		PM lithic vc BX
C ? CARB	sharp					basalt hyalo
	sharp	205				basalt hyalo
	sharp					PM vc BX some v large basalt clasts (to 65mm). mostly basalt + minor chert
	sharp					basalt hyalo.
	sharp					
		210				
	sharp			SHD1-3		basalt hyalo w/ PM base.
	sharp					PM vc BX basalt + ls.
		215				
	sharp					PM vc BX
	sharp					
		220				

LOG

SHD1

date: 15/03/00 | scale 1:100

structure	m	grainsize (.063, 1, 2, 8, 32, 64, 256 mm)		s	description
alt^n	220				
	225		SHD1_4		
CS CARB	230				
	235				
sharp			SHD1_5		hyalo (basalt) w/ partly alt. sandy carb matrix
	240				
	245				

LOG

SHD1

date: 15/03/00 | scale 1:100

alt^n	structure	m	grainsize (.063, 1, 2, 8, 32, 64, 256 mm)		s	description
	sharp	245				basalt hyalo.
	sharp (Qz+Ep+ CARB VEIN)					
C± CARB						basaltic vc ss
	fairly sharp	250				
				SHD1	6	fm vc BX w/- pre. basalt w/- minor chert & rhy, some rhy very large, more monomictic to base
		255				
	grad →					↓ back to normal basalt breccia
	sharp ≡ (Qz+Ep+ CARB VEIN)					
		260				
	sharp					fm vc BX basaltic ms/sis & ss units
	sharp			SHD1	7	fm vc BX/ss mostly basalt & 1° clasts w/ occ charty clast, few 1° beds interbedded
C+ H+ CARB ≡		265				
	sharp					basaltic ms/sis & ss units ← some small clasts of ms/sis
C+ CARB (veins mostly)		270				

LOG

SHD1

date: 15/03/00 | scale 1:100

structure	m	grainsize (.063, 1, 2, 8, 32, 64, 256 mm)	s	description
alt^n	270			
C± CARB	275			
	280			rhy clasts (fairly large)
	285			
C+A	290			
	295			

pm VC SS/BX graded units

VC SS

F - phyric

+ rhy clasts

LOG

SHD1

date: 15/08/00

scale 1:100

structure	m	grainsize (.063 1 2 8 32 64 256 mm)	s	description
C+A	295			vc ss (F phyric)
	300			
C+ CARB				vc ss (F-phyric + carb interbeds?)
C+H +CARB	305			ls
				(trilos)
S				F + minor Q xbals ss
C+H +CARB	310			ls
S				F + minor Q xbals ss
C+H+ CARB	315			ls breccia (auto?)
C+H				PM? vc ss
	320			F-phyric + c/H alt basalt?

LOG

SHD 1

date: 15/03/00

scale 1:100

structure	m	grainsize (.063, 1, 2, 8, 32, 64, 256 mm)		s	description
	320		SHD1	8	
C+H	325				
			SHD1	9	
	330				10 SS
C+S			SHD1	10	
	335				
			SHD1	11	
C+H					
	340				
	345				

LOG

SHD1

date: 15/03/00 | scale 1:100

structure	m	grainsize (.063, 1, 2, 8, 32, 64, 256 mm)		s	description
alt^n	345				
C+H					
	350				basalt? clasts to 55 mm x 30 mm
	355				
			SHD1	12	coherent basalt? (dyke)?
C+S	360				
	365				basalt clasts

thin? to 315.45

LOG

SHD1

date: 15/08/00

scale 1:100

structure		m	grainsize (.063, 1, 2, 8, 32, 64, 256 mm)	s	description
alt^n		370			
C+S					
S+f		375			more silicic? fe-stained
					vc SS
C+S					basaltic? c/carb alt sists (well bedded)
		380			
					vc SS
+S					
		385			
	sharp?				
C					
		390			[illegible] grit from grained
C+S					
	sharp?				vc SS
S+ + C					[illegible]
		395			

LOG

SHDI

date: 02/05/00

scale 1:100

structure	altn	m	grainsize (.063, 1, 2, 8, 32, 64, 256 mm)	s	description
		395			
(ass S to base)					
		400			dactic? vc SS.
CxS					
	sharp →				
		405			
					vc SS.
		410			
	grad →				
CxS					vc SS + clasts (larger) (to ~4cm).
		415			
	grad →				
		420			vc SS (as 64 411m)

LOG

SHD1

date: 02/05/00 | scale 1:100

structure	m	grainsize (.063, 1, 2, 8, 32, 64, 256 mm)	s	description
alt^n	420			
	425			
GS				
	430			hyalo? / breccia clasts of coherent? in matrix of upper & lower
	435			
GS				
++p	440			Fe-rich fluids [illegible] & [illegible] into [illegible] carb/Fe replacing vesicles? ~~basaltic [illegible]~~ basalt / basalt or just deformed ← breccia?
			SHD1-13	
GS				same as above, but fewer vesicles/amygdales.
	445			

LOG

SHD1

date: 02/05/00 | scale 1:100

structure (alt)		m	grainsize (.063, 1, 2, 8, 32, 64, 256 mm)	s	description
sharp →		445			
		450			
C+S					vc SS
		455			
	??				hydrothermal clasts of coherent in matrix of upper
	sharp→				
C+S		460			
C+S		465			wk jointed sitstone beds?
		470			

LOG

SHD1

date: 02/05/00 | scale 1:100

structure	m	grainsize (.063, 1, 2, 8, 32, 64, 256 mm)	s	description
a 1m	470			
C-S				
S-C				
	475			
S ↑ pseudo-breccia (S alt) ↓				sericite btw 'clasts'
Qtz-CTE VEIN	480	Qtz-CTE		qtz + Fe/cte vein
+S	485			
++S				breccia & pseudo-breccia (S alt)
+ S				*1st 30cm vc ss. vc ss from below + strong S alt of parts (½ core lengthways)
	490			
grad →				
C-S				vc ss mom clasts ↓ basaltic clasts.
	495			↓ SPILLWAY BASALT SUCCESSION ?

LOG

SHD1

date: 02/05/00

scale 1:100

grainsize: .063 | 1 | 2 | 8 | 32 | 64 | 256 mm

structure	m		s	description
alt"	494			vc SS
C+S		SHD1	14	stranger pumice breccia? chl-seri alt seri chl basalt?? "A maybe pseudo-b[illegible] pm bx? w/ few chl pumice? qtz-porph"
+ P				
C+S	490			clastic vc SS basaltic
*S+C	sharp (chilled)	SHD1	15	coherent? basalt / breccia similar alt in part to one above
C+S	sharp → (structural? minor faulting & folding) sharp → (top? bottom)			basalt breccia (pepperitic??) clastic vc SS some vcSI basaltic
*S+C	sharp			fine g vc SS
C+S	480			clastic vc SS basaltic more angular
	sharp			
C+S + F	470			vc SS
C+F	460			

LOG

SHD1

date: 03/05/00 | grainsize | scale 1:200/1:100

structure	m	grainsize (.063, 1, 2, 8, 32, 64, 256 mm)		s	description
a 1m	520				
	530				vc ss
C+Fe					
	540				
Qz+Fe Py					silicification of vc ss. intense qtz veining (VI), then Fe overprinting (small veinlets) (large veins) + pyrite in w/r Fe (large amounts up to 5%)
	550				
C+Fe					vc ss
qtz+Cte vein					vein
C+Fe					
	560				vc ss
sharp (erosional?)				SHD1 16	
++ H CARB VES					cement basalt v. vesicular
sharp (chill??)					
Fe	565				vc ss

1:100

LOG

SHD1

date: 03/05/00 | scale 1:200 / 1:100

structure (alt)		m	grainsize (.063 1 2 8 32 64 256 mm)		s	description
		565				
+Fe						v.c. s.s
Qtz ± Fe-Ctc →						veinlets
						v.c. s.s
		575				
++Fe+Py +CARB VEINS	FAULT?					PM. BX at top to mm w/- broken core small band near base of PM again clasts mostly v.c.ss, some more silicic/chloritic.
++Fe+ Py						v.c. s.s
++Fe+ +Py	broken core (sharp) fault? sharp →	580		SHD1	17	basalt breccia w/- PM top
++Py+ ++Fe+ C						
++Fe+ Py Qz VEINED	sharp (chilled)					coherent basalt? w/- chilled margins (darker less vesicles) vesiculated (amygdales), red (Fe) pyrite nodules, qtz veining, some carb veining
	sharp (chilled)	585		SHD1	18	
						v.c. s.s. some PM clasts (reddy chloritic)
		595				

1:200 1:100

LOG

SHD13

date: 05/05/00 | scale 1:200 | page 1 of 4

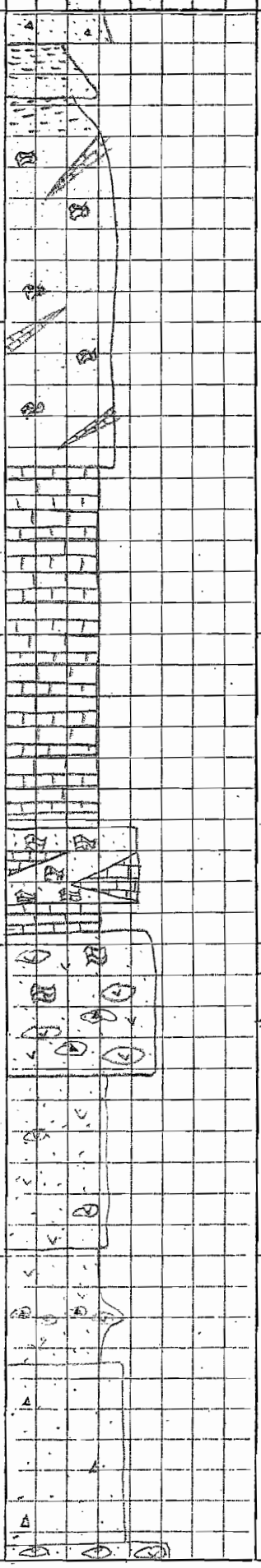

structure	m	s	description
+C	sharp →		vc ss
			vc sis/ss
+C + CARB (veining)			vc sis/ss w/- ls clasts, veining & interbeds
	grad →		
CARB H+C			bedded ls w/- some trilobs.
	sharp →		
H+C +C. NB			ls bx w/- interbeds
CARB H—C	sharp →		bedded slo w/- trilobs
H+C +CARB (VEINS)	sharp →	1DX3 22X12 / SHD3- 1	45 pm bx w/- pred. basalt clasts, also ls & cherty
	sharp →		basaltic? vc ss w/- fine basalt clasts
H+C			
+H+C +K SPAR? (orange-pink)	sharp →		basaltic vc ss w/- middle bx w/- cherty & basalt clasts
C+SH +CARB			vc ss some clasts of basalt
	fairly sharp →		← basalt clasts (dyke) ↓

LOG

SHD13

date: 05/05/00 | scale 1:200 | page 2 of 4

structure		m	grainsize (.063 1 2 8 32 64 256 mm)	s	description
C←H		650			basalt bx w/- some coherent sections
	grad →				basalt hyaloclastite
	sharp →				as bH hyaloclastite
+C←H		660			vc SS w/- some basalt clasts
	sharp →				
+H+C				SHD13 2	basalt bx (auto ??)
	sharp →				
H←C		670			coherent basalt dyke
				SHD13 3	
+H+C	sharp → grad →				basalt bx (auto ??)
+H+ C←S (to base)					vc SS w/- some basalt clasts
		680			
				SHD13 4	
++H+C (ARB VEINS)	sharp → (chilled)				basaltic dyke
H←C←S	grad → sharp → sharp → grad →				breccia at base. vc SS w/- basalt clasts jigsaw-fit at top (basalt)
+H→C	(fractured, overlying intrusive)	690		SHD13 5	basaltic dyke.
+C→S			shear zone		
+C←H					
++H→C	sharp →				basaltic breccia, some foreign clasts?
C←H	contact missing, removed as sample				basaltic dyke.
	grad →	700			

LOG

SHD13

date: 05/05/00 | scale 1:200

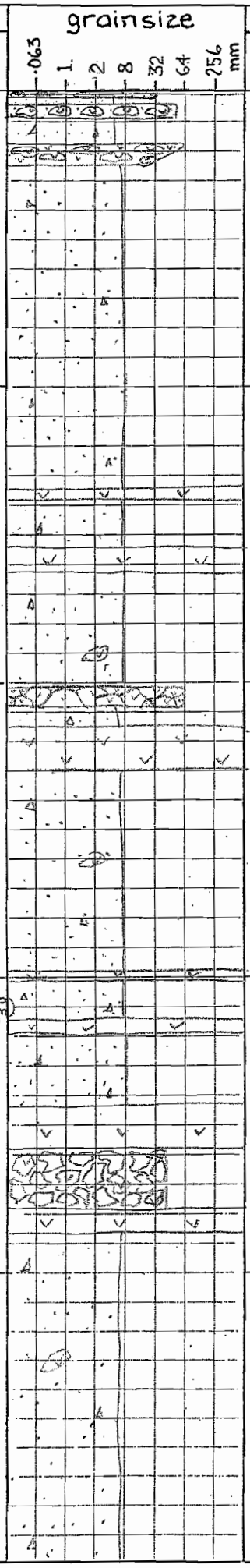

structure		m	s	description
+C+H	grad →	700		basalt bx (700.40 – 700.90)
	grad →			701.70 – 702.10 dyke bx
				702.10 – 702.40 less vesicular basalt bx
+H+C				
				vc ss
C↑				
+S		710		
	chilled? sharp →			basaltic dyke
++S				
+C+H +S	sharp →			
++S	sharp → (chilled)			basaltic dyke
C→S				vc ss (some basaltic clasts)
	sharp (chilled)	720		
+E +H	(veins) sharp?			bx^d basalt dyke
	sharp →			
++E +H	→			basaltic dyke
	(not chilled)			
C→S				vc ss (some basaltic clasts)
	sharp (chilled)			bottom 10-15cm?
+H+C	sharp →	730		basalt dyke
C+S	(faulted? slickenside)	breccia ~1cm +vein		vc ss
+H+C	sharp (chilled)			bottom 20-25cm same as 104. basalt dyke (repeat of bx)
C→S				vc ss (some basalt clasts?)
	sharp → (chilled)			basalt dyke
	sharp → (chilled)			hyaloclastite? (bx^d dyke)
C→H	grad-sharp →			basalt dyke
	sharp → (chilled)			
		740		
C→S				vc ss (some basalt clasts)
		750		

page 3 of 4

LOG

SHD13

date: 05/05/00 | scale 1:200 | page 4 of 4

structure		m	grainsize (.063, 1, 2, 8, 32, 64, 256 mm)		s	description
a H^		750				
leaS to basalt		760				
H+C	sharp → (chilled)	770		SHD13	7	basalt dyke vc SS hyaloclastite (broken/bx^d dyke)
C				SHD13	8	
+H ++Pg +C	fault (brokenly core) broken but not all sheared → sharp (chilled??)					
+C+H						
C+S	sharp → (chilled)					vc SS
	sharp → (chilled)	780				basaltic dyke? 783 – 785.2 ?
+ C						
+C +H	sharp →			SHD13	9	vc SS w/- basalt bx some clasts fluidal w/- chilled margins
		790				
+C -S						vc SS
		800				

LOG

SHD14

date: 04/05/00 | scale 1:200

structure	m	grainsize (.063, 1, 2, 8, 32, 64, 256 mm)	s	description
	0			Broken & weathered core
C+A				F-phyric vc ss
FAULT	10			10.40
				med. dark grey mostly mon. vc ss w/ some poly but pred. dark grey green mafic? clasts some (andesitic?)
				v. large (greater than core 15/20cm) clasts are deformed through shearing (longer more than fatter) & mafic more than felsic (rhy)
				sandy matrix deformed around (shearing not too bad)
	20			* some clasts broken to jigsaw fit (brecciation through transport)
				* some sed. clasts (sandstone, maybe cherty)
				* some clasts are rimmed
C				matrix supported
	30			↓ matrix lighter in colour to light grey
	40			
grad→				more even clast size to base, but still occassional v large clast (from about 43 m, change abrupt but gradational)
	50			matrix darker again, but lightening ↓

LOG

SHD14

date: 04/05/00 | scale 1:200

alt^n	structure	m	grainsize (.063, 1, 2, 8, 32, 64, 256 mm)	s	description
		50			
		60			clasts more jigsaw fit to base, almost clast-supported
	sharp (Q vein)				F-phyric silica-alt^d vc SS some v. large clasts of rhy? & and
qtz & minor chl veining					
C+AQ stronger to base (some massive C)		70			lower 1/3 of unit has v. little veining.
	sharp				graded units of vc SiS/SS well bedded, some small units (5-10cm). * esp to base.
+C					
	sharp				
C		80			PM BX (rhy, mafic, ls)
C+A?	sharp				
	sharp				F-phyric (large alt^n) vc SS massive. some small beds. m breccia
C+A					PM BX w/ clasts of pred. C+A alt F-phyric vc SS (some a+epi veining to base)
	sharp				
		90			
C+A					F-phyric vc SS massive as b4
	sharp ~~ fault?				broken core / puggy vc BX/SS w/ clasts of rhy? & same.
		100			

LOG

SHD14

date: 04/05/00 | scale 1:200

structure		m	grainsize (.063, 1, 2, 8, 32, 64, 256 mm)	description
		100		
H±C	grad. → grad. → sharp →			ls Bx ls w/- trilos
		110		pm vc Bx/ss - sections of Bx & sections of ss
		120		← sections of more mm basaltic? lithic Bx ↓
		130		
		140		
	sharp→			
+S				pumiceous? vc ss!
S±H/V ±S	sharp→	150		basaltic? lithic vc ss (basaltic!)

LOG

SHD 14

date: 04/05/00 | scale 1:200

structure	m	grainsize (-.063, 1, 2, 8, 32, 64, 256 mm)	mm	%	description
	150				
C+SH			10x1 10x3	15	
	160		10x2 30x3	25	
sharp			5x2 50x7	30	vein of Q, K'spar & calcite w/ included bits of surrounding rock (undeformed)
H+C +S	170		15x1 20x3	20	
			SHD14 1		
H+S +C			13x2 27x4	10	
	180		20x7 20x20	55	large variety of clast altⁿ: – H rimmed C – C – H – S – S rimmed H
H+C +S			SHD14 2		12x2 40x12 50
	190		6x3 20x8	45	
H+S-C Py disem					
H+C			15x3 20x5	50	
	200		15x2 40x10	40	

LOG

SHD14

date: 04/05/00 | scale 1:200

structure (alt)		m	grainsize (.063, 1, 2, 8, 32, 64, 256 mm)		s	description
H+C		200		30x4 70Dx28	50	
		210		SHD14 30x3 50x11	3 45	
	sharp					qtz+calcite+k'spar vein w/ v small amounts of rock in
				15x3 40x15	55	
H+C		220		12x2 20x4	45	
				20x3 40x7	40	
+ P		230		13x2 50x8	40	
H+S+C + H + Py (dis)						bed clasts
				20x1 35x3	35	
	barite vein (SHD14p)					barite vein w/ bits (conformable) of vc BX in
+S +C + H + Py (dis)		240		25x3 50x18	45	
				SHD14	4	
				15x2 23x12	30	
+S +H + C + Py						
		250		10x3 22x4	40	

LOG

SHD14

date: 04/05/00 | scale 1:200 | page 6 of 7

structure	m	grainsize (.063, 1, 2, 8, 32, 64, 256 mm)		s	description
C+H +C	250		15x3 7CDx6	45	
	260		12x3 45x20	85	
fault?					} broken core - fault?
C+H +S			20x2 7CDx35	30	
			SHD14	5	
	270		20x2 7CDx60	50	
			SHD14 7x1 50x7	6 40	
C+S +H.	280		6x3 35x7	45	
			10x1 15x4	25	} veined / sheared / brecciated (broken core etc)
C+S +H			SHD14	7	
	290				qtz-phyric (20% of rock) {about 4mm av} maybe small basalt clasts?
H+C			SHD14	6	sheared
					qtz porphyry
	300				

LOG

SHD14

date: 04/05/00 | scale 1:200

structure		m	grainsize (.063, 1, 2, 8, 32, 64, 256 mm)		s	description
C+H		300				
		310				
	sharp →					
±C +S -H		320		15x2 35x5	20	basaltic? lithic (only smaller & fine) vc ss(basaltic?)
				SHD14	9	
	sharp →					
C+H(Fe) -S						
C+H		330				
C+H(Fe) -S						qtz-porphyry
	sharp →					
		340				large qtz (~1cm) blobs in otherwise siliceous vc. ss? dacitic?
Qz+Fe -C						
		350				

LOG

SHD21

date: 03/03/00 | scale 1:100 | page 1 of 6

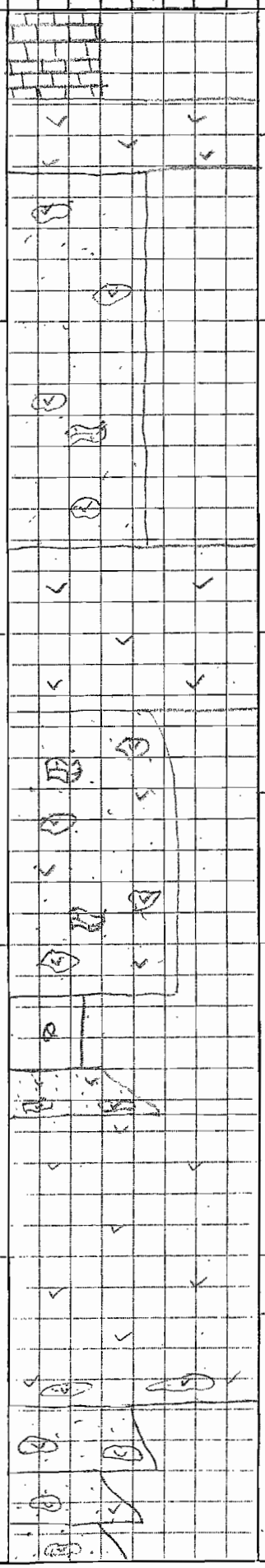

alt^n	structure	m	s	description
H+ CARB		170		massive 1s minor carb veins.
minor H minor	CO_3 veins sulph veins		SHD21_1	strongly hat alt basalt
S	sheared +	175		basalt breccia w/ minor ls clasts
CARB + Q		180		coherent basalt vesicles replaced by carb numerous carb + qtz veins
S			SHD21_2	basalt breccia + carb lithics
	sharp	185		Qtz + Chl vein + CO_3.
CARB S	sheared + sharp			basalt breccia
CARB - Q		190	SHD21_3	coherent basalt vesicles replaced by carb. numerous veins of carb & minor qtz
S. c	grad → grad →	195		

LOG

SHD21

date: 03/03/00 | grainsize | scale 1:100

alt^n	structure	m	s	description
		195		
S				coherent dacite
				basalt breccia. coherent dacite
S+				strongly hac alt basalt? breccia, v. fol^d & sheared broken core
+H	fol^d ++ shear zone?	200		
S				dacitic vc ss.
+S	fol^d ++ shear zone?			strongly fol^d & sheared. (broken core).
S		205		dacite lithic breccia w/- v. occasional basalt clasts
-C	sharp		SHD21_04	v. flattened / sheared FM's? ? speckling rock (pale green grey) vc SS?
S				
-C	?			coherent basalt ? ? dss?
S	shear	210		coherent? dacite
	sharp			
S+C				dacitic breccia
+S		215		
S				
		220		

LOG

SHD21

date: 07/03/00 | scale 1:100

structure	m	grainsize (.063, 1, 2, 8, 32, 64, 256 mm)		s	description
alt^n	220				
S+P -CARB (veins)					dacitic breccia
					breccia ?vcbx? (f.g. lithic) ??
	225				dacitic VC SS
					← polymictic lithic breccia? base
S+C+ Py (dis)	230				
					numerous small graded units of polymictic lithic VC SS.
			SHD21_5		clasts of basalt, dacite & cherty?
	235				
	240				
			SHD21_6		
	245				

LOG

SHD21

date: 07/03/00 | scale 1:100

structure (α-ltn)	m	grainsize (.063, 1, 2, 8, 32, 64, 256 mm)	s	description
SrC	245			becoming more basalt-rich w/- depth.
SrC				minor S alt speckled chl? replaced FMs
+S+C	250			
			← SHD21-7	
S+P +C				darker than rest w/- fg at top & almost purple breccia (mud/py?) base.
	255			
S				polymictic lithic breccia pre basalt + cherty + dacite?
+S**	260		SHD21-8	
	265			polymictic lithic
new sequence S**				
	270			

LOG

SHD21

date: 08/03/00 | grainsize | scale 1:100

alt^n	structure	m	SAMPLE No.	s	description
		270			
S					massive lithic-rich unit (medium to dark green)
	sheared	275	SHD21-9		
S+					more sericitic to base / closer to contact (sharp) but are some qtz veins to 15 cm from contact
	sharp →				
S++ C+	sheared sharp →	280			polymictic basaltic, dacitic? lithic, sheared & highly sericitized & chloritized (pale green)
S+C+					occasional large clast (to 20cm) of basalt (chl alt)? and more often pyrite-rich
		285			
P phenocrysts ↓ out					
S++	sharp (Q vein → ~35mm)				288.5 - 289.0 broken core & little of, poss shear zone?
S+C		290			polymictic basaltic/dacitic? lithic
S+C					(basaltic sheared, other (dacite?) fol^n is around, therefore more resistant, or v. pl altered when sheared)
S+C		295			294.62 - 294.78 - pyritic siltstone (sil)

LOG

SHD21

date: 08/08/80 | scale 1:100 / 1:200

structure	alt^n	m	grainsize (.063, 1, 2, 8, 32, 64, 256 mm)	s	description
	??	295		SHD21-10	polymictic pyritic sils / pyr alt basaltic sils, basaltic lithic vc breccia.
					maybe not clasts but small inclusions as basalt clasts btw
					polymictic basaltic lithic vc breccia.
		300			
≡S^+ + C					
		305			
				SHD21-11	
		310			
	Q VEIN (~30mm)				
	Q vein (~35 mm)				PM vc SS grades a little to contact w/ porphyry, by increase in sericite & addition of H & C alt forming small veins/interbeds?
CARB+H +SrC	sharp	315			
S^+ + P					Q-porphyry breccia
P^+ + C^+ + S^+ + P					massive sulph. breccia Q-porph breccia cherty lithic breccia w/ pyr bedded (~10cm) bedded (at top) & breccia at base. v. sulph. rich (massive vc sulph) w/ few cherty clasts interbedded vc SS (sil) & Q-porph? broken core shear
		325			massive Q-porph ?

LOG

SHD25

date: 29/02/00 | scale 1:200

structure (alt^n)		m	grainsize (.063, 1, 2, 8, 32, 64, 256 mm)	s	description
		0			no core recovery 0 – 4.2 m
WEATHERED A+C		5			matrix-supp vc breccia
		15			f.g. cherty lithics (large) + qtz-feld stals
	graded units	25			feld stals + feld stal rich rhyo/dacite ? (large).
A+C		35			numerous normally graded units of feld stal lithic vc ss, w/- larger lithic clasts of rhy/dac ?
		45			

LOG

SHD25

date: 29/02/00

scale 1:200

structure		m	grainsize (.063, 1, 2, 8, 32, 64, 256 mm)	s	description
alt		45			
		55			
A+C		65			
		75			
		85			
		95			f.g. silty ss lithic-rich VC

LOG

SHD25

date: 29/02/00

scale 1:200

structure altn	m	grainsize (.063, 1, 2, 8, 32, 64, 256 mm)	s	description
	96	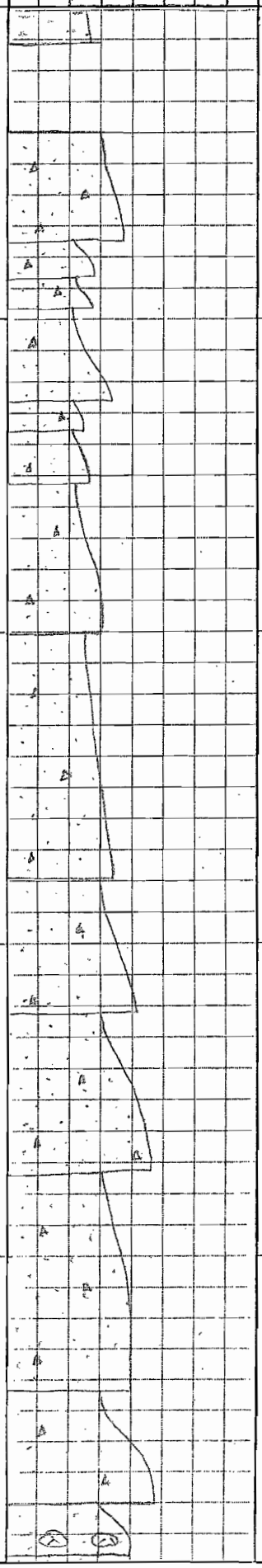		Core Loss / broken core. 96.2 - 99.0 m
	105			
A+C				larger normally graded units of feldspar rich lithic VC SS, becoming more massive +
	115			
	125			
	135			
C+A	145			

LOG

SHD25

date: 29/02/00 | scale 1:200 / 1:100

alt	structure	m	grainsize (.063, 1, 2, 8, 32, 64, 256 mm)	MAX/AV SIZE (MM)	s	description
		145				
C+A						graded (normally) volcaniclastic sequences. w/- rhy clasts becoming more abundant
		155				
minor P/C stripes pattern						- mostly rhy clasts + few ls clast supp in a few places.
C						- clast-less matrix, few pink (alb) bands in C.
						- monomictic rhy lithic breccia in strongly chl matrix matrix supp
					MM	
	grad →					
		165				polymictic lithic breccia w/- ls, dacite & rhy? clasts, also carb veining thru out
CARB +C	sheared but not as obvious					matrix to clast to matrix supported
					PM	
	grad →					
		175				pred. rhyolitic lithic breccia
Q+A + C					MM	
C ARB +C	grad →				PM	polymictic breccia w/- ls & dacite? clasts. Some ls beds?
H-C	sharp →					fossiliferous (tr. ls) ls
C+CARB	sheared					matrix-supp dacitic autobreccia
-C	sharp → minor shear fault, obl to bed					f.g. bedded?/foliated sis w/ numerous minor faults {k'spar/alb phenos to 5mm} + sulphides (py)
Q+ A+C	shear fault??			SHD25.1		qtz, epi, k'spar/ab. chl veining thru chl, alb alt stalin
		185			B	M°2
	sharp →			70 80 90 SHD25.2		interlocking (photo #12)
H+C						
	grad sharp?					unsorted qtz, k'spar? black {ferromag?
		195				

1:200

1:100

LOG

SHD25

date: 28/02/00 | scale 1:100 | BASALT BRECCIA

alt^n	structure	m	grainsize (.063, 1, 2, 8, 32, 64, 256 mm)	MAX/AV SIZE (mm)	B % M?	description
		190		25x7/12x4	40%	
				50x15/10x4	40%	photo #13 basalt? lithic breccia clasts are less vesicular & some are less affected by shearing. Most appear fairly well rounded but some, the less sheared are more angular. Some foreign clasts which are more siliceous w/ qtz grains & are orange/pink maybe qtz/alb alt?
	sheared	195				
H+C				30x6/8x3	55%	
Qtz alt or sound clasts?		200				
				20x2/8x3	45%	
	grad →					
		205		SHD25_3		perlitic clast (photo #14). more bedded, but still wf brecciated mostly carb, some patches w/ v. strong c alt.
CARB				(16) 70x8/15x4	20%	some fossiliferous (trilo)
		210		(16) 40x20/20x3	25%	
	grad →					carb & m. basalt lithic breccia w/ minor carb veins & some fossiliferous clasts (trilo)
H+C				(16) 40x60/20x5	40%	
	grad →	215				basalt breccia

LOG

SHD25

date: 28/02/00 | scale 1:100 | BASALT BRECCIA

alt^n	structure	m	grainsize (.063, 1, 2, 8, 32, 64, 256 mm)	MAX/AV SIZE (MM)	B%	description
		215				
	shear fault?					core loss, broken core 215.4 – 217.1
H-C CARB						basalt breccia w/ fine ls clasts & carb veins.
		220				
CARB H-C			v. carbolt	30×15 20×5	20%	basalt breccia, carb alt
		225				ls breccia > massive ls
-C	grad					
						basalt breccia, carb alt.
H-C						
				SHD25_4		(photo ~~at~~ 16)
		230		CD×60 15×3	35%	
H-C						
				SHD25_5		
CARB +C	sharp.->			30×20 20×5	30%	ls & minor basalt breccia v carb + C alt.
	grad->	235				carb veined basalt breccia
H-C CARB						
CARB +C	grad ->			CD×40 20×10	60%	carb & basalt breccia carb+C alt. ls breccia?
C						
C	sharp					ls breccia?
C		240				

LOG

SHD25

date: 28/02/00 | scale 1:100 | BASALT BRECCIA

calt^n	structure	m	grainsize (.063 1 2 8 32 64 256 mm)	max/av size (mm)	B %	description
-C		240				
CARB C-H				50x25/15x3	50%	more carb alt breccia more carb veins & more ? C inf.
	grad →					
		245				basalt breccia w/ occasional carb vein
				40x8/8x2	25%	
H+C						
	sheared					
		250		50x30/10x2	40%	
H.C				80x15/15x2	30%	
		255				
	grad →					
CARB +H.C				40x10/10x2	35%	
		260				strongly carb alt. basalt breccia (carb veins/bands etc).
				70D x 20/15x3	30%	
CARB -C	grad →					carb beds
	sharp →					basalt SS & carb interbeds
+C CARB		265				

LOG

SHD25

date: 28/02/00 | scale 1:100 | BASALT BRECCIA

alt	structure	m	grainsize (.063 1 2 8 32 64 256 mm)	MAX/AV SIZE (MM)	BS MPa	description
C ARB	sheared	265		25x20/5x3	25%	basalt & m carb breccia w/ carb veining/bedding
C-H	grad→					
C						
	grad→					
C-H		270		40x20/15x2	30%	basalt breccia w/ minor carb veins
				SHD25_6		
H-C						basalt breccia & carb veining
	sheared			40x20/10x2	30%	
C		275				
						minor carb veins basalt breccia
H-C				50x30/15x3	35%	
	grad →	280				carb + m basalt breccia w/ carb veining & banding, strong C alt + m. sulphides.
C				40-50° carb veins & clasts		
	sharp? →					basalt breccia
H						
C						
H		285				breccia of mostly carb w/ minor basalt. carb veining & C alt. → carb clasts (v. minor sulphides). carb? clasts less sheared. (∴ post-def alt?)
C	grad			20x10/2.0x0	45%	
H-C						
		290				

LOG

SHD25

date: 26/02/00 | scale 1:100 | BASALT BRECCIA

alt	structure	m	grainsize (.063, 1, 2, 8, 32, 64, 256 mm)	MAX/AV SIZE (mm)	B %	description
		290		80x60/20x1	45%	
C						
				50x20/20x1	25%	
		295		SHD25-7		chlorite alt B clast (photo # 17)
	sharp vein					
C						carb veins to 6 cm & also strong minor veining. Strong C alt.
				30x12/"	52	
		300				photo # 15
						harder to see clasts now as no boundaries
				50x25/8x2	45%	zones of ~10 cm where C alt over H. also larger basalt clasts have H edges around C (1 green) cores, & white carb vesicles
		305				
						basalts are v strongly H. vesicles appear as rims. massive little basalt breccia wt pervasive H alt (also minor C alt)
H-C -CARB veins	sheared			40x30/15x2	30%	
						minor carb band/vein/clast?
		310		50x10/10x2	50%	
	grad →					chlor more C alt. basalt? cores less alt??
						~1cm soft l. green w/ d. green clasts
						clasts (carb?) alt to larger or smaller like? soft like carb but more clayey (haematisation)
H-C + CARB VEINS	sheared			SHD25-8		
						few large l. green clasts ~5cm × >4cm (core). (photo # 16)
						white clasts? → carb (alt?)
	shear? vein?	315				lots of haematite bands only in pervasive chlor

Monomictic

Polymictic

epi + carb + qtz

LOG

SHD25

date: 29/02/00 | scale 1:200

structure	m	grainsize (.063, 1, 2, 8, 32, 64, 256 mm)	s	description
alt*				epi + chl + hae + qtz veining
+ H	315			monomictic andesitic lithic breccia (puzzle) w/- pervasive carbonate veining btw clasts, w/. occasional more bedded lo. units
shear vein?				
H	325			∴ clast-supp.
				{less carb veining 316.5 - 333.0 m}
grad				lo w/ carb haloed & alt. andesite clasts
H+ CARB	335			
+ EPI				← epi veins 2 @ 10cm each
	345			
puzzle breccia				
	355			
	365			

LOG

NC1

date: 08/05/00 | scale 1:200 | page 1 of 10

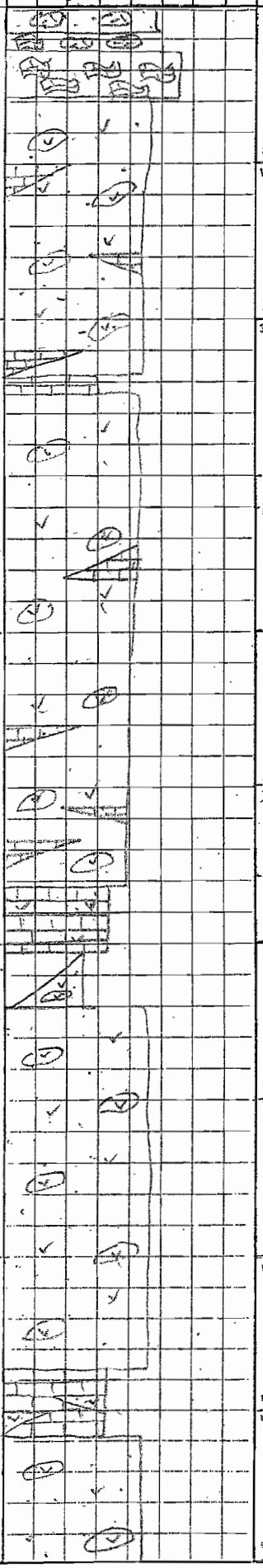

structure		m	mm	%	description
C+A +C ARB	grad →	305			fairly mm bx (rhy) vc (occ. ls clast)
C+ +H +C ARB	sharp →				Pm bx ls bx ls & rhy vc
			25x4 100x23	40	basalt bx (some more coherent dyke? pieces)
H+ +C +C ARB (veins)					some interbeds of b
		315	30x2 50x30	35	
CARB+H	grad →				ls.
			40x2 50x7	65	
			NC1	1	
H+ +C +C ARB (veins)					
		325	20x2 40x8	40	
					more ls beds to base
mostly CARB to base			68x4 70x150	65	
			NC1	2	
CARB +C +H	grad →				basaltic lithic ls.
CARB +Qz+C	sharp →	335	7x1 10x2	40	carb+qtz+chl vein
H+C+ CARB	sharp fault?				vein + basalt bx (due to low ∠ to bedding)
			15x1 70x15	35	
					basaltic lithic bx
H+ +C +C ARB (veins)					
		345	20x4 120x8	50	
CARB +H +C	sharp →		10x1? 10x2?	5	ls w/ few b bx intervals.
H+ +C +CARB	sharp (but more grad than top)				basalt lithic bx
		355	15x3 40x4	40	

LOG

NC1

date: 08/05/00

scale 1:200

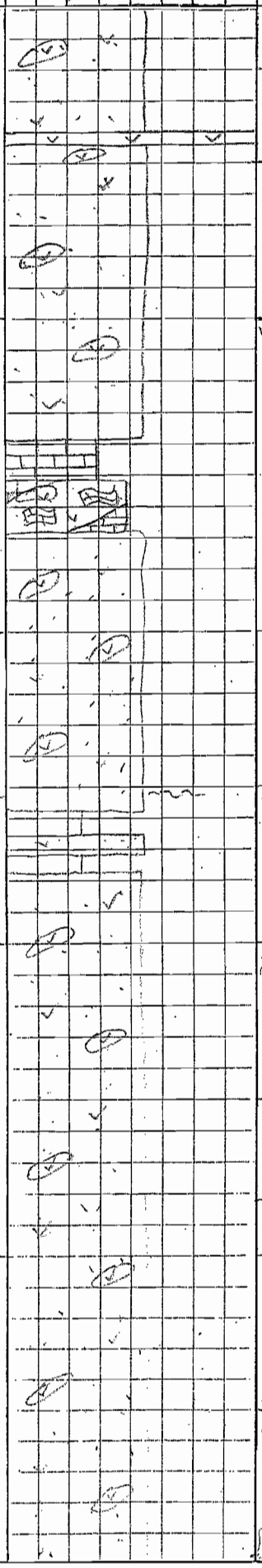

structure alt	structure	m	mm	%	description
		355			
			NC1	3	
C	grad/sharp (broken box)		20x2 60x6	40	dyke??
H+C CARB	tension? gashes almost ⊥ to foln (carb)				
		365	10x2 100x3	60	
CARB +C+H	grad → grad →				bo. bo box + b clasts + bs bedding rounded
	grad → (sharper than 2 b4)				
		375	20x3 60x8	70	
			30x4 150x15	70	
CARB C CARB	shear zone? sharp				> qtz + atc + chl veins.
		385	30x5 200x50 (dyke?)	80	
			15x4 60x25	70	
C- CARB					basalt bx.
			NC1	4	
		395	20x4 50x9	40	
			20x3 150x30	65	
C+H +CARB					
C-CARB			NC1 20x20 40x30	5 90	(dyke bx?)
		405			

LOG

NC1

date: 06/05/00 | grainsize | scale 1:200 / 1:400 / 1:200

structure		m	mm	%	description
		405			
H+C -CARB					
C	sharp (chilled)		70x6 / 200x18	95	dyke
H+ +C +CARB					
		415	15x3 / 120x15	45	
			NC1 10x2 / 35x4	6 / 40	
	sharp				
CARB+ C+H		425			
					is massive - bedded
		435			
more C to base					
		445			
	sharp				
		455	5x1 / 15x4	30	is w/ small basalt? clasts (H+C+H)
CARB + H+C	sharp		NC1 7x2 / 12x3	7 / 20	
		465			
					is bedded
	sharp/irr		5x2 / 50x20	5	is w/ small basalt? clasts (H+C+H)
	sharp/irr	475			

Grainsize: .063 | 1 | 2 | 8 | 32 | 64 | 256 mm

LOG

NC1

date: 08/08/00 | scale 1:200 | page 4 of 10

structure		m	grainsize (.063, 1, 2, 8, 32, 64, 256 mm)	mm	%	description
CARB + H	sharp	475				
				10x2 35x6	40	basalt bx prod mm but some PM (½) sections + minor ½ beds
H+C -CARB						
		485		30x2 220x25	45	
				15x2 150x20	55	
C	sharp (chilled)					dyke
H+C	shear (sharp)	495		20x2 30x3	30	
C+H				15x4 780x70 NC1..	90 8	
		505		20x5 70x25	95	basalt bx clasts much larger than UH more fragmental rather than fluidal?
H+C						
				10x4 120x18	70	
C+H						
		515		20x3 60x5	55	
H+C				25x4 230x10	65	
		525		25x3 120x4	70	

LOG

NC1

date: 09/05/00 | scale 1:200

structure		m	grainsize (.063, 1, 2, 8, 32, 64, 256 mm)		s	description
a H+		525				
				NC1	9	
				10x3 60x30	80	
		535		30x4 80x5	60	
				20x3 80x20	65	
		545		25x5 140x26	55	
				NC1	10	
CA RB ←H	sharp					
H+ +C	sharp →					
	sharp →			20x3 35x7	65	
CA RB ←H		555				
	sharp →			20x11 30x12	60	
H+ +C		565		35x6 100x9	80	
				15x2 90x12	65	
		575		30x4	90	

more basalt (generally) more indur? bx^n → less interstitial material → larger clasts of basalt → more uniform sized clasts

more coherent, less of a bx

~~A~~more vesicular after last dyke (amygdales)

* possible chilling to lb kedo? (less vesicles + bx^n)

7350 x 730

LOG

NCI

date: 09/05/00 | scale 1:200 | page 6 of 10

structure		m	grainsize (.063, 1, 2, 8, 32, 64, 256 mm)		s	description
		575				
	sharp →					cte+chl vein
coarse + Cr+H	fairly sharp →					
Fe⁺+C				15x3 / 30x5	85	basalt bx
	fairly sharp →					
		585		NCI / 10x15 / 300x50	90	(sheared?) basalt w/ crack bx? (hyalo?)
				25x12 / 200x40	85	
		595		25x10 / 120x70	85	
C⁺+H				30x4 / 200x45	75	
	grad →					
		605		20x10 / 120x35	70	
				20x8 / 120x40	75	basalt bx (more jigsaw fit)
		615		25x7 / 60x15	70	
some Sify				40x8 / 60x20	55	
		625		50x15 / 150x70	85	

LOG

NC1

date: 09/05/00 | scale 1:200

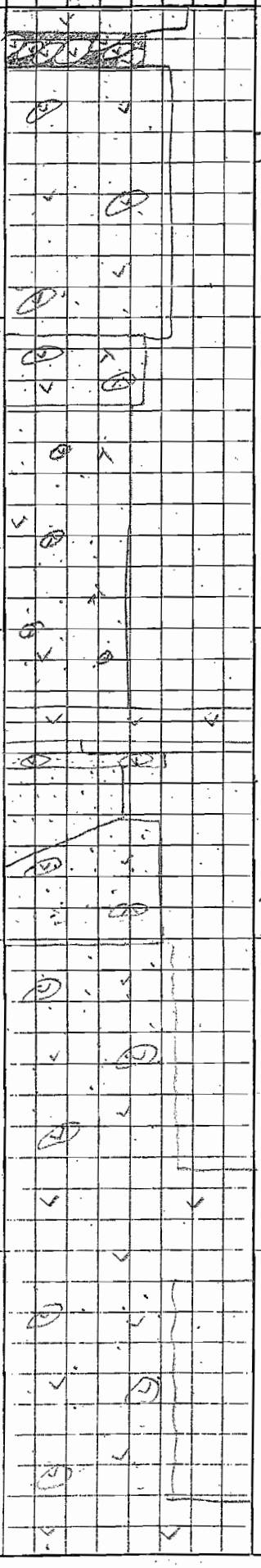

alt^n	structure	m		s	description
+Py →	sharp →	625			basalt + carb infilling
C+RB +H					
C+Py -S			NC1	12	
					basalt bx (some vesicles appear unfilled by carb)
		635			
C+S -H	sharp →				PM BX (basalt + rhy?)
	sharp →				
C+-Py +A					vc ss? (basalt + rhy/dacite?)
		645			
C+A	sharp				dyke (basalt)
Q-C A	veins (Q+C+Q) sharp				Q-chl veins basalt dyke? hyalo?
	shear? sharp?	~	~?		
C-A					dacitic? vc ss
AnS+C	sharp →				PM vc ss/bx (dacitic ss? + basalt?) + some small sulph clasts
	~		~		
	sharp? →	655			
C+H -(A+S)					basalt bx
Py(Fe) +C	shear zone				broken core (v brittle)
C+H -(A+S)					
	? → (missing)				
+C					basalt - coherent
		665			
	sharp → (vein)				
C+H -(A+S)					basalt bx (more purple-grey) (brittle cutter?)
	faisly sharp				
		675			basalt - coherent

LOG

NC1

date: 10/05/00 | scale 1:200

structure		m	grainsize (.063, 1, 2, 8, 32, 64, 256 mm)		s	description
alt^n						
	fairly sharp →	675				
				NC1	13	
C+H - (A+S)						
				NC1	14	basalt bx. (? non coherent) brittle - hyalo? (A?) - jigsaw - fit.
		685				
A?+H						
	fairly sharp					
C+H - A						
	shear?	695				basalt coherent
A?+H						
	sharp →					
C+A+H						basalt (appears different than overlying)
				NC1	15	
	sharp (chilled?)	705				
C+A?						ductile vs. [illegible]
		715				
	sharp (chilled?)					
C+S						basalt dyke.
		725				

LOG

NC1

date: 10/05/00 | scale 1:200

alt^n	structure	m	grainsize (.063, 1, 2, 8, 32, 64, 256 mm)		s	description
		725				
		735				
C+-A						dacitic vc SS
		745				
		755				
	sharp (chilled)					basalt dyke w/ bx^d bottom contact (chilled)
C+-S	sharp (chilled)					vc SS
	sharp (chilled)					basaltic hyalo?
	semi-grad	765				basalt dyke (larger phenocrysts)
				NC1	16	
						basalt dyke (larger phenocrysts) bx^d top & bottom
	grad fairly sharp					
C+S-A						vc SS
		775				

LOG

NC1

date: 10/05/00 | scale 1:200

alt^n	structure	m	grainsize (.063, 1, 2, 8, 32, 64, 256 mm)	s	description
		775			
C+S -Py(dis)	sharp → (chilled all around) →				uneven edge of basalt
		785			dacitic vc ss
	sharp →				
C, Q/A		795			vc ss qtz? porph (glomero?)
	sharp (vein) →	805			
Py(Fe)+ C,A+S +Q					vc ss w/ clasts of dac? & basalt?
	sharp? (chilled??)				
C-S -H(Fe)		815			basalt dyke
	sharp →				qtz vein box dyke? lo green minerals
	sharp → (chilled)				vc ss
	sharp → (chilled)				basalt (cd homent) & bx^d → hyalo?
		825			vc ss to 829.6 then start of another dyke (chilled contact)

LOG

NC4

date: 10/03/00

scale 1:200

structure	m	grainsize (.063, 1, 2, 8, 32, 64, 256 mm)	s	description
	0			no core recovery. 0 - 2.7 m
				strongly weathered & sections of broken core. 2.7 - 10.9 m
	10			Q+F VC SS
A+C				
	20			F+Q
	30			F - Q
	40			
	50			

LOG

NC4

date: 10/03/00

scale 1:200

structure alt^n		m	grainsize (.063, 1, 2, 8, 32, 64, 256 mm)		s	description
		50				F VC SS
						graded mass flow units
		60				
		70				
A+C						
		80				
		90				
		100				

LOG

NC4

date: 10/03/00 | scale 1:200

alt^n	structure	m	grainsize (.063, 1, 2, 8, 32, 64, 256 mm)	s	description
↓ C ↑		100			
					← veined top w/ clasts within
		110			
C→Q - A					
					vc SS/breccia.
		120			
C→Q - A +C→CB					pumice? in carb veins. vc BX w/ pre. carb clasts.
C→A - Q					vc SS.
C→CB +C	all mixed up convoluted	130			vc BX carb clasts + couple of rhy clasts? & few vc SS beds (minor) or clasts at base
C					dacitic vc bx? (dacitic hyalo w/ vc SS)
					fragmental/pumice base.
		140			" (as above)
					"
					pyrite veins & diss. in vc SS/bx
P-C C→CB (veins)		150			

LOG

NC4

date: 10/03/00 | scale 1:200 / 1:100

structure (alt^n)		m	grainsize (.063, 1, 2, 8, 32, 64, 256 mm)		s	description
		150				
C ARB	vein? →					
		160				← consolidated at base
C+A Fig+C-CARB						VC SS. ss/bx.
C+A	vein (~15cm) (Q+C-CARB)	170				
						VC SS.
		180				
CARB + Fig-C						massive carb (ls) fossils → tribs, peloids? almost all clast supported
		190				massive carb (ls)
S+C				NC4	1	poss. semi alt basalt lithic BX /SS
				NC4	2	? polymictic breccia
+HC		195		NC4	3	basalt lithic VC BX (poly & tex) + dacite + chert

1:200

1:100

LOG

NC4

date: 10/02/00 | grainsize | scale 1:100

alt^n	structure	m	grainsize (.063, 1, 2, 8, 32, 64, 256 mm)		s	description
		195		NC4	4	
	Q vein fault? →					
SHC		200				poss polymictic basaltic lithic VC BX
				NC4	5	
		205				
	grad? →					
		210				polymictic lithic vc bx some easily identified basalt clasts, other unsure
HC?	folded? sheared					?
		215				
				NC4	6	pre monomictic basalt lithic vc bx.
		220				

LOG

NC4

date: 10/03/00

scale 1:100

structure / alt^n	m	grainsize (-.063, 1, 2, 8, 32, 64, 256 mm)		s	description
	220				
Stg +Py					
	225				
slightly red-brown submetallic coatings, esp. on carb veins [ankerite?]					
	230		NC4-7		
+CARB					
	235				
	240				
			NC4-8		
grad →					vc SS (w/- minor seri alt. Basalt vc bx at top - interbedded?)
CGS +CARB					
	245				

LOG

NC4

date: 10/03/00 | grainsize | scale 1:200

structure	alt^n	m	grainsize (.063, 1, 2, 8, 32, 64, 256 mm)		s	description
		245				dacitic ??
				NC4	9	* poss dacitic clasts
				NC4	10	
		255				
	C+Py?	265				
	sharp			NC4	11	cherty basalt (fg) dyke? (chilled margins)
		275				vc ss (dacitic?) massive.
				NC4	12	
		285				
	grad?					vc ss (dacitic?)
	C+Py? + Al					
	sharp					vc ss (coarse) sil clasts (dac?) bx Py?
		295				

LOG

NC4

date: 13/03/00 | grainsize | scale 1:200

structure	m	grainsize (.063, 1, 2, 8, 32, 64, 256 mm)		s	description	page 8 of 13
alt^n	295					
	305					
sharp			NC4	13	coherent basalt?? dyke (rhy?) chilled margins	
	315				vc ss w/ increasing clasts to bottom	
c^			NC4	14		
sharp	325				dacitic hyaloclastite? or vc bx (clasts to about 25mm max)	
					vc ss (dacitic w/ occ clasts of dacite?) ? pumaceous ?	
	335				clasts more mafic w/ depth?	
			NC4	15		
	345					

LOG

NC4

date: 13/08/00 | scale 1:200

structure	m	grainsize (.063, 1, 2, 8, 32, 64, 256 mm)		s	description
	345				
					vc ss
	355				
			NC4_16		
					basaltic dyke - some small sections of auto-BX? - some included country rock
			NC4_17		
	365				
C^{+}_{1} + A					vc ss
					includes clasts of light grey sil. material (cherty) (dacitic siltstone - sometimes clasts?)
grad → P^{+}_{1} + C	375				
grad →					dacitic ss ?? basaltic dyke ?? (dac ss)
sharp →					dacitic sltst/ss basaltic dyke (dacite)
C + P_1					dacitic - lithic polymictic vc ss/bx?
					clasts? (ign?? or dac vc ss/bx) dacitic vc ss?
	385				dacitic bx?
					hyaloclastite (dacitic?) or bx (poly?)
P^{+}_{1} + C					dacitic vc ss/bx or ign?? hyaloclastite
	395				

LOG

NC4

date: 18/08/00 | scale 1:200

structure	m	grainsize (.063, 1, 2, 8, 32, 64, 256 mm)		s	description
alt^n	395				← ruggy section in hyalo ~15cm ?
					coherent dacite (massive)
C.A					
?	405				hyalo? (dacite?)
					coherent dacite
C.A?					?? dacite?
					coherent dacite
C.A?			NC4	18	?? dacite?
					coherent dacite
	415				
					hyalo - clast supported + dacitic ss?
?					
					hyalo matrix supported
	425				hyalo - clast supported.
sharp	435				dacitic vc cs/bx
folding evident (esp. of veins)					
					vc ss.
	445				

LOG

NC4

date: 13/03/00 | scale 1:200

structure	m	grainsize (.063, 1, 2, 8, 32, 64, 256 mm)		s	description
alt^n	445				?? dacitic vc ss
intense Py veins (to 8mm diam)			NC4	19	basaltic dyke?
					?? dacitic vc ss
C					vc ss.
			NC4	20	basaltic dyke
	455				
			NC4	21	
					vc ss. (some poly?)
					veined & mineral up
	465				
					more coherent
	475				vc ss dacitic
					vc ss) basaltic dykes?
CHS -A					dacitic ss (vc)
	485				
A-C					
Py in veins (lots)					
	495				

LOG

NC4

date: 14/03/00 | scale 1:200

structure	m	grainsize (.063, 1, 2, 8, 32, 64, 256 mm)	s	description
alt^n	495			
A-C +Py (in veins)				coherent dacite
	505			
sharp (vein) →				
				dacitic vc ss
	515			
minor carb veins throughout most of core from basalt bx/ts down				coherent dacite w/ small sections of vc ss & minor bx/hyalo.
	525			
A-C				
				dacitic vc ss w/ occ small sections of polymictic bx.
	535			
	545			

LOG

NC4

date: 14/03/00 | scale 1:200

structure alt^n		m	grainsize (.063, 1, 2, 8, 32, 64, 256 mm)		s	description
		545				polymictic lithic vc bx w/- bands of coherent dacite, matrix pre. dacitic ss
		555				contains clasts of below + qtz phenos & wispy grey brown (+ qtz)
A±C		565		NC4	22	
A+C						coherent dacite
C-A		575		NC4	23	polymictic dacite / andesite breccia. 577.2 EOH. qtz-porphy hyalo/bx?
		585				

Appendix B

B-1 XRF analyses

B-2 Carlo-Erba analyses and recalculations

B-3a Short-wave infra-red spectrum stack

B-3b PIMA results

Appendix B-1

XRF ANALYSES — School of Earth Sciences, University of Tasmania — Analyst Phil Robinson 09/25/2000

XRF sample preparation by Katie McGoldrick

SMAJOR2 program (checked) — ScMo X-ray tube

Ident	SiO2	TiO2	Al2O3	Fe2O3	MnO	MgO	CaO	Na2O	K2O	P2O5	C	CO2	H	H2O	Loss Inc. S-	Total	Total 2	S
BLANK(7/9/00)	95.71	0	<0.01	5.01	0.01	<0.01	0	<0.03	0	0					0	100.68	100.73	0
TASBAS(2/9)	44.54	2.32	14.17	12.63	0.18	8.34	7.83	5.43	1.94	0.95					1.56	99.89	98.37	0.04
NC1-11	47.49	1.04	18.65	10.16	0.14	4.19	5.25	4.43	1.65	0.33	1.03	3.77	0.56	5.00	6.88	100.21	103.708767	0.01
NC4-19	53.63	0.87	17.92	10.02	0.85	1.35	1.17	0.04	6.42	0.26	1.16	4.25	0.37	3.31	6.96	99.49	102.817074	1.2
SHD1-1	46.84	0.98	20.6	8.08	0.18	2.28	6.9	3.02	3.37	0.35	1.20	4.40	0.44	3.93	7.26	99.86	102.609228	0.04
SHD1-14	51.65	1.14	21.9	10.53	0.13	2.41	0.63	0.69	5.7	0.37	0.09	0.33	0.55	4.92	4.28	99.43	101.08512	0.05
SHD13-5	59.06	0.97	17.41	8.45	0.15	1.41	1.79	3	3.24	0.33	0.33	1.21	0.34	3.04	3.55	99.36	100.73774	0.01
SHD21-6	31.25	0.52	14.15	26.51	2.49	5.39	6.19	0.42	0.35	0.17	2.34	8.57	0.89	7.95	12.59	100.03	107.697979	0.5
SHD25-2	52.25	0.83	17.09	7.04	0.08	2.18	7.48	4.27	1.96	0.31	1.24	4.54	0.35	3.13	6.29	99.78	102.761464	0.01

MO4 program (ScMo X-ray tube) — AU1 program (gold tube)

MO4 program		Y	Zr	Nb	La	Ce	Nd
NC1-11		41	163	7	21	46	22
NC4-19		22	108	5	37	75	32
SHD1-1		31	161	8	45	96	42
SHD1-14		59	372	18	93	172	78
SHD13-5		34	155	7	37	77	35
SHD21-6		36	197	9	36	65	32
SHD25-2		36	105	5	31	68	29
det. limit	ppm	1	1	1	2	4	2
AWQUARTZb		<1	<1	<1	<2	<4	<2
AGV1		19.0	232.0	13.7	37.1	69.9	32.1
TASBAS(4x)		20.8	254.3	54.7	44.0	85.1	39.8
TASGRAN(4x)		33.2	154.3	13	39.8	79.6	34.4

Appendix B-2

Helen Scott samples 25/9/2000

Sample ID	%C	CO2	%H	H2O	%S
NC 1-11	1.03	3.77	0.56	5.00	nd
NC 4-19	1.16	4.25	0.37	3.31	1.03
SHD 1-1	1.20	4.40	0.44	3.93	nd
SHD 1-14	0.09	0.33	0.55	4.92	nd
SHD 13-5	0.33	1.21	0.34	3.04	nd
SHD 21-6	2.34	8.57	0.89	7.95	0.28
SHD 25-2	1.24	4.54	0.35	3.13	nd

G.Rowbottom 09/25/2000

Appendix B-3a

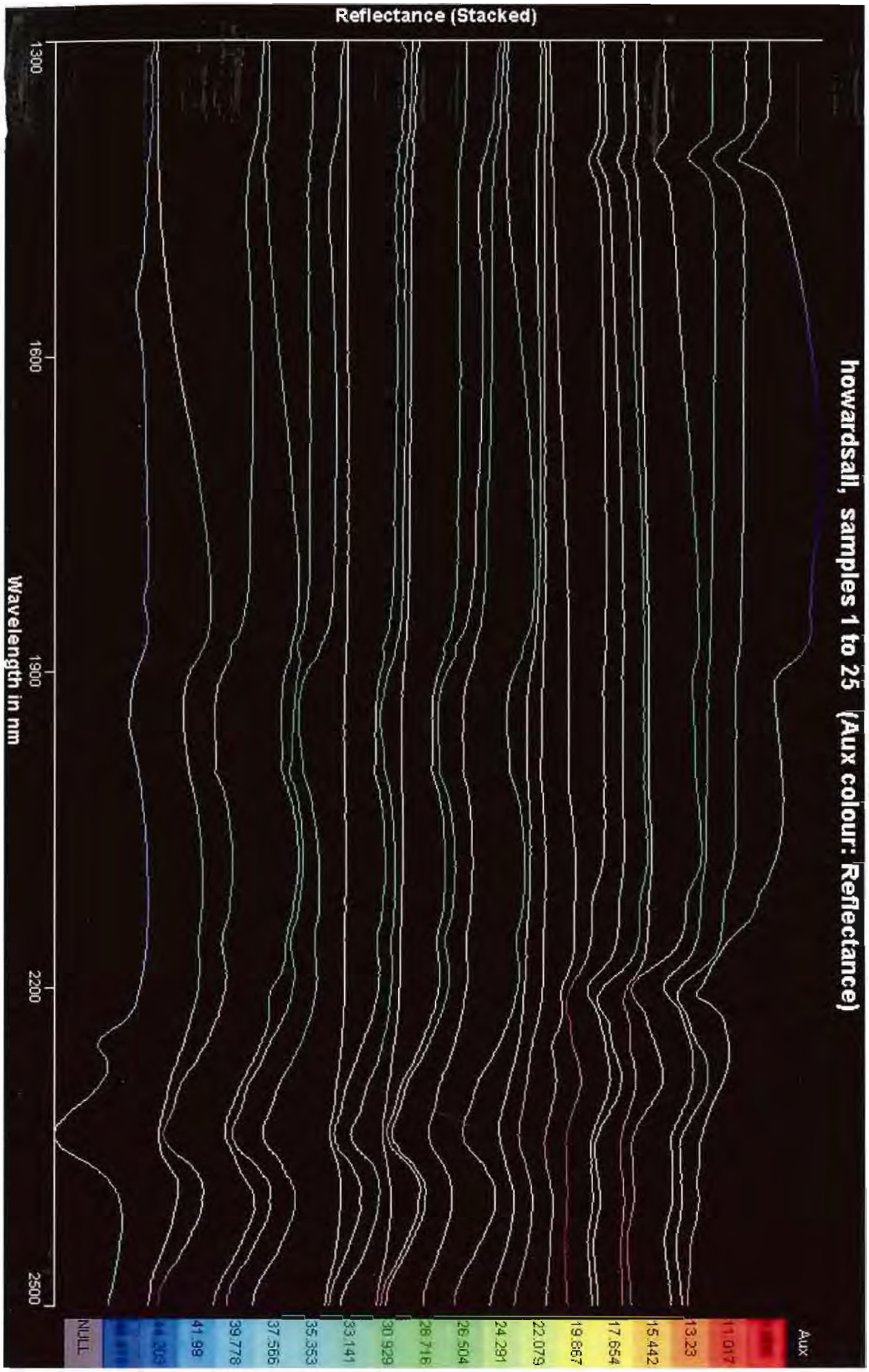

Appendix B-3b

Sample No.	Carbonate 1	Weight %	Carbonate 2	Weight %	Accuracy
SHD1_2	Calcite	0.796	Phlogopite1	0.204	11.984
SHD1_5	Calcite	0.803	Phlogopite1	0.197	12.096
SHD1_6	FeChlorite	1	NULL	NULL	86.8
SHD1_7	Calcite	1	NULL	NULL	60.312
SHD1_14	Muscovite	0.554	FeChlorite	0.446	132.217
SHD1_15	Muscovite	1	NULL	NULL	122.282
SHD1_16	Phengite	1	NULL	NULL	94
SHD13_3	FeChlorite	0.632	Calcite	0.368	26.251
SHD13_9	Calcite	0.561	Phlogopite2	0.439	50.165
SHD14_2	Muscovite	0.789	Paragonite	0.211	41.612
SHD14_3	Ankerite	1	NULL	NULL	46.983
SHD14_8	Calcite	0.72	Dolomite	0.28	24.632
SHD21_7	Muscovite	1	NULL	NULL	78.436
SHD25_1	Epidote	1	NULL	NULL	30.094
SHD25_6	Calcite	0.769	Dolomite	0.231	12.312
SHD25_8	Calcite	0.848	Epidote	0.152	18.718
NC1_1	Calcite	1	NULL	NULL	15.984
NC1_7	Calcite	0.793	Dolomite	0.207	11.56
NC1_9	Calcite	1	NULL	NULL	33.289
NC1_12	Calcite	1	NULL	NULL	60.799
NC1_13	Kaolinite	0.53	Illite	0.47	59.206
NC1_16	Muscovite	1	NULL	NULL	117.007
NC4_9	Calcite	0.597	Phlogopite2	0.403	62.448
NC4_11	Calcite	0.574	Phlogopite2	0.426	62.46

Appendix C

Literature Review – Fire Fountain Basalts: Processes and Products

Basaltic Fire Fountaining:

Processes and Products

Helen J. Scott
BAppSc

University of Tasmania

CODES SRC
Centre for Ore Deposit Research

A literature review submitted in partial fulfilment of the requirements of the Degree of Bachelor of Science with Honours

School of Earth Sciences
July 2000

Abstract

Fire fountain eruptions involve numerous and dynamic processes, and therefore produce a wide variety of products. Both the processes and products formed are strongly influenced by physical properties such as viscosity, gas content and eruption velocity of the magma. Fire fountain eruptions occur in both subaerial and subaqueous conditions, and sometimes result in very similar deposit characteristics. There are strong similarities between the deposits formed in the two settings, but differences are still numerous enough for ease in discrimination between those formed on land and those at sea. One of the more notable differences is the formation of pillow lavas in only subaqueous settings, whereas most of the other products have been found to a certain degree in both.

Contents

Abstract i

List of Illustrations iv

Chapter 1: Introduction 1

Chapter 2: Subaerial basaltic explosive eruptions 2

2.1 Introduction 2

2.2 Controls on eruption style 2

2.2.1 Magma rise speed 2

2.2.2 Gas content 2

2.2.3 Viscosity 3

2.2.4 Drainback and ponding 3

2.3 Subaerial fountaining eruption styles and fragmentation mechanisms 4

2.3.1 Magma fragmentation 4

2.3.2 Sporadic – Strombolian 4

2.3.3 Steady – Hawaiian 4

2.3.4 Low fountain – Intermediate 4

2.4 Products of subaerial fire fountain eruptions 5

2.4.1 Types of pyroclasts 5

Scoria 5

Spatter 6

Achneliths 6

2.4.2 Macroscopic – deposits 6

Strombolian - Scoria cones 6

Hawaiian - Spatter cones and ramparts 7

Littoral cones 8

Fountain fed lavas 8

Chapter 3: Subaqueous fire fountain eruptions 10

3.1 Introduction 10

3.2 Controls on eruption style 10

3.2.1 Hydrostatic pressure **10**
3.2.2 Gas content **11**
3.2.3 Viscosity **11**
3.3 Subaqueous explosive eruption styles and fragmentation mechanisms ... **12**
3.3.1 Magma-water interaction **12**
Magma explosivity 12
Steam explosivity 12
Cooling-contraction granulation 13
3.3.2 Shallow water and emergent **13**
Continuous-uprush eruption 14
3.3.3 Deep water **14**
3.4 Products of subaqueous fire fountains **15**
3.4.1 Modern examples **15**
Macroscopic character 15
Shallow water – Surtseyan eruption products 15
Deep water – Hyaloclastites 16
Clast morphology 16
3.4.2 Ancient examples **17**
Macroscopic character 17
Clast morphology 17

Chapter 4: Discussion and conclusions **18**

References **19**

List of illustrations

Figures	Description	
1.1	Hydromagmatic landforms	1
2.1	Strombolian – Hawaiian transition	2
2.2	Magma rise speed Vs gas content	3
2.3	Fountain dynamic structure	5
2.4	Accumulation rate Vs temperature	6
2.5	Littoral cone formation	9
3.1	Depth ranges of fragmentation processes	11
3.2	Contact-surface steam explosivity	12
3.3	Continuous-uprush	15

Photos

2.1	Pele's tears	7
2.2	Pele's hair	7
3.1	Kavachi – Shallow water	16
4.1	Stromboli – Fire fountaining	18

Chapter 1: Introduction

The aim of this literature review is to outline the major processes and products formed by explosive basaltic eruptions, focusing on fire fountaining behavior.

Explosive basaltic eruptions in subaerial and subaqueous settings are similar in many ways. Many of the eruption styles occur in both settings, and many of the eruption products have similar textures, as shown in work by Gill *et al.* [1990], Carlisle [1963], Cas *et al.* [1989], Moore [1985] and Tazieff [1972]. Similar processes and products occur in both settings, with controlling factors including gas content, external water (Figure 1.1) viscosity, eruption velocity and pressure.

A number of papers have been selected from a large range of sources, on both subaerial and subaqueous explosive basaltic eruptions of varying types. Conflicting views of authors are noted as well as unanimous agreement on some issues, especially in the field of subaqueous fire fountaining, which is still a strongly theoretical field of study. Possible use of the identification of products of fire fountains to constrain environments of deposition is also addressed.

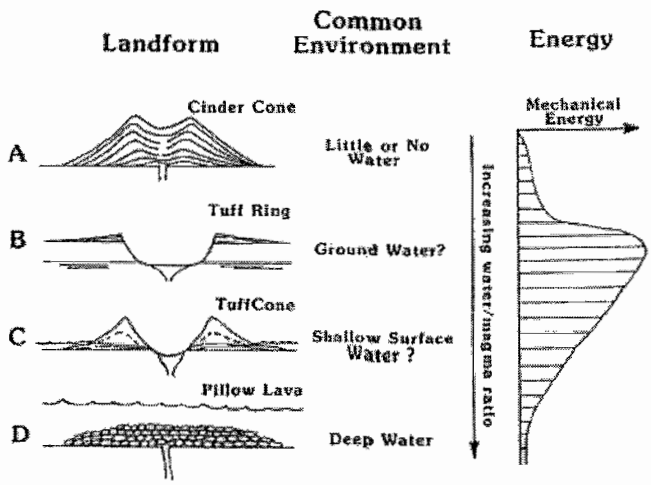

Figure 1.1 Relationships of hydromagmatic landform to environment and mechanical energy for basaltic volcanism. [Wohletz & Sheridan, 1983 p410]

Chapter 2: Subaerial basaltic explosive eruptions

2.1 Introduction

There has been much study into the various forms of subaerial basaltic explosive eruptions, including work into Hawaiian and Strombolian styles, and formation of numerous pyroclastic deposits produced by these styles. The transition of Hawaiian to Strombolian eruption styles is relatively sharp, and is not determined by the gas content of the magma, but by the speed of ascent [Parfitt & Wilson, 1995; Fisher & Schmincke, 1984]. Therefore the gas content of the magma cannot be accurately determined from the height of the fountain as was previously thought [Head & Wilson, 1987, 1989].

2.2 Controls on eruption style

2.2.1 Magma rise speed

The greatest control on the eruption style of basaltic magmas from subaerial vents is the speed at which it rises [Parfitt & Wilson, 1995; Fisher & Schmincke, 1984]. This determines the amount of accumulation of gas bubbles in the magma column, which in turn determines the style of eruption upon reaching the surface vent. The change from Strombolian to Hawaiian-style occurs in a narrow speed range of about 0.01-0.3ms^{-1} as shown in Figure 2.1.

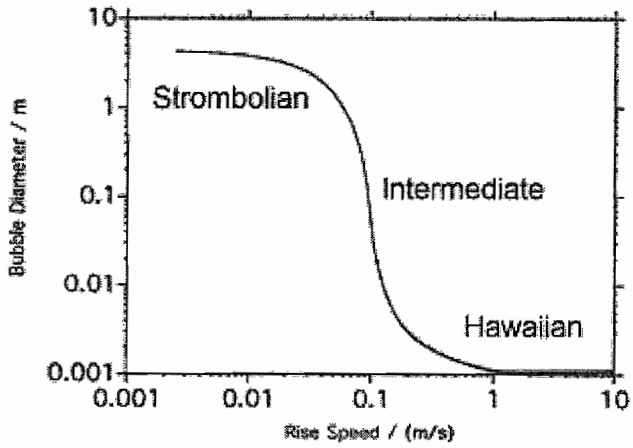

Figure 2.1 The variation with magma rise speed of the diameter of the largest bubble than can be formed by coalescence of smaller bubbles, in a magma with viscosity 30 Pa s and total initial volatile content 0.5 wt per cent; the volatile is assumed to consist entirely of H_2O. [modified from Parfitt & Wilson, 1995 p227]

2.2.2 Gas content

The gas content of the magma determines the vesicularity, as well as influencing the style of eruption. Lowering of the magmatic gas content alters the style of eruption from fountaining to effusive eruption of vesicular magma [Parfitt & Wilson, 1995]. Mangan & Cashman [1992] calculated a required change of about 0.05 wt% dissolved water to achieve this. To alter Hawaiian fountaining to Strombolian, a coupled decrease in magma rise speed and gas content would be required, as shown in Figure 2.2.

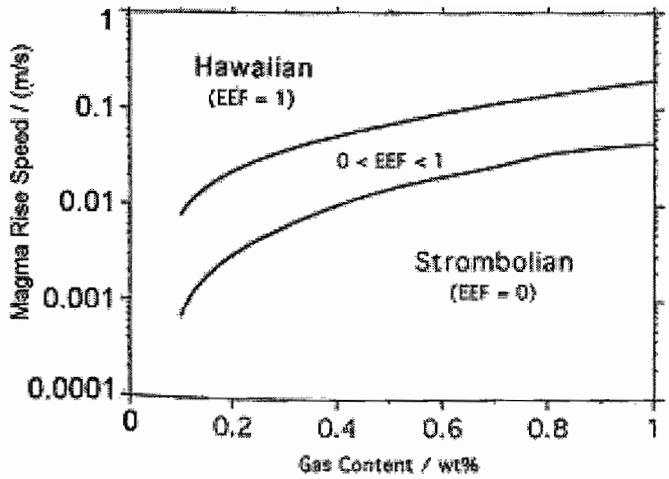

Figure 2.2 The variation in style of explosive basaltic eruptions shown as a function of magma rise speed and total magma water content. [Parfitt & Wilson, 1995 p231]

2.2.3 Viscosity

The composition, temperature, crystallinity and degree of exsolution of gaseous phases determine the viscosity of the melt. This in turn aids in determining the eruption style of the magma, with low viscosity generally resulting in fountaining, and high viscosity in effusion of vesicular lavas.

2.2.4 Drainback and ponding

Drainback is the process by which erupted lava falls back within the vent area or is entrained in flows that re-enter the vent; draining lava may also form ponds in the vent, which restrict eruption. Central vents are more likely to be affected by drainback than fissure vents due to the long lateral extent of the fissure type. Wilson *et al.* [1995] stated that a high exsolved gas content yields a high fountain, and low content a low fountain; a high exsolved gas content coupled with a lava pond results in an intermediate fountain height. The presence of a lava pond lowers the fountain height because the lava in the pond close to the fountain will be entrained, decreasing the fountain's energy, and thus reducing its upward momentum [Wilson *et al.*, 1995]. The degree of entrainment of ponded lava is increased by a low mass flux and high gas content, resulting in a lower fountain. The heights attained by fountains from circular vents are greatly reduced in a pond environment. This also holds true for fissure vents, which are even more susceptible to entrainment [Wilson *et al.*, 1995].

Entrainment may suppress steady fountaining and give the impression of Strombolian eruption. This is due to the presence of degassed lava in the vent (degassing occurs when vent is inactive for a significant length of time) inhibiting newer gaseous lava from erupting in a fountaining manner. This pseudo-Strombolian behavior will persist until the older degassed lava is removed, by eruption, from the vent.

2.3 Subaerial fountaining eruption styles and fragmentation mechanisms

2.3.1 Magma fragmentation

During rise of magma in the conduit, different gas species exsolve out to form bubbles. The process begins with CO_2 exsolving at depth and continues with H_2S and H_2O exsolving closer to the surface. The amounts of these gases in the magma, especially CO_2, influences some of the properties of the eruption, including the fragmentation depth [Papale & Polacci, 1999]. As magma rises in the conduit, gases continually exsolve. When the rate of rise exceeds the rate of exsolution, explosive fragmentation occurs [Mangan & Cashman, 1996]. Explosive fragmentation occurs at a critical gas volume fraction, usually taken as 75%, though Sparks [cited in Parfitt & Wilson, 1995, p227] gives a range from <60% - >90% gas.

2.3.2 Sporadic – Strombolian

Strombolian-style eruptions are characterised by sporadic explosions and fountaining of lava, and can be associated with hydrovolcanic (interactions between hot magma and water) activity (e.g. Peridot Mesa, Arizona; Crater Elegante, Mexico [Wohletz & Sheridan, 1983], and Taal, Philippines [Kokelaar, 1986]). This type of eruption occurs as the result of a low magma rise speed, and a high degree of bubble coalescence. This leads to zones within the magma being enriched and depleted in gas because the fragmentation level (critical gas volume 75%) is not reached. Vesicular, gas-depleted lava ponds in the vent, and is only disturbed when gas-enriched zones move up through the magma column and burst. As the distribution of enriched and depleted zones are relatively random, sporadic explosions result.

2.3.3 Steady – Hawaiian

Hawaiian-style eruptions are characterised by a steady fountaining of lava from fissure or central vents. Usually eruption is initiated along a fissure and over time becomes localised at one or two vents, which may develop spatter or cinder cones [Wilson *et al.*, 1995; Fisher & Schmincke, 1984]. Lava fountains are the result of high magma rise speeds, leading to fragmentation at deep levels and high pressure. Subsequent expansion of the gas as pressure decreases causes acceleration of the magma within the conduit, and a high eruption velocity [Parfitt & Wilson, 1995; Macdonald & Abbott, 1970]. Wilson *et al.*, [1995] reported fountain heights of up to 580m for eruptions from central vents (1959 eruption of Kilauea) and of less than 100m for fissure vents (Kilauea). Mangan & Cashman [1996] reported a fountain height of about 300m for Kilauea, and exit speeds of greater than $40ms^{-1}$.

2.3.4 Low fountain – Intermediate

Low fluctuating fountains are formed when the critical volume fraction is reached only at shallow depth and low pressure due to large bubbles coalescing and small bubbles not

coalescing. Only low fountain velocities are attained by this type of eruption. This is due to the scarcity of acceleration attributable to gas expansion occurring at shallow depths. Hawaiian-like fountaining, therefore, occurs but attains an inferior elevation and fluctuates around a mean height, due to changes in bubble density [Parfitt & Wilson, 1995].

2.4 Products of subaerial fire fountain eruptions

Figure 2.3 gives an overview of fountain dynamics, eruption deposits and facies and morphology of fire fountain eruptions. Head & Wilson [1989] described pyroclastic deposits with relation to temperature of clasts and the rate of accumulation, as shown in Figure 2.4.

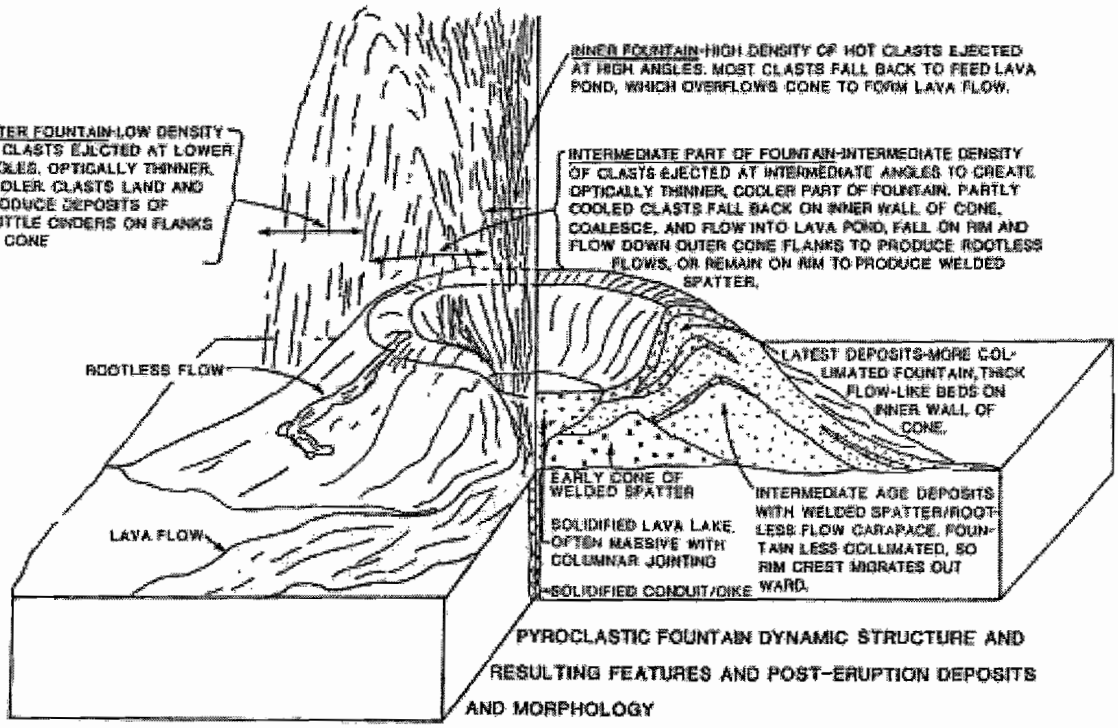

Figure 2.3 Sketch of the relationship of pyroclastic fountain dynamic structure and resulting post-eruption facies, deposits, and morphology. These relationships apply over a wide range of scales observed in basaltic pyroclastic eruptions. [Head & Wilson, 1989 p268]

2.4.1 Types of pyroclasts

Scoria

Scoria is a vesicular basaltic pyroclast that is produced in great abundance through explosive subaerial (dominant), hydromagmatic and shallow/emergent eruptions. Mangan & Cashman [1996] showed that scoria from a Kilauea lava fountain had a vesicle content between 70-85% of volume, and a clast size generally less than 15cm. Reticulite, a highly vesicular form of scoria and the product of high lava fountaining, had a vesicle content between 95-99% of volume, with the fragility of the structure leading to sizes generally less than 5cm.

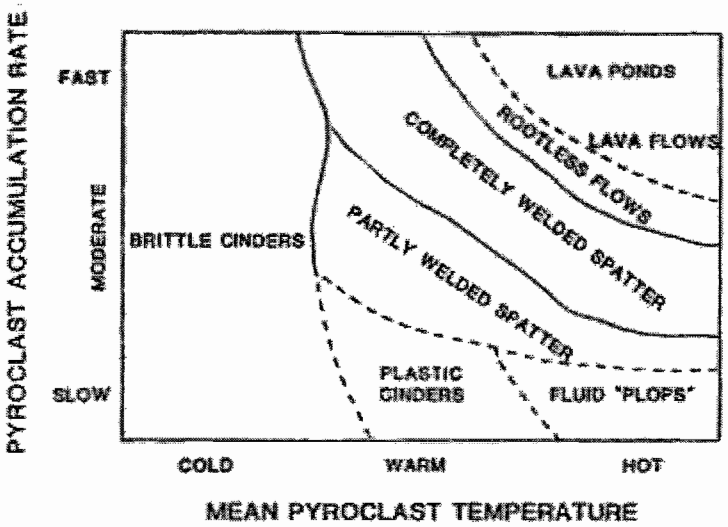

Figure 2.4 Pyroclast/deposit diagram illustrating the relationship between pyroclast temperature and pyroclast accumulation rate. [modified from Head & Wilson, 1989 p265]

Spatter

Spatter is basaltic magma which is erupted in a semi-fluid state by fire fountaining. Due to its fluid nature spatter readily agglutinates to form cones, and may even form rootless flows if fluid enough when the ground is impacted after eruption.

Achneliths

Achneliths are smooth-surfaced glass fragments that are commonly formed by Hawaiian fire fountaining events [Johnson, 1989]. They are very often associated with Pele's hair and tears, the latter being teardrop-shaped pyroclasts of volcanic glass (Photo 2.1) that represent chilled droplets of magma formed when they were flung into the air by a fountaining episode. Fisher [1968] mentions drawn glass and frozen droplets with bent and bizarre shapes and sometimes teardrop-shaped. Pele's hair are delicate needles and threads of volcanic glass (Photo 2.2) [Johnson, 1989] that are formed by the natural drawing out of liquid magma within the fountain. They are commonly attached to the narrow end of Pele's tears. Pele's hair was noted by Macdonald & Abbott [1970] to be coarse and stiff when produced by large fountains and fine when produced by small fountains.

2.4.2 Macroscopic – Deposits

Strombolian – Scoria cones

Strombolian deposits are commonly composed of scoria cones and various bombs proximal to vents, with scoria deposits in more distal areas. Scoria cones are the result of the accumulation of vesicular chilled lava pieces, and are usually accompanied by spherical, ribbon and spindle bombs [Johnson, 1989; Macdonald & Abbott, 1970]. The bombs are

Photo 2.1 Pele s tears. Photograph by J.D. Griggs USGS Nov 1984 http://volcanoes.usgs.gov

Photo 2.2 Pele s hair. Photograph by D.W. Peterson USGS 27 March 1984 http://volcanoes.usgs.gov

formed while the lava is still semi-fluid and moving through the air; by the time they come to rest they are already chilled and so do not deform further plastically. The scoria deposits may be stratified (variations resulting from changes in eruption style, flux and wind direction), and may show normal or reverse grading that reflect changes in column height and dispersal [Johnson, 1989].

Hawaiian — Spatter cones and ramparts

Spatter cones are the product of Hawaiian-style fire fountaining from a central vent , and are the result of the accumulation and agglutination of semi-fluid fragments of lava called spatter [Macdonald & Abbott, 1970]. Similar eruptions from fissure vents form elongate spatter ramparts, which parallel the erupting vent [Johnson, 1989; Wilson *et al.*, 1995]. Spatter deposits commonly include plastically deformed bombs such as the cow-dung bomb, which forms when semi-fluid clots of lava fall to earth, impact and resemble their namesake. Smaller fluidal volcanic glass fragments called achneliths, are also formed by these processes [Johnson, 1989].

Littoral cones

Littoral cones are formed where lava flows contact water (e.g. coasts of seas and lakes) [Jurado-Chichay *et al.*, 1996]. The typical Hawaiian littoral cone is typified by small cinder cones formed during rigorous hydromagmatic explosions involving a'a lava [Moore & Ault, 1965]. Some cones also have occasional plastically deformed bombs. Some bombs display extreme impact deformation, and are inferred to have been highly fluid and gas-rich when they came to rest [Fisher, 1968].

A more recent paper than Moore & Ault [1965], by Jurado-Chichay *et al.* [1996] describes littoral cones of a pahoehoe origin. Commonly these have an initial scoria and lapilli ring formed at a distance from the site of interaction, with various numbers of inner spatter rings formed during explosions. The accumulation of some of the spatter may have fed short lava flows that welled within the rings of the deposit [Jurado-Chichay *et al.*, 1996]. These cones have full circular pyroclastic deposits, and differ from typical cones that form crescent deposits. The remainder of the pyroclastic ejecta is reworked by the sea [Jurado-Chichay *et al.*, 1996]. The processes outlined here for the formation of littoral cones are further detailed in Figure 2.5.

Fountain fed lavas

Fire fountain activity can form extensive rootless lava flows by the accumulation of fluid pyroclasts erupting from the vent. These lavas can flow away from a fountain, but may also flow back into the cone to form a lava pond.

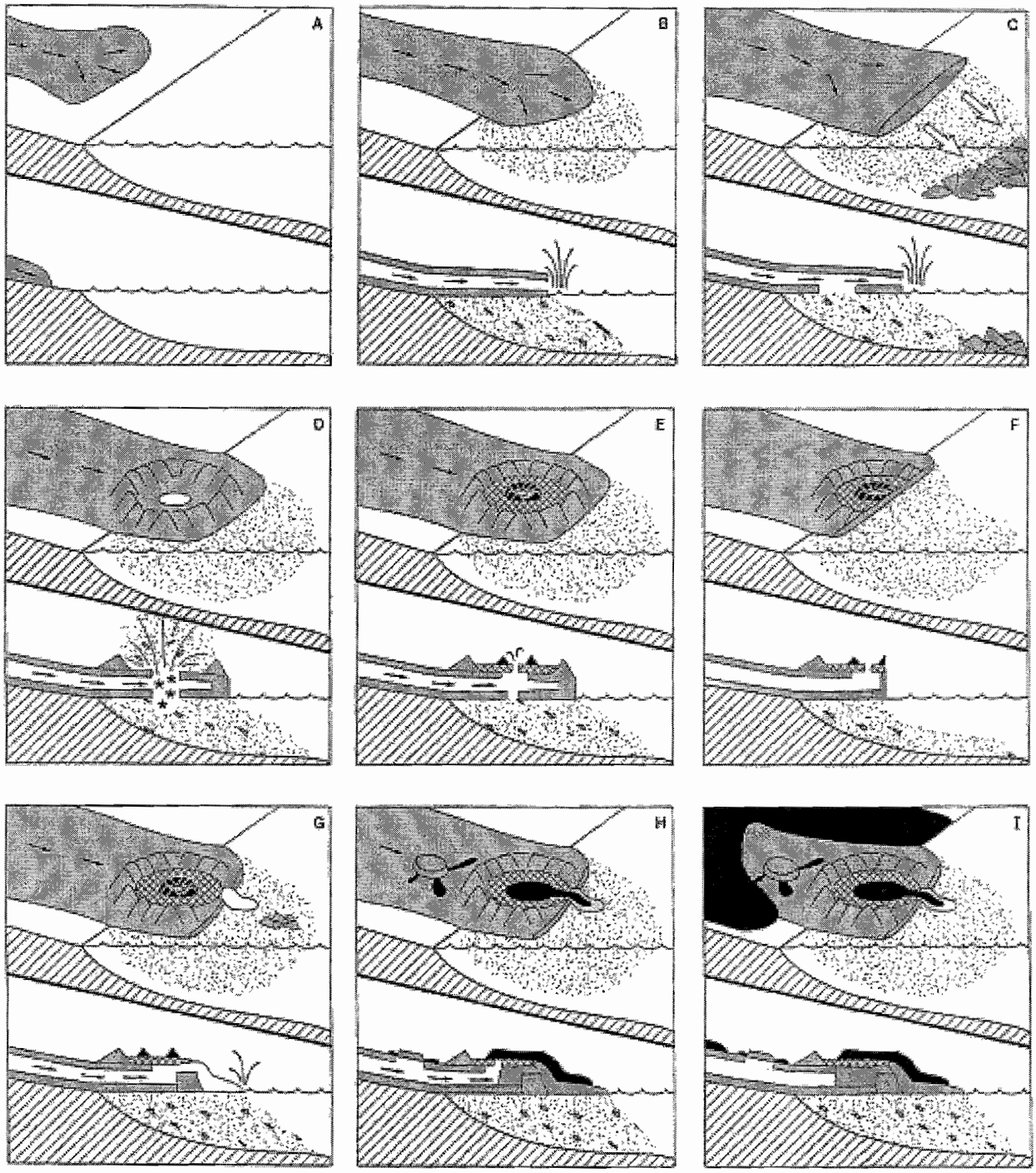

Figure 2.5 Sequential diagrams (*upper boxes*) and cross sections (*lower boxes*) show the sequence of circular littoral cone formation: **A** Lava approaches the coastline. **B** Small littoral explosions form hyaloclastites over which the lava extends, forming a lava delta. C The front of the delta collapses, Inland, disturbances in the hyaloclastites allow the tube to collapse downward. **D** Molten lava mixes explosively with underlying wet hyaloclastites. Explosions (*asterisks*) break through the tube roof to start building the main littoral cone. **E** Water supply diminishes and explosions weaken to spattering and produce the inner rims (*black*), lava ponds within the main rim (*cross-hatched lines*). **F** Erosion/collapse occurs due to marine action (Pu'u Ki and Three-rim cone are at this stage). **G** At 'Au'au Cone – collapse takes place while molten lava remains in the ponded zone and a small lava flow extends oceanward accompanied by spattering. **H** Latestage 'a'a (*black*) occupies the tube and erupts through the ponded flows to cover the floor of the main cone and to mantle the small peninsula. Just uphill of the main rim a lava rise forms and leaks small 'a'a and toothpaste lava flows (also *black*). **I** The last 'a'a (*black*) surrounds the cone. (Figure drafted by N. Hulbrit) [Jurado-Chichay *et al.*, 1996 p480]

Chapter 3: Subaqueous and emergent fire fountain eruptions

3.1 Introduction

Subaqueous fire fountaining behavior is a relatively new concept, and as with subaerial fountaining, the products of these eruptions are rarely preserved. The explosive eruption of basaltic magma in an aqueous environment in a relatively non-violent fashion has been the cause of much ongoing debate. Many authors have suggested that subaqueous fire fountaining produces hyaloclastites in deep-sea environments [Batiza *et al.*, 1984; Smith & Batiza, 1989; Tazieff, 1972; Kokelaar, 1986]. High-density gravity flows, that deposit volcaniclastic material great distances from the vent, may also be related to fire fountaining activity [Lowe cited in Smith & Batiza, 1989 p97; Menard cited in McBirney, 1963 p468; Dolozi & Ayres, 1991]. In shallow water and emergent settings, Strombolian-style fountaining is predominant, and is commonly associated with hydrovolcanic activity. Hawaiian-type fire fountaining commonly occurs as a late stage eruption style in the emergence of young volcanic islands (e.g. Capelinhos, Azores [Williams & McBirney, 1979], Surtsey, Iceland [Williams & McBirney, 1979; Moore, 1985; Kokelaar, 1986], and Bear Lake, Canada [Dolozi & Ayres, 1991]). Dolozi & Ayres [1991] believed that the study of mafic fragmental units could provide information more able to constrain volcano morphology, water depth and eruptive processes, than studies of lava flows.

3.2 Controls on eruption style

3.2.1 Hydrostatic pressure

Hydrostatic pressure is the largest control on the eruption of magma into an aqueous environment. Unlike subaerial eruptions, subaqueous eruptions are constricted by pressure imposed by an overlying water column; pressure increases with water depth. Sigvaldason [1968] attributed a facies change, from effusive pillow lavas to fragmental pillow-breccias, to a decrease in hydrostatic pressure. The decrease in external pressure caused an increase in the internal pressure of the lava, resulting in more violent eruption. McBirney [1963] asserted that explosive eruptions will not occur below 2000m due to the inability of water vapour to expand sufficiently, resulting in effusive eruption. Kokelaar [1986] defined the volatile or pressure compensation level as the depth where transition from effusive to fragmental processes occurs, and noted that the level is influenced by the composition of the magma, especially the original volatile (H_2O) content (Figure 3.1).

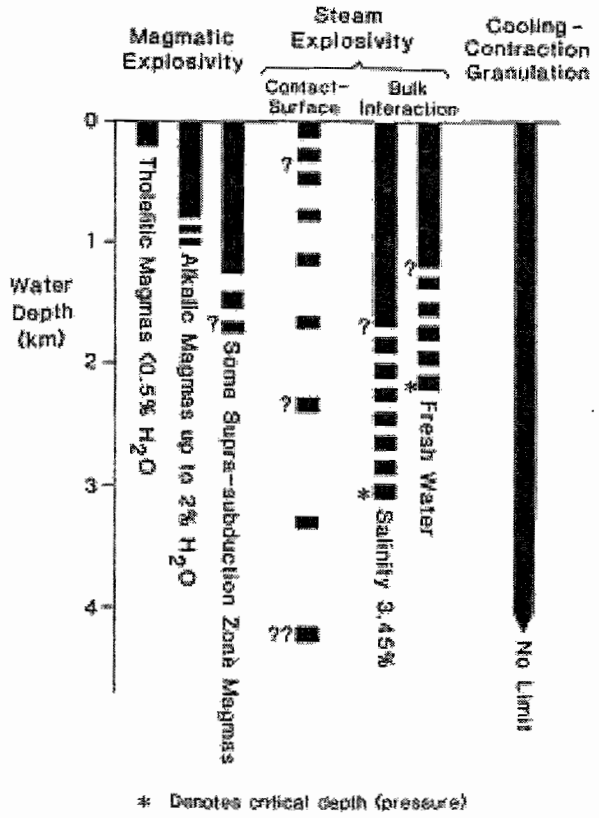

Figure 3.1 Depth ranges of major clast-forming processes, illustrating (1) that magmatic explosivity is not necessarily the major factor controlling the onset of clast formation, and (2) that very little is known about pressure limitation of clast-forming explosive behaviour [Kokelaar, 1986 p277]

3.2.2 Gas content

Gas content is an important factor in the vesiculation and fragmentation of magma. Original gas content of a basaltic magma is a strong influence on the volatile compensation depth, at which transition occurs between effusive and fragmental eruption styles. Friedman [cited in McBirney, 1963 p462] determined an original magma water content of 0.06-0.1% for basalts, which would restrict explosive eruption to less than 500m depth except for extremely enriched magmas [McBirney, 1963]. Gill *et al.* [1990] found greater magmatic water content in backarc rift volcanics than in hyaloclastites formed by fire fountaining on intraplate seamounts, showing that supra-subduction zone magmas should be more prone to fragmentation.

3.2.3 Viscosity

As in subaerial eruptions, the viscosity of the magma influences the style of eruption. In a subaqueous setting this is an important factor, with the main control on viscosity being the temperature of the magma, which is strongly controlled by the degree of crystallisation of the magma [Hall, 1996].

3.3 Subaqueous explosive eruption styles and fragmentation mechanisms

3.3.1 Magma-water interaction

There are four magma-water interaction processes that lead to magma fragmentation [Kokelaar, 1986]:

1. Magma explosivity
2. Contact-surface steam explosivity
3. Bulk interaction steam explosivity
4. Cooling-contraction granulation

Magma explosivity

This process involves the expansion of volatiles inherent to the magma. Expansion can lead to direct fragmentation, or may simply accelerate the eruption of the magma, so leading to fountaining and spatter formation and other fragmentation mechanisms [Kokelaar, 1986].

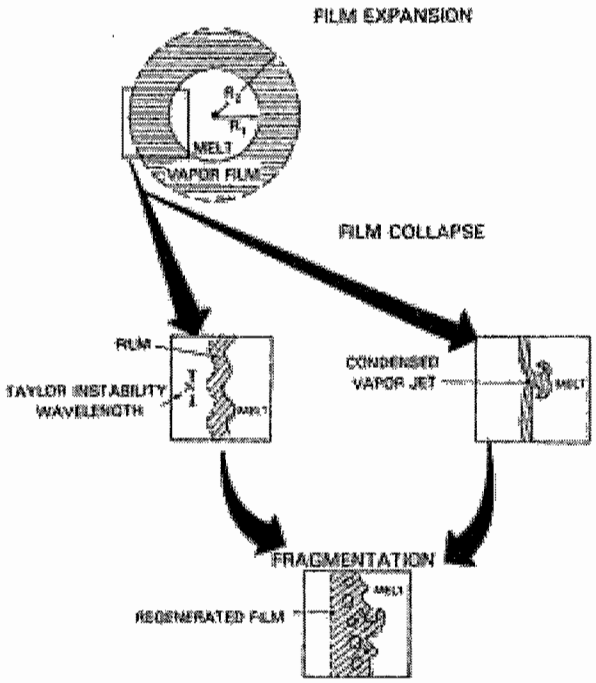

Figure 3.2 Diagrammatic illustration of the film collapse model showing fragmentation during collapse by Taylor instabilities and water jetting. [Wohletz 1983 p52]

Steam explosivity

Steam is produced at the interface between the erupting magma and the surrounding water, and forms an insulating film. The film can be disturbed by explosive expansion and collapse [Kokelaar, 1986] (Figure 3.2). Tazieff [1972], in a study of the pyroclastics in subaerial and subaqueous eruptions, showed that the ratio of explosive to effusive clasts is greater in subaqueous, than in subaerial eruptions. He concluded that steam explosions (secondary phreatic) cause greater fragmentation than initial magmatic explosions. He also

asserted that secondary phreatic explosions in subaqueous environments increase the momentum of clasts, producing greater fountain height than subaerial eruptions (600-1200m versus 100-300m). Smith & Batiza [1989] suggested that the elastic strain energy built up during intrusion of magma may add to the propelling force during eruption, resulting in greater fountain height.

Explosive contact-surface steam explosivity occurs when the insulating steam film around molten lava is disturbed or collapses. Clasts formed are very small and are commonly near spherical, bulbous or irregular in shape [Kokelaar, 1986]. Kokelaar [1986] noted that explosive contact-surface steam explosivity is initiated by strong mechanical impulses, such as forceful impact between magma and water (e.g. waves breaking on lava).

Non explosive contact-surface steam explosivity occurs when the steam film partially insulates the boundary between the magma and the water, causing slower heating and less violent interaction. The chilled extremities of pillow lavas typify this. Kokelaar [1986] mentioned that the stability of steam films increased with depth and subsequent hydrostatic pressure, resulting in a lower likelihood of explosive reactions in deep sea environments.

Bulk interaction steam explosivity occurs when amounts of water are trapped in close proximity to hot magma resulting in explosive behavior. Bulk interaction of magma and water may lead to contact-surface interactions [Kokelaar, 1986].

Cooling-contraction granulation

Cooling-contraction granulation occurs as a result of the temperature differential between the interior and exterior surfaces of erupted magma. As the outside of the lava quickly becomes solid the continued contraction on the inside causes the chilled rim to fragment.

3.3.2 Shallow water and emergent

Shallow water explosive basaltic eruptions are common along divergent and convergent ocean-ocean boundaries, and intraplate hotspots where island chains are developed (e.g. Iceland, Aleutians, and Hawaii). These types of eruptions are generally characterised by Surtseyan behavior, which is strongly explosive and produces highly fragmented deposits through a process known as continuous-uprush (e.g. Capelinhos, Azores and Taal, Philippines) [Moore, 1985].

Continuous-uprush eruption

Continuous-uprush eruptions occur at a specific water to lava ratio. If the ratio is large continuous-uprush eruptions will not occur, and tephra finger explosions (Photo 3.1) will be produced (e.g. Surtsey, Iceland, Anak Krakatau, Capelinhos and Kavachi, Solomon Islands). If the ratio is small, steam-rich lava fountaining occurs (e.g. Heimaey, Iceland and Kilauea, Hawaii). Continuous-uprush eruptions occur in the following stages:

- Initial intrusion of magma into water-logged debris under flooded vent.
- Heating of porewater and surface water.
- Boiling of water to form a bubble column which reduces hydrostatic pressure locally.
- Reduced pressure allows exsolution of magmatic gases which froths up the magma.
- Greater surface area allows for greater magma-water interaction and the production of more steam.
- Small explosions build crater rims and clear debris and water from the vent area, space is effectively filled with steam, pyroclasts and minor lithics [Kokelaar, 1986] as shown in Figure 3.3.
- Lava moves into the crater bottom and proceeds to fountain in the pressure-reduced environment.
- Any water entering the vent area either through the debris pile, or over the crater rim must be little enough to be quickly flashed to steam otherwise the process will falter.
- Explosions excavate deep into the underlying debris pile until the walls collapse inward, during a break in explosions, and cover the lava.

This process will continue in a cyclic pattern of eruption and quiescence as long as the eruption requirements are met. Due to the deep excavating nature of this process, volcanic bombs and glassy droplets may, and have been found at depth in the debris pile [Moore, 1985].

3.3.3 Deep water

The study of seamounts near the East Pacific Rise using submersibles, has led to the correlation of hyaloclastites (often associated with the seamounts) with subaqueous fire fountaining activity. This activity is thought to be initiated along ring fractures that develop during caldera formation and enlargement [Batiza *et al.*, 1984]. Study of the structure of seamounts suggests initial mound building by effusion of pillow lavas. During the waning stages of growth, an increase in magmatic pressure results in the generation of lava fountains by a water hose effect [Schmincke & Sunkel, 1987]. Bonatti [1967] inferred that fissure eruptions will occur quietly and behave plastically due to proximity to the magma reservoir.

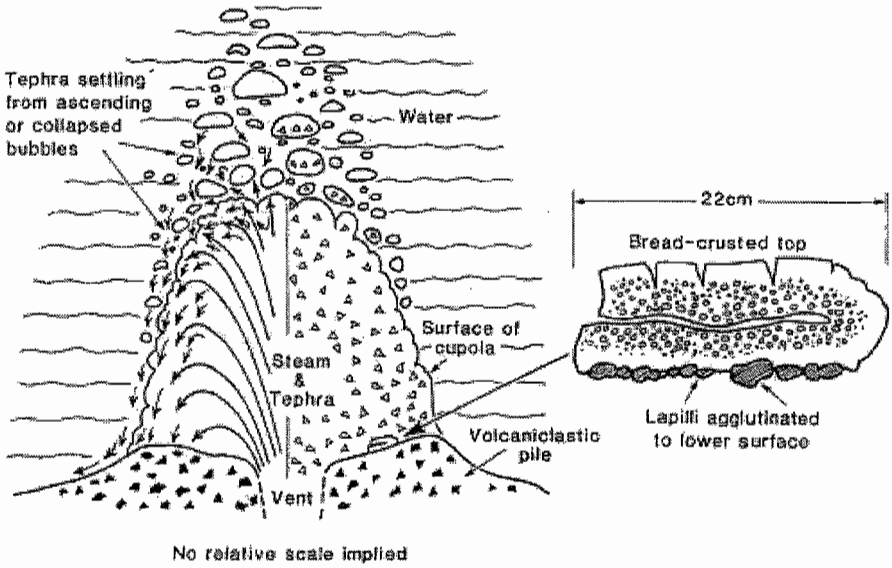

Figure 3.3 Schematic diagram of a cupola of steam enclosing the gas-thrust jet and much of the fallout during continuous eruption; arrows indicate movement direction of tephra. Fine tephra carried away by water current, and bouyant scoria, are not shown. It is important to appreciate that the cupola mostly contains a high concentration of tephra, and is not merely a steam-filled void into which tephra is ejected. Tephra-free bubbles may, however, break free. Diagrammatic section of a folded slab of basaltic spatter deposited at about 45 m below sealevel at Surtla. [Kokelaar, 1986 p282]

On the other hand, seamount eruptions will involve explosive shattering because lavas tend to travel further and are more viscous. He also noted the influence of effusion rate and the amount of magma-water interaction on eruption style. Allen [1994] commented that a high discharge rate results in fountaining of magma erupting from extensional faults, rather than passive effusion, and Kokelaar [1986] suggested fountaining occurred when magma was erupted through a constricted vent at a high discharge rate.

3.4 Products of subaqueous fire fountains

3.4.1 Modern examples

Macroscopic character

McBirney [1963] suggested that block faulting or earthquakes rupturing the sediment layer on the ocean floor may initiate the growth of seamounts. Tazieff [1972] commented on the similarity between seamounts and shallow subaqueous ash-rings (e.g. Erta'Ale range and Kokmaraea, Afar, Ethiopia). He attributed the similarity to identical mechanisms of pyroclastic ejection, but differing dispersal patterns (controlled by the eruptive depth).

Shallow water – Surtseyan eruption products

Tazieff [1972] described the relationship between the diameter/height ratio and depth of eruption of ash-rings formed in a shallow marine environment. He attributed the dispersal of pyroclasts along parabolic flight paths to be affected directly, relative to the depth at which the clast originated. Shallower vents will produce pyroclasts with higher trajectories and a

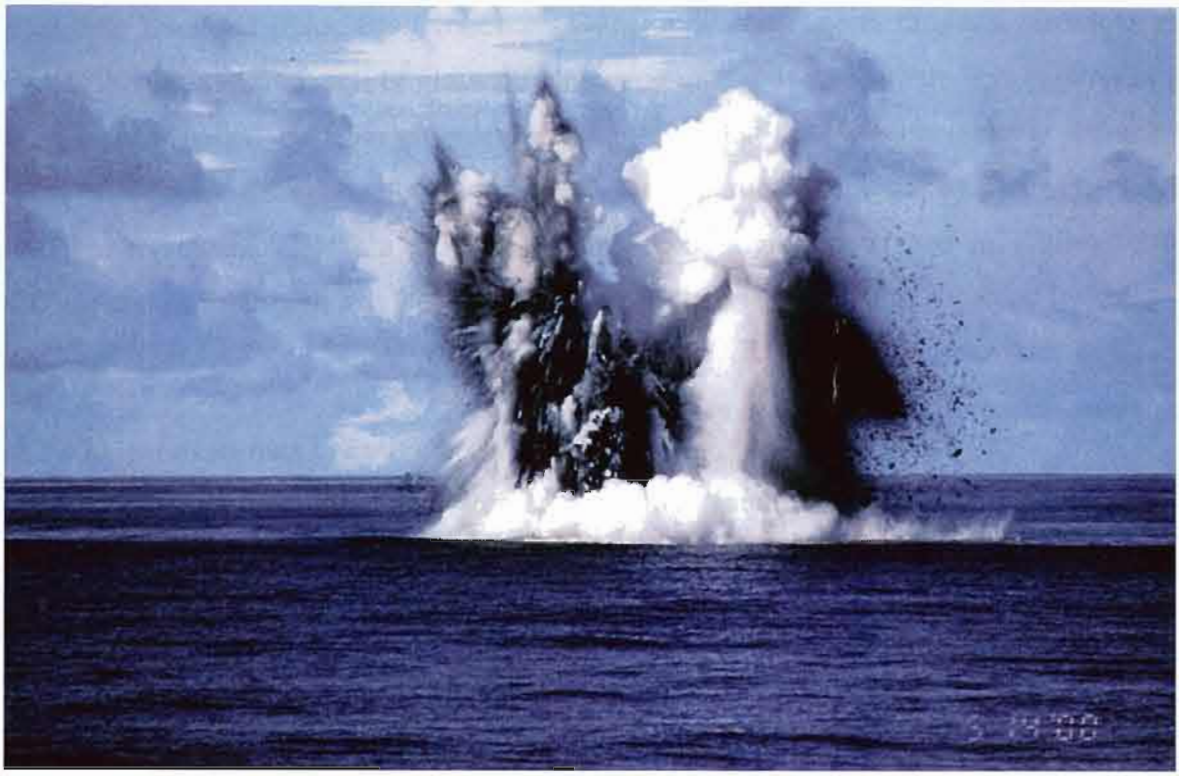

Photo 3.1 Kavachi, Solomon Islands double fountain eruption. Photograph by Neil Cheshire, CSIRO RV Franklin May 14 2000 http://www.syd.dem.csiro.au/research/hydrothermal/kavachi

wider dispersal. He gave ratios of up to 10:1 for rings formed from subaqueous vents and ratios generally of 1:1 for ash-rings formed in subaerial settings. Sheridan & Wohletz [1983] noted that the deposits of explosive shallow water hydromagmatic eruptions are composed of sand-sized clasts and are well stratified.

Deep water — Hyaloclastites

As subaqueous fire fountaining has never been directly witnessed [Dolozi & Ayres, 1991] the resulting products are inferred. Lonsdale & Batiza [1980] proposed that some eruptions form hyaloclastites whereas others form lavas on similar terrain. McBirney [1963] asserted that there are special conditions which allow eruption of magma on to the ocean floor, and certain physical or chemical properties that result in hyaloclastite flows. Kokelaar [1986] stated that deep-water hyaloclastites may be formed by granulation of fountained or cascaded material.

Clast morphology

The style of fragmentation is determined by yield strength, viscosity and surface tension [Wohletz, 1983]. Production of pyroclasts with fluidal shapes and high surface area, are formed by fluid basalt magmas that undergo explosive eruption [Wohletz, 1983]. Carlisle [1963] noted that violent explosions in magmas of very low viscosity would result in fluidal

rather than fractured pyroclasts. Kokelaar [1986] attributed magma droplets, stretched and twisted ribbons, and filaments of glass to fountaining mechanisms. Carlisle [1963] remarks on puzzle-fit shards derived from globules. He suggested that the globules (already deposited) shatter when their steam envelopes dissipate. Plastic particles reported by Dolozi & Ayres [1991] in a volcaniclastic are thought to have been originally erupted in shallow water (<100m) due to their high original vesicularity, and then redeposited downslope by creep or slumping.

3.4.2 Ancient examples

The origin of products formed by fire fountaining activity is commonly misinterpreted. Products can strongly resemble fragmented pillow lavas, and resedimented hyaloclastite breccias and tuffs. Subsequently ancient deposits have, in the past, been interpreted to be the result of effusive eruption, and completely unrelated to fountaining activity. Such false interpretations are now being reassessed on the basis of new research findings.

Macroscopic character

Schmincke & Sunkel [1987] described a Carboniferous submarine succession that may, in part, have been formed by Strombolian submarine fountaining in the later stages of pillow lava mound development. Dolozi & Ayres [1991] described a Proterozoic volcanic sequence in which fragmental rocks are the dominant deposit, and are thought to have been formed in a Surtseyan-type eruption. Fire fountaining is thought to have accompanied explosive hydromagmatic eruptions, and Dolozi & Ayres [1991] suggested that Surtseyan-type steam cupola exclusion (majority of water is excluded from reacting with newly erupted lava) may have been active around the vent at the time of eruption.

Clast morphology

Clasts within recognised ancient subaqueous deposits are believed to have been formed by the same processes as more modern analogues. Dolozi & Ayres [1991] detailed tuff-breccia, breccia, lapilli-tuff and broken bombs within the Early Proterozoic Bear Lake rocks, that they attributed to extensive, Surtseyan-type fragmentation mechanisms. Cas *et al.* [1989] employed similar mechanisms in their interpretation of a Surtseyan-type deposit at Otago, New Zealand; clast types included rare fluidal spindle shapes and breadcrust bombs. Schmincke & Sunkel [1987] described lava stringers, bombs and lapilli inter-bedded with effusive lava units, that show changes in the dominant eruptive and fragmentary mechanisms active at the time.

Chapter 4: Discussion and conclusions

Fire fountain eruptions are a very important component of explosive basaltic volcanism, as they provide information on the structure and environmental setting of the volcano. Fragmental fire fountain deposits can be used to provide a higher degree of precision than other fragmental facies, in the study of the pre- and post-eruption settings. This is due to the highly constrained, both physical and chemical, environments that fire fountains erupt into.

Some components of subaerial and subaqueous deposits can be clearly identified due to their unique attributes (e.g. pillow lavas - subaqueous, welded-spatter cones - subaerial). Although some characteristics of subaerial and subaqueous deposits are very similar, the suite of clasts as well as the macroscopic form of the deposits are influenced strongly by the depositional environment. For example, the formation of seamounts, from which common fire fountaining is postulated, are usually accompanied by pillowed flows. Quite often pillowing is the initiating eruption process, and forms a mound upon which both lavas and fragmental deposits accumulate to build the seamount.

Fire fountain eruptions, whether in a subaerial or subaqueous environment, are controlled primarily by magma rise and eruption velocity, gas content, viscosity and confining or changing pressure. Fragmentation processes are also highly dependant on these factors, as is evident from the differing degrees and severity of fragmentation produced by fountaining. At least some of the characteristics of deposits are unique to the environment and style of eruption that formed them. Deposit characters are most strongly influenced by the temperature of the clasts that formed them, the accumulation rate and accumulation process of the clasts, and the influence of external and environmental factors after emplacement.

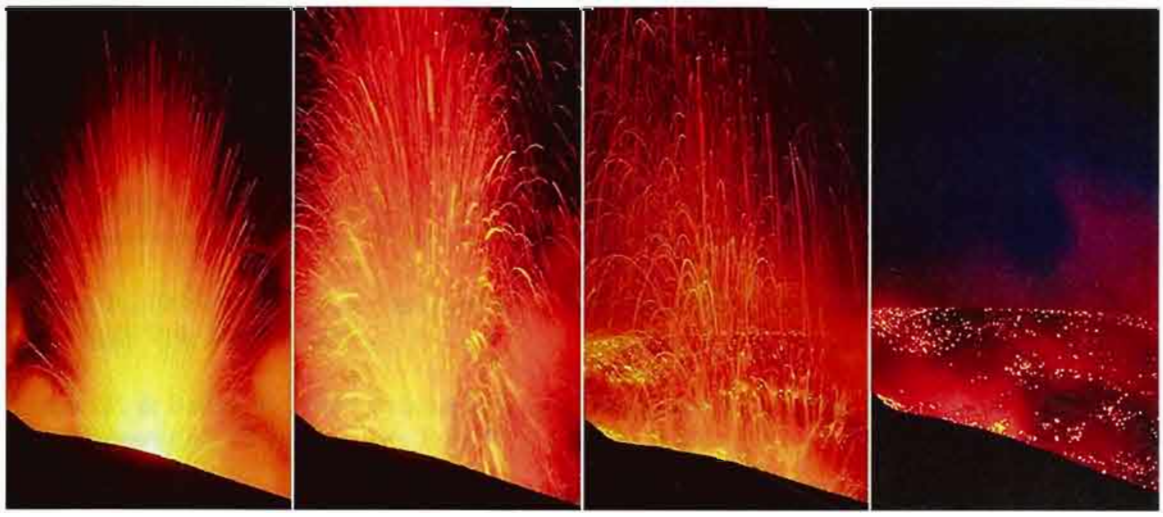

Photo 4.1 Sequence of fountaining on Stromboli, Italy. Photograph by J. Alean STROMBOLI *on-line* http://stromboli.net

References

Allen, R.L., 1994 *Interpretation of the volcanic sequence and mineralization, Yolande-Newton Creek area* **in** Pasminco report TCR-94-3590

Batiza, R., Fornarl, D.J., Vanko, D.A. & Lonsdale, P., 1984 *Craters, Calderas, and Hyaloclastites on Young Pacific Seamounts* J. Geophys. Res. 89: 8371-8390

Bonatti, E., 1967 *Mechanisms of Deep-sea volcanism in the South Pacific* **in** Abelson, P.H.(ed.), *Researches in Geochemistry Vol. 2* John Wiley & Sons, Inc.: New York pp453-491

Carlisle, D., 1963 *Pillow Breccias and their Aquagene Tuffs, Quadra Island, British Columbia* J. Geol. 71: 48-71

Cas, R.A.F., Landis, C.A. & Fordyce, R.E., 1989 *A monogenetic, Surtla-type, Surtseyan volcano from the Eocene-Oligocene Waiareka-Deborah volcanics, Otago, New Zealand: a model* Bull. Volc. 51: 291-298

Dolozi, M.B. & Ayres, L.D., 1991 *Early Proterozoic, basaltic andesite tuff-breccia: downslope, subaqueous mass transport of phreatomagmatically-generated tephra* Bull. Volc. 53: 477-495

Fisher, R.V., 1968 *Puu Hou littoral cones, Hawaii* Geol. Rund. 57: 837-864

Fisher, R.V. & Schmincke, H-U., 1984 *Pyroclastic Rocks* Springer-Verlag: Berlin 472p

Gill, J., Torssander, P., Lapierre, H., Taylor, R., Kaiho, K., Koyama, M., Kusakabe, M., Aitchison, J., Cisowski, S., Dadey, K., Fujioka, K., Klaus, A., Lovell, M., Marsaglia, K., Pezard, P., Taylor, B. & Tazaki, K., 1990 *Explosive Deep Water Basalt in the Sumisu Backarc Rift* Science 248: 214-217

Hall, A., 1996 *Igneous Petrology* (2nd Edn.) Addison Wesley Longman Limited: Essex 551p

Head, J.W. & Wilson, L., 1987 *Lava fountain heights at Pu'u 'O'o, Kilauea, Hawaii: Indicators of amount and variations of exsolved magma volatiles* J. Geophys. Res. 92: 13715-13719

Head, J.W. & Wilson, L., 1989 *Basaltic pyroclastic eruptions: Influence of gas-release patterns and volume fluxes on fountain structure, and the formation of cinder cones, spatter cones, rootless flows, lava ponds and lava flows* J. Volc. Geotherm. Res. 37: 261-271

Johnson, R.W.(ed.), 1989 *Intraplate Volcanism in Eastern Australia and New Zealand* Cambridge University Press: London 408p

Jurado-Chichay, Z., Rowland, S.K. & Walker, G.P.L., 1996 *The formation of circular littoral cones from tube fed pãhoehoe: Mauna Loa, Hawai'i* Bull. Volc. 57: 471-482

Kokelaar, P., 1986 *Magma-water interactions in subaqueous and emergent basaltic volcanism* Bull. Volc. 48: 275-289

Lonsdale, P. & Batiza, R., 1980 *Hyaloclastite and lava flows on young seamounts examined with a submersible* Geol. Soc. Am. Bull. 91: 545-554

Macdonald, G.A. & Abbott, A.T., 1970 *Volcanoes in the Sea: The Geology of Hawaii* University of Hawaii Press: Honolulu 441p

McBirney, A.R., 1963 *Factors governing the nature of submarine volcanism* Bull. Volc. 26: 455-469

Mangan, M. & Cashman, K., 1992 *Vesiculation of basaltic magma during eruption - low energy versus high energy events* EOS Trans. 73: 629

Mangan, M.T. & Cashman, K.V., 1996 *The structure of basaltic scoria and reticulite and inferences for vesiculation, foam formation, and fragmentation in lava fountains* J. Volc. Geotherm. Res. 73: 1-18

Moore, J.G., 1985 *Structure and eruptive mechanisms at Surtsey Volcano, Iceland* Geol. Mag. 122: 649-661

Moore, J.G. & Ault, W.U., 1965 *Historic Littoral Cones in Hawaii* Pacific Science 19: 3-11

Papale, P. & Polacci, M., 1999 *Role of carbon dioxide in the dynamics of magma ascent in explosive eruptions* Bull. Volc. 60: 583-594

Parfitt, E.A. & Wilson, L., 1995 *Explosive volcanic eruptions-IX. The transition between Hawaiian-style lava fountaining and Strombolian explosive activity* Geophys. J. Int. 121: 226-232

Schmincke, H-U. & Sunkel, G., 1987 *Carboniferous submarine volcanism at Herbornseelbach (Lahn-Dill area, Germany)* Geol. Rund. 76: 709-734

Sheridan, M.F. & Wohletz, K.H., 1983 *Hydrovolcanism: Basic considerations and review* J. Volc. Geotherm. Res. 17: 1-29

Sigvaldason, G.E., 1968 *Structure and products of subaquatic volcanoes in Iceland* Contr. Min. Pet. 18: 1-16

Smith, T.L. & Batiza, R., 1989 *New field and laboratory evidence for the origin of hyaloclastite flows on seamount summits* Bull. Volc. 51: 96-114

Tazieff, H., 1972 *About deep-sea volcanism* Geol. Rund. 61: 470-480

Williams, H. & McBirney, A.R., 1979 *Volcanology* Freeman, Cooper and Company: New York 97p

Wilson, L., Parfitt, E.A. & Head, J.W., 1995 *Explosive volcanic eruptions-VIII. The role of magma recycling in controlling the behaviour of Hawaiian-style lava fountains* Geophys. J. Int. 121: 215-225

Wohletz, K.H., 1983 *Mechanisms of hydrovolcanic pyroclast formation: grain-size, scanning electron microscopy, and experimental studies* J. Volc. Geotherm. Res. 17: 31-63

Wohletz, K.H. & Sheridan, M.F., 1983 *Hydrovolcanic explosions II. Evolution of basaltic tuff rings and tuff cones* Am. J. Sc. 283: 385-413

Appendix D

Rock Catalogue

Appendix D

Catalog#	Field#	Rock Name	Rock description
145622	SHD1_1	breccia	grn plag phyric bx'd andt, str chl alt
145623	SHD1_2	breccia	grn plag phyric bx'd andt, str chl alt, w. calc veins
145624	SHD1_3	sandstone	gy polymictic v'clastic sst, chl alt
145625	SHD1_5	breccia	grn & pink andt bx, w. calc veins
145626	SHD1_6	breccia	grn polymictic v'clastic bx, chl alt, w. calc vein
145627	SHD1_7	breccia	grn andt bx, str chl+carb-hem-ser alt, w. red hem+carb amygdales
145628	SHD1_14	breccia	grn andt bx, str chl+ser alt
145629	SHD1_15	breccia	light gy-grn andt bx, ser+chl alt
145630	SHD1_16	andesite	gy andt, str ser alt
145631	SHD13_3	andesite	gy-brn & grn bx'd andt, ser alt, w. chl & calc veins
145632	SHD13_5	andesite	dark gy pink & grn plag phyric jig-saw fit bx'd andt, chl alt
145633	SHD13_9	sandstone	dark gy-grn andt'c v'clastic sst/bx, str chl alt, w. calc-ankerite veins
145634	SHD14_2	sandstone	yellow & gy andt'c v'clastic sst/bx, str ser-chl alt
145635	SHD14_3	sandstone	dark grn andt'c v'clastic sst, v str chl alt w. minor gal & calc vein
145636	SHD14_8	dacite	purple-grn dac'c qz porph, chl & hem alt, w. calc vein
145637	SHD21_6	sandstone	dark grn basalt? clast w. carb amygdales, v str chl alt & minor dissem gal
145638	SHD21_7	breccia	light gy-grn polymictic v'clastic bx, str ser+chl alt, w. calc vein
145639	SHD25_1	breccia	dark grn fspr? phyric andt? bx, chl alt, w. ep, chl & calc veins
145640	SHD25_2	breccia	purple-gy plag phyric bx'd andt, hem alt
145641	SHD25_4	breccia	purple andt bx w. carb amygdales, str hem+carb-chl alt, calc veins
145642	SHD25_6	breccia	purple andt bx, str hem+carb-chl alt, calc veins
145643	SHD25_8	breccia	purple andt bx w. carb amygdales, str hem+carb-chl alt, calc veins
145644	NC1_1	breccia	purple andt bx w. carb amygdales, str hem+carb-chl alt, calc veins
145645	NC1_7	breccia	white & purple andt clasts, chl+hem alt in rextalised carb matrix
145646	NC1_9	breccia	purple-grn andt bx, chl+ser-carb alt, w. calc veins
145647	NC1_11	andesite	grn bx'd plag phyric andt, chl alt
145648	NC1_12	breccia	yellow-grn bx'd andt, str chl+py-ser alt, calc amygdales
145649	NC1_13	breccia	pink plag phyric andt bx, v str ser+py alt
145650	NC1_16	andesite	grn plag phyric andt, chl alt
145651	NC4_1	breccia	grn & purple andt bx, chl+ser-hem alt
145652	NC4_3	breccia	purple andt bx, chl+hem alt
145653	NC4_9	sandstone	grn v'clastic sst, chl alt, w. calc-ankerite vein
145654	NC4_11	andesite	gy-brn bx'd and, ser alt w. minor dissem py, ankerite veins
145655	NC4_14	breccia	gy polymictic v'clastic bx, chl alt
145656	NC4_17	andesite	grn-brn bx'd andt, ser alt
145657	NC4_18	breccia	dark green bx'd andt?, chl alt
145658	NC4_19	andesite	gy-grn andt, chl alt, calc veins

Metamorphism	AMG Northing	AMG Easting	Full Map Title	Map Scale
low grade	5358917.63	380946.27	in-house Goldfields Exploration - South Henty	1:5 000
low grade	5358916.73	380943.38	in-house Goldfields Exploration - South Henty	1:5 000
low grade	5358915.59	380939.71	in-house Goldfields Exploration - South Henty	1:5 000
low grade	5358912.94	380931.28	in-house Goldfields Exploration - South Henty	1:5 000
low grade	5358911.56	380926.92	in-house Goldfields Exploration - South Henty	1:5 000
low grade	5358910.31	380922.95	in-house Goldfields Exploration - South Henty	1:5 000
low grade	5358877.48	380813.04	in-house Goldfields Exploration - South Henty	1:5 000
low grade	5358876.6	380810.04	in-house Goldfields Exploration - South Henty	1:5 000
low grade	5358865.43	380770.58	in-house Goldfields Exploration - South Henty	1:5 000
low grade	5358881.53	380962.71	in-house Goldfields Exploration - South Henty	1:5 000
low grade	5358881.2	380951.88	in-house Goldfields Exploration - South Henty	1:5 000
low grade	5358880.75	380888.49	in-house Goldfields Exploration - South Henty	1:5 000
low grade	5358846.43	380782.22	in-house Goldfields Exploration - South Henty	1:5 000
low grade	5358840.29	380764.79	in-house Goldfields Exploration - South Henty	1:5 000
low grade	5358823.06	380698.07	in-house Goldfields Exploration - South Henty	1:5 000
low grade	5358891.11	380805.46	in-house Goldfields Exploration - South Henty	1:5 000
low grade	5358891.3	380801.83	in-house Goldfields Exploration - South Henty	1:5 000
low grade	5357924.04	381044.45	in-house Goldfields Exploration - South Henty	1:5 000
low grade	5357924.02	381043.46	in-house Goldfields Exploration - South Henty	1:5 000
low grade	5357923.92	381017.75	in-house Goldfields Exploration - South Henty	1:5 000
low grade	5357924.45	380991.22	in-house Goldfields Exploration - South Henty	1:5 000
low grade	5357925.25	380965.45	in-house Goldfields Exploration - South Henty	1:5 000
low grade	5357322.05	381179.09	in-house Goldfields Exploration - South Henty	1:5 000
low grade	5357325.18	381158.55	in-house Goldfields Exploration - South Henty	1:5 000
low grade	5357326.75	381147.94	in-house Goldfields Exploration - South Henty	1:5 000
low grade	5357328.54	381139.85	in-house Goldfields Exploration - South Henty	1:5 000
low grade	5357330.33	381133.88	in-house Goldfields Exploration - South Henty	1:5 000
low grade	5357332.71	381127.6	in-house Goldfields Exploration - South Henty	1:5 000
low grade	5357338.26	381117.46	in-house Goldfields Exploration - South Henty	1:5 000
low grade	5358529.49	380983.55	in-house Goldfields Exploration - South Henty	1:5 000
low grade	5358529.52	380982.79	in-house Goldfields Exploration - South Henty	1:5 000
low grade	5358529.82	380962.1	in-house Goldfields Exploration - South Henty	1:5 000
low grade	5358529.63	380952.37	in-house Goldfields Exploration - South Henty	1:5 000
low grade	5358528.44	380928.44	in-house Goldfields Exploration - South Henty	1:5 000
low grade	5358526.67	380907.09	in-house Goldfields Exploration - South Henty	1:5 000
low grade	5358523.58	380879.86	in-house Goldfields Exploration - South Henty	1:5 000
low grade	5358521.33	380861.55	in-house Goldfields Exploration - South Henty	1:5 000

Map comments	DDH	Depth (m)	Azimuth	Inclination	Area
may be available through Goldfields Exploration	SHD1	190.8	251.5	-72.2	EL 8/96
may be available through Goldfields Exploration	SHD1	200.2	252.8	-71.2	EL 8/96
may be available through Goldfields Exploration	SHD1	211.9	252.8	-71.2	EL 8/96
may be available through Goldfields Exploration	SHD1	238.1	252.5	-70.2	EL 8/96
may be available through Goldfields Exploration	SHD1	251.4	252.5	-70.2	EL 8/96
may be available through Goldfields Exploration	SHD1	263.4	252.5	-69.7	EL 8/96
may be available through Goldfields Exploration	SHD1	497	253.5	-51	EL 8/96
may be available through Goldfields Exploration	SHD1	501.9	253.5	-51	EL 8/96
may be available through Goldfields Exploration	SHD1	563	254.5	-46.2	EL 8/96
may be available through Goldfields Exploration	SHD13	670.9	267.5	-53.4	EL 8/96
may be available through Goldfields Exploration	SHD13	688.7	268.5	-52.2	EL 8/96
may be available through Goldfields Exploration	SHD13	788.2	271	-48.8	EL 8/96
may be available through Goldfields Exploration	SHD14	185	249.5	-43	EL 8/96
may be available through Goldfields Exploration	SHD14	209.2	251	-39	EL 8/96
may be available through Goldfields Exploration	SHD14	292.8	256.5	-32.3	EL 8/96
may be available through Goldfields Exploration	SHD21	244.4	275	-62.8	EL 8/96
may be available through Goldfields Exploration	SHD21	252.1	273	-62	EL 8/96
may be available through Goldfields Exploration	SHD25	184.6	269	-54.5	EL 8/96
may be available through Goldfields Exploration	SHD25	186.3	269	-54.5	EL 8/96
may be available through Goldfields Exploration	SHD25	229.3	270	-53.1	EL 8/96
may be available through Goldfields Exploration	SHD25	272.1	273	-51	EL 8/96
may be available through Goldfields Exploration	SHD25	311.8	271	-48.8	EL 8/96
may be available through Goldfields Exploration	NC1	321	281	-82.5	EL 8/96
may be available through Goldfields Exploration	NC1	459	278	-81	EL 8/96
may be available through Goldfields Exploration	NC1	528	278	-81	EL 8/96
may be available through Goldfields Exploration	NC1	584.5	278	-81	EL 8/96
may be available through Goldfields Exploration	NC1	629.1	286	-82	EL 8/96
may be available through Goldfields Exploration	NC1	677.4	286	-82	EL 8/96
may be available through Goldfields Exploration	NC1	766.1	295	-82	EL 8/96
may be available through Goldfields Exploration	NC4	192.5	272	-70	EL 8/96
may be available through Goldfields Exploration	NC4	194.7	272	-70	EL 8/96
may be available through Goldfields Exploration	NC4	249.9	272	-70	EL 8/96
may be available through Goldfields Exploration	NC4	272.5	272	-70	EL 8/96
may be available through Goldfields Exploration	NC4	322.6	267	-61	EL 8/96
may be available through Goldfields Exploration	NC4	364	267	-61	EL 8/96
may be available through Goldfields Exploration	NC4	413.8	263	-56	EL 8/96
may be available through Goldfields Exploration	NC4	446.3	263	-56	EL 8/96

State	Country	Biostratigraphy	Era	Eon	Lithostratigraphy	Group
Tasmania	Australia	Middle Cambrian	Palaeozoic	Phanerozoic	Lynchford Mb	Tyndall Gp
Tasmania	Australia	Middle Cambrian	Palaeozoic	Phanerozoic	Lynchford Mb	Tyndall Gp
Tasmania	Australia	Middle Cambrian	Palaeozoic	Phanerozoic	Lynchford Mb	Tyndall Gp
Tasmania	Australia	Middle Cambrian	Palaeozoic	Phanerozoic	Lynchford Mb	Tyndall Gp
Tasmania	Australia	Middle Cambrian	Palaeozoic	Phanerozoic	Lynchford Mb	Tyndall Gp
Tasmania	Australia	Middle Cambrian	Palaeozoic	Phanerozoic	Lynchford Mb	Tyndall Gp
Tasmania	Australia	Middle Cambrian	Palaeozoic	Phanerozoic	Lynchford Mb	Tyndall Gp
Tasmania	Australia	Middle Cambrian	Palaeozoic	Phanerozoic	Lynchford Mb	Tyndall Gp
Tasmania	Australia	Middle Cambrian	Palaeozoic	Phanerozoic	Lynchford Mb	Tyndall Gp
Tasmania	Australia	Middle Cambrian	Palaeozoic	Phanerozoic	Lynchford Mb	Tyndall Gp
Tasmania	Australia	Middle Cambrian	Palaeozoic	Phanerozoic	Lynchford Mb	Tyndall Gp
Tasmania	Australia	Middle Cambrian	Palaeozoic	Phanerozoic	Lynchford Mb	Tyndall Gp
Tasmania	Australia	Middle Cambrian	Palaeozoic	Phanerozoic	Lynchford Mb	Tyndall Gp
Tasmania	Australia	Middle Cambrian	Palaeozoic	Phanerozoic	Lynchford Mb	Tyndall Gp
Tasmania	Australia	Middle Cambrian	Palaeozoic	Phanerozoic		
Tasmania	Australia	Middle Cambrian	Palaeozoic	Phanerozoic	Lynchford Mb	Tyndall Gp
Tasmania	Australia	Middle Cambrian	Palaeozoic	Phanerozoic	Lynchford Mb	Tyndall Gp
Tasmania	Australia	Middle Cambrian	Palaeozoic	Phanerozoic	Lynchford Mb	Tyndall Gp
Tasmania	Australia	Middle Cambrian	Palaeozoic	Phanerozoic	Lynchford Mb	Tyndall Gp
Tasmania	Australia	Middle Cambrian	Palaeozoic	Phanerozoic	Lynchford Mb	Tyndall Gp
Tasmania	Australia	Middle Cambrian	Palaeozoic	Phanerozoic	Lynchford Mb	Tyndall Gp
Tasmania	Australia	Middle Cambrian	Palaeozoic	Phanerozoic	Lynchford Mb	Tyndall Gp
Tasmania	Australia	Middle Cambrian	Palaeozoic	Phanerozoic	Lynchford Mb	Tyndall Gp
Tasmania	Australia	Middle Cambrian	Palaeozoic	Phanerozoic	Lynchford Mb	Tyndall Gp
Tasmania	Australia	Middle Cambrian	Palaeozoic	Phanerozoic	Lynchford Mb	Tyndall Gp
Tasmania	Australia	Middle Cambrian	Palaeozoic	Phanerozoic	Lynchford Mb	Tyndall Gp
Tasmania	Australia	Middle Cambrian	Palaeozoic	Phanerozoic	Lynchford Mb	Tyndall Gp
Tasmania	Australia	Middle Cambrian	Palaeozoic	Phanerozoic	Lynchford Mb	Tyndall Gp
Tasmania	Australia	Middle Cambrian	Palaeozoic	Phanerozoic	Lynchford Mb	Tyndall Gp
Tasmania	Australia	Middle Cambrian	Palaeozoic	Phanerozoic	Lynchford Mb	Tyndall Gp
Tasmania	Australia	Middle Cambrian	Palaeozoic	Phanerozoic	Lynchford Mb	Tyndall Gp
Tasmania	Australia	Middle Cambrian	Palaeozoic	Phanerozoic	Lynchford Mb	Tyndall Gp
Tasmania	Australia	Middle Cambrian	Palaeozoic	Phanerozoic	Lynchford Mb	Tyndall Gp
Tasmania	Australia	Middle Cambrian	Palaeozoic	Phanerozoic	Lynchford Mb	Tyndall Gp
Tasmania	Australia	Middle Cambrian	Palaeozoic	Phanerozoic	Lynchford Mb	Tyndall Gp
Tasmania	Australia	Middle Cambrian	Palaeozoic	Phanerozoic	Lynchford Mb	Tyndall Gp
Tasmania	Australia	Middle Cambrian	Palaeozoic	Phanerozoic	Lynchford Mb	Tyndall Gp
Tasmania	Australia	Middle Cambrian	Palaeozoic	Phanerozoic	Lynchford Mb	Tyndall Gp
Tasmania	Australia	Middle Cambrian	Palaeozoic	Phanerozoic	Lynchford Mb	Tyndall Gp
Tasmania	Australia	Middle Cambrian	Palaeozoic	Phanerozoic	Lynchford Mb	Tyndall Gp

Formation	Member	Depositional environment	Basin	Preps
Comstock Fm	Lynchford Mb	shallow to deep marine	Mount Read Volcanics	R,TS,CR,PD
Comstock Fm	Lynchford Mb	shallow to deep marine	Mount Read Volcanics	R
Comstock Fm	Lynchford Mb	shallow to deep marine	Mount Read Volcanics	R,TS
Comstock Fm	Lynchford Mb	shallow to deep marine	Mount Read Volcanics	R
Comstock Fm	Lynchford Mb	shallow to deep marine	Mount Read Volcanics	R
Comstock Fm	Lynchford Mb	shallow to deep marine	Mount Read Volcanics	R
Comstock Fm	Lynchford Mb	shallow to deep marine	Mount Read Volcanics	R,CR,PD
Comstock Fm	Lynchford Mb	shallow to deep marine	Mount Read Volcanics	R
Comstock Fm	Lynchford Mb	shallow to deep marine	Mount Read Volcanics	R
Comstock Fm	Lynchford Mb	shallow to deep marine	Mount Read Volcanics	R
Comstock Fm	Lynchford Mb	shallow to deep marine	Mount Read Volcanics	R,TS,CR,PD
Comstock Fm	Lynchford Mb	shallow to deep marine	Mount Read Volcanics	R
Comstock Fm	Lynchford Mb	shallow to deep marine	Mount Read Volcanics	R
Comstock Fm	Lynchford Mb	shallow to deep marine	Mount Read Volcanics	R
		shallow to deep marine	Mount Read Volcanics	R
Comstock Fm	Lynchford Mb	shallow to deep marine	Mount Read Volcanics	R,CR,PD
Comstock Fm	Lynchford Mb	shallow to deep marine	Mount Read Volcanics	R
Comstock Fm	Lynchford Mb	shallow to deep marine	Mount Read Volcanics	R
Comstock Fm	Lynchford Mb	shallow to deep marine	Mount Read Volcanics	R,CR,PD
Comstock Fm	Lynchford Mb	shallow to deep marine	Mount Read Volcanics	R,TS
Comstock Fm	Lynchford Mb	shallow to deep marine	Mount Read Volcanics	R
Comstock Fm	Lynchford Mb	shallow to deep marine	Mount Read Volcanics	R
Comstock Fm	Lynchford Mb	shallow to deep marine	Mount Read Volcanics	R
Comstock Fm	Lynchford Mb	shallow to deep marine	Mount Read Volcanics	R,TS
Comstock Fm	Lynchford Mb	shallow to deep marine	Mount Read Volcanics	R,TS
Comstock Fm	Lynchford Mb	shallow to deep marine	Mount Read Volcanics	R,CR,PD
Comstock Fm	Lynchford Mb	shallow to deep marine	Mount Read Volcanics	R
Comstock Fm	Lynchford Mb	shallow to deep marine	Mount Read Volcanics	R
Comstock Fm	Lynchford Mb	shallow to deep marine	Mount Read Volcanics	R,TS
Comstock Fm	Lynchford Mb	shallow to deep marine	Mount Read Volcanics	R
Comstock Fm	Lynchford Mb	shallow to deep marine	Mount Read Volcanics	R,TS
Comstock Fm	Lynchford Mb	shallow to deep marine	Mount Read Volcanics	R
Comstock Fm	Lynchford Mb	shallow to deep marine	Mount Read Volcanics	R
Comstock Fm	Lynchford Mb	shallow to deep marine	Mount Read Volcanics	R
Comstock Fm	Lynchford Mb	shallow to deep marine	Mount Read Volcanics	R
Comstock Fm	Lynchford Mb	shallow to deep marine	Mount Read Volcanics	R,TS
Comstock Fm	Lynchford Mb	shallow to deep marine	Mount Read Volcanics	R,CR,PD